Thesis for a Ph.D. Degree

Assessment of aerosol optical depth and estimation of lidar ratio from CALIOP measurements

CALIOP 에어로졸 광학 두께의 검증과 라이다 상수 산정에 관한 연구

Man-Hae Kim

February 2014

School of Earth and Environmental Sciences

Graduated School

Seoul National University

Assessment of aerosol optical depth and estimation of lidar ratio from CALIOP measurements

by

Man-Hae Kim

Dissertation Submitted to the Faculty of Graduated School of Seoul National University in Partial Fulfillment of the Requirement for the Degree of Doctor of Philosophy

Degree Awarded:

February 2014

Advisory Committee:

Professor	Byung-Ju Sohn,	Chair
Professor	Soon-Chang Yoon,	Advisor
Professor	Young-Sung Ghim	
Professor	Jhoon Kim	
Professor	Sang-Woo Kim	

이학박사학위논문

CALIOP 에어로졸 광학 두께의 검증과 라이다 상수 산정에 관한 연구

Assessment of aerosol optical depth and estimation of lidar ratio from CALIOP measurements

2014년 2월

서울대학교 대학원

지구환경과학부

김 만 해

ABSTRACT

Assessment of aerosol optical depth and estimation of lidar ratio from CALIOP measurements

Man-Hae Kim

School of Earth and Environmental Sciences

The Graduated School

Seoul National University

The Cloud-Aerosol Lidar with Orthogonal Polarization (CALIOP) is a space-borne lidar system onboard the Cloud-Aerosol Lidar and Infrared Pathfinder Satellite Observation (CALIPSO) satellite. CALIOP is a unique instrument that can provide aerosol extinction profile and AOD on a global scale for both day and night. However, the uncertainty in CALIOP AOD is relatively high compared to other passive sensors. In order to assess the uncertainty in CALIOP AOD and investigate potential sources of uncertainty, CALIOP AOD was compared with MODIS-Aqua (hereafter referred to MODIS) AOD over ocean by separating aerosol type

defined in CALIOP level 2 algorithm. Such comparisons have been performed for five different aerosol subtypes classified by CALIOP algorithm, namely clean marine, dust, polluted dust, polluted continental, and biomass burning, over the ocean from June 2006 to December 2010. MODIS AOD at 550 nm (0.111 ± 0.079) for the collocated data pairs is about 63% higher than CALIOP AOD at 532nm (0.068 ± 0.073). For clean marine, MODIS AOD (0.110 ± 0.064) is almost twice the CALIOPAOD (0.056 ± 0.038), and the difference between the AOD values has a strong latitude dependence likely related to the surface wind speed over the ocean. The difference in AOD for dust (13%) is observed to be the lowest among the five aerosol types under consideration, but it shows a slight regional variation. The discrepancy of AOD for dust also shows strong dependency on the layer mean of the particulate depolarization ratio. CALIOP AOD is higher than MODIS AOD for both polluted dust and polluted continental by 15% and 29%, respectively, for most of the ocean. One of the possible reasons for the difference is the misclassification of clean marine (or marine + dust) as polluted dust and polluted continental in the CALIOP algorithm. For biomass burning, uncertainty in the layer base altitude is thought to be one of the main reasons for the lower value of CALIOP AOD.

Current CALIOP level 2 algorithm uses pre-determined $\boldsymbol{S_{aer}}$ for classified aerosol types. However, not only using single values of $\boldsymbol{S_{aer}}$ for each aerosol type but also aerosol classification algorithm could be sources of uncertainties in aerosol extinction retrieval. In this study, to improve currently used $\boldsymbol{S_{aer}}$ in CALIOP level 2 algorithm, $\boldsymbol{S_{aer}}$ is determined from CALIOP by using AOD from AERONET and MODIS-Aqua as a constraint without any assumption. Using 4-year measurements (2006-2010) of elastic-backscatter lidar and SKYNET sun/sky radiometer at Seoul National University of Seoul, Korea, mean lidar ratio is estimated to be 61.7±16.5 sr. Lidar ratios are also retrieved using ground-based lidar and AERONET sun/sky radiometer during Distributed Regional Aerosol Gridded Observation Networks (DRAGON) Northeast Asia Campaign 2012. Mean lidar ratios at Seoul and Osaka were retrieved as 65.41±21.42 sr and 65.04±20.62 sr, respectively. Mean lidar ratios from Seoul and Osaka, which are metropolitan cities in East Asia, are almost same and comparable to the lidar ratio for pollution used in CALIOP algorithm.

Dust aerosol is easily recognized from depolarization ratio measurements due to its non-spherical shape. *Burton et al.* [2013] reported that aerosol type classification for dust is the most accurate in CALIOP algorithm. For this reason, lidar ratios are retrieved mainly focused on dust

aerosol and compared other studies and CALIOP Level 2 Product. The lidar ratio for dust conditions are estimated to be 51.7±13.7 sr using 4-year measurements of elastic-backscatter lidar and SKYNET sun/sky radiometer at Seoul National University of Seoul, Korea. During DRAGON 2012 NE Asia campaign, lidar ratio for dust event on 27-28 April 2012 in Seoul is retrieved as 48.02±9.38 sr from elastic-backscatter lidar and AERONET sun/sky radiometer. From a synergy of CALIOP and AERONET, lidar ratio for Saharan/Arabian dust is derived to be 47.45±16.52 sr. Lastly, using CALIOP and MODIS measurements together, dust lidar ratio is retrieved as 45.50±15.17 sr. Especially, the mean lidar ratio for Asian dust is estimated much larger as 53.04±18.30 sr. All the lidar ratios for dust aerosol retrieved in this study using AOD constrained method show larger values than currently used lidar ratio for dust in CALIOP algorithm (40 sr), which suggests that dust lidar ratio in CALIOP algorithm is underestimated and needs to be increased.

Keywords: CALIOP, aerosol optical depth, aerosol type, lidar ratio, MODIS

Student Number: 2005-20504

TABLE OF CONTENTS

LIST OF FIGURES

LIST OF TABLES

CHAPTER 1. INTRODUTION

1.1. Background and motivation

1.1.1. The importance of aerosol vertical distribution on radiative forcing

Aerosols continue to contribute one of the largest uncertainties to estimate and interpret of the Earth's changing energy budget. Aerosol-climate feedbacks occur mainly through changes in the source strength of natural aerosols or changes in the sink efficiency of natural and anthropogenic aerosols; a limited number of modelling studies have bracketed the feedback parameter within ±0.2 W m^{-2} $°C^{-1}$ with low confidence [*Boucher et al.*, 2013]. The impact of aerosols on Earth' radiation budget mainly depends on their optical properties and horizontal/vertical distribution. The vertical distribution of aerosols, especially light-absorbing aerosol, is very important because they can modify the radiative heating in the atmosphere [e.g., *Won et al.*, 2004; *Ramanathan et al.*, 2007; *Ramana et al.*, 2010].

Lidar (light detection and ranging) is a useful instrument, which can provide vertical distribution of aerosols to estimate aerosol direct radiative

forcing and atmospheric heating rate. In June 2006, the Cloud-Aerosol Lidar and Infrared Pathfinder Satellite Observation (CALIPSO) satellite which contains space-borne lidar system, the Cloud-Aerosol Lidar with Orthogonal Polarization (CALIOP), has been launched [*Winker et al.*, 2003; *Vaughan et al.*, 2009]. Therefore, it is a great opportunity for us to estimate aerosol direct radiative forcing and atmospheric heating rate using CALIOP measurements on a global scale. *Huang et al.* [2009] used CALIOP data to estimate dust aerosol radiative forcing and atmospheric heating rate over the Taklimakan Desert in Northwestern China. On a global scale, however, the estimation of aerosol radiative forcing using observed aerosol profile data is still insufficient.

1.1.2. Aerosol extinction retrieval from CALIOP measurements

CALIOP is a space-borne lidar system onboard CALIPSO. CALIOP is an elastic lidar system having three channels: two channels measuring orthogonally polarized components of backscatter at 532 nm and one measuring total backscatter at 1064 nm. The CALIOP data products are divided into level 1, level 2 and level 3. The CALIOP level 1 product is calibrated, range-corrected lidar signal and the CALIOP level 2 aerosol product is intended product for use by science community, including

aerosol extinction profiles and other optical properties. The CALIOP level 3 aerosol product reports monthly mean profiles of aerosol optical properties on a uniform spatial grid. The CALIOP level 2 extinction retrieval algorithm has three steps. First, it detects cloud and aerosol layers from level 1 dataset. Then it classifies detected layers by type using several indicators such as backscatter intensity, depolarization ratio, surface (region) type. The last step of the algorithm is performing extinction retrievals for the layers which are determined at step 1 [*Winker et al.*, 2009; *Omar et al.*, 2009; *Young and Vaughan*, 2009]. The CALIOP data flow within the level 2 data processing system is shown in Figure 1.1.

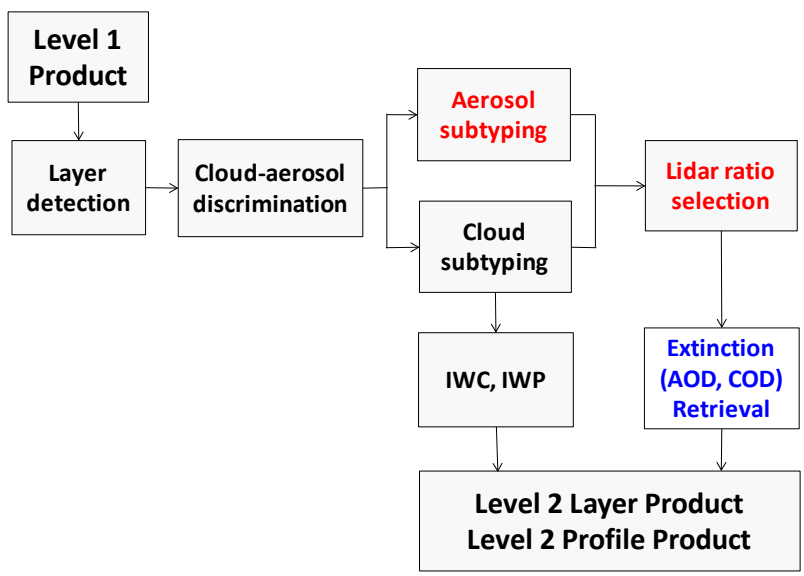

Figure 1.1. A schematic diagram of the CALIOP operational data process to produce the level 2 products (http://www-calipso.larc.nasa.gov/).

The expected error for CALIOP aerosol optical depth (AOD) is ± (0.05 + 40%) over both land and ocean [*Winker et al.*, 2009; *Omar et al.*, 2013]. The relative error of CALIOP AOD is quite large compared to the expected error for MODIS (Moderate Resolution Imaging Spectroradiometer) AOD of ± (0.05 + 15%) over land and ± (0.03 + 5%) over ocean [Remer et al., 2005]. The main sources of uncertainties in the CALIOP extinction retrieval are errors in (1) instrument calibration, (2) feature detection, (3) identification of feature types, (4) multiple-scattering function, and (5) specification of the corresponding lidar ratios [*Winker et al.*, 2009; *Omar et al.*, 2013; *Young et al.*, 2013]. Because values for lidar ratios can vary over a large range, even for a particular feature type, lidar ratio is the largest source of uncertainty in the retrievals [*Young et al.*, 2013]. Omar et al. [2009] declared that the goal is to constrain the uncertainty in the lidar ratio to no more than 30%. However, the uncertainties in the lidar ratio are known to be larger than 30%. The currently used lidar ratios in CALIOP algorithm for each aerosol type and their uncertainties are shown in Table 1.1. Moreover, errors in identification of feature types are directly related with uncertainty in the lidar ratio, thus an effect of the lidar ratios on the accuracy of CALIOP AOD is significant.

Table 1.1. Lidar ratios for the aerosol types identified in the version 3 CALIOP algorithm, together with the one standard deviation uncertainties and relative uncertainties [*Young et al.*, 2013].

type	Lidar ratio (sr)	Uncertainty (sr)	Relative uncertainty (%)
Clean Marine	20.0	6.0	30
Dust	40.0	20.0	50
Clean Continental	35.0	15.8	45
Polluted Continental	70.0	24.5	35
Polluted Dust	55.0	22.0	40
Biomass Burning	70.0	28.0	40

1.1.3. Determination of aerosol lidar ratio (S_{aer}) for the elastic lidar

Elastic backscatter lidars are commonly used to derive the aerosol extinction profile using lidar equation [*Klett*, 1981; *Fernald*, 1984]. However, the lidar equation has two unknown variables; aerosol extinction and backscatter coefficients. To solve ill-posed problem of the elastic lidar equation, the aerosol extinction-to-backscatter ratio or aerosol lidar ratio (hereafter, referred to as $\boldsymbol{S_{aer}}$) should be determined. $\boldsymbol{S_{aer}}$ is a key parameter, which is a function of aerosol physical and chemical properties such as aerosol size, shape, refractive index and chemical composition. It is frequently either assumed or inferred from additional measurements.

Various techniques have been implemented to avoid the assumption of $\boldsymbol{S_{aer}}$. The Raman lidar technique [*Ansmann et al.*, 1990] and the high spectral resolution lidar (HSRL) technique [*Shipley et al.*, 1983] can derive aerosol extinction profiles needless to assume the $\boldsymbol{S_{aer}}$ by separating aerosol returns from molecular returns. The elastic lidar, however, cannot measure or derive the aerosol $\boldsymbol{S_{aer}}$ by itself. So, additional measurements are needed to determine $\boldsymbol{S_{aer}}$ for the elastic lidar. *Doherty et al.* [1999] calculate $\boldsymbol{S_{aer}}$ from in-situ measurements. They used modified Nephelometer to measure aerosol scattering coefficient and 180° backscatter coefficient and particle soot absorption

photometer (PSAP) to obtain aerosol absorption coefficient. *Dubovik et al.* [2006] and *McPherson et al.* [2010] used aerosol phase function, and other aerosol optical properties from AERONET (Aerosol Robotic Network) sun/sky radiometer measurements to derive $\boldsymbol{S_{aer}}$. *Kaufman et al.* [2003] and *Leon et al.* [2003] used similar way to calculate $\boldsymbol{S_{aer}}$, but they used aerosol models with one fine and one coarse mode and MODIS (Moderate Resolution Imaging Spectroradiometer) measurements instead of AERONET. The CALIPSO lidar ratio selection algorithm also uses aerosol models [*Omar et al.*, 2009], which based on cluster analysis of a multiyear AERONET dataset [*Omar et al.*, 2005].

Welton et al. [2000] used an independently measured AOD with MPL (Micro Pulse Lidar) measurement to determine $\boldsymbol{S_{aer}}$. They used AOD as a constraint to produce the aerosol extinction profiles. The advantage of this technique is that information of $\boldsymbol{S_{aer}}$ is not required. The similar technique was used by *Burton et al.* [2010]. They retrieved aerosol extinction profiles from CALIPSO lidar measurements using MODIS derived AOD as a constraint to determine $\boldsymbol{S_{aer}}$ and evaluated this result by comparing with coincident measurement of airborne HSRL. The comparison of 37 profiles shows that the resulting retrievals agree well with HSRL measurements within $\pm 20\%$.

1.2. Objectives of this study

CALIOP is a unique instrument that can provide aerosol extinction profile and AOD on a global scale for both day and night. However, the uncertainty in CALIOP AOD is relatively high compared to other passive sensors such as MODIS, POLDER (Polarization and Directionality of the Earth's Reflectances), MERIS (Medium Resolution Imaging Spectrometer), and SEVIRI (Spinning Enhanced Visible and Infrared Imager). In order to assess the uncertainty in CALIOP AOD and investigate potential sources of uncertainty, CALIOP AOD was compared with MODIS-Aqua (hereafter referred to MODIS) AOD over ocean by separating aerosol type defined in CALIOP level 2 algorithm. MODIS AOD was chosen because expected error over ocean (± 0.03 ± 5%) is much less than the expected error for CALIOP AOD (± 0.05 ± 40%). Moreover, as part of the A-train satellite constellation, CALIPSO and Aqua can provide numerous collocated datasets to compare with. AOD from CALIOP Version 3.01 Aerosol Profile Products has been compared with AOD from MODIS-Aqua Collection 5.1 MYD04-L2 data over the ocean by considering aerosol subtypes classified by the CALIOP scene classification algorithms [*Omar et al.,* 2009; Winker et al., 2009].

Potential sources for the discrepancies in AOD between the two sensors are discussed for each aerosol type.

Because uncertainty in S_{aer} is the largest source of uncertainty in the CALIOP AOD, It is desirable to improve S_{aer} values used in CALIOP algorithm to retrieve accurate AOD (or aerosol extinction). Current CALIOP level 2 algorithm uses pre-determined $\boldsymbol{S_{aer}}$ for classified aerosol types. However, not only using single values of $\boldsymbol{S_{aer}}$ for each aerosol type but also aerosol classification algorithm could be sources of uncertainties in aerosol extinction retrieval. In this study, to improve currently used $\boldsymbol{S_{aer}}$ in CALIOP level 2 algorithm, $\boldsymbol{S_{aer}}$ is determined from CALIOP by using AOD from AERONET and MODIS-Aqua as a constraint without any assumption. Then, the characteristics of $\boldsymbol{S_{aer}}$ will be discussed for each aerosol type.

CHAPTER 2.
ASSESSMENT OF CALIOP AOD BY COMPARING WITH MODIS

2.1. Introduction

CALIOP onboard CALIPSO satellite is a space-borne lidar system that can measure the vertical structure of aerosol and cloud distributions on a global scale [*Winker et al.*, 2007, 2009]. Several studies validating CALIOP with ground-based measurements have shown reasonable agreements for the CALIOP Level 1 product with ground-based lidar [e.g., *Chazette et al.*, 2010; Kim et al., 2008, 2011].

The CALIOP Level 2 product, on the other hand, shows a much larger variation when compared with ground-based or airborne measurements. *Mielonen et al.* [2009] have found that 70% of the CALIOP Level 2 aerosol subtypes are in agreement with the AERONET-derived aerosol types. *Schuster et al.* [2012] found a CALIPSO 532 nm AOD bias of -13%, corresponding to an absolute bias of -0.029 relative to AERONET. However, the relative and absolute biases are reduced to -3% and -0.005, respectively, when they exclude dust aerosols. *Burton et al.* [2013] showed

that 62% of CALIOP ‘clean marine’, 54% of ‘polluted continental’, and 80% of ‘dust’ agree with airborne HSRL-1 classification results. However, agreement is poorer for CALIOP smoke (13%) and polluted dust (35%). *Kacenelenbogen et al.* [2011] have shown that CALIOP AOD is a factor of two lower than MODIS, POLDER, airborne HSRL and AERONET. *Bréon et al.* [2011] found that CALIOP-derived AODs show little resemblance to AERONET-derived AODs, with a root-mean-square (RMS) difference of 0.404 at 500 nm. *Omar et al.* [2013] showed that CALIOP AODs are lower than AERONET AOD, especially at low AODs. Furthermore, they reported that the median of relative AOD difference between CALIOP and AERONET (500 nm) is 25% of AERONET AOD for AOD > 0.1. *Misra et al.* [2012] reported the mean backscatter difference ranges from -0.004 to 0.023 km-1 sr-1 by comparing CALIOP Level 2 aerosol backscatter profile with ground-based Micro Pulse Lidar Network (MPL-NET) measurements.

Comparison of CALIOP AOD with ground-based instruments, such as sunphotometer and lidar, however, is more limited than space-borne passive sensors, such as MODIS, POLDER, MERIS, and SEVIRI. This is because CALIOP has a very narrow field of view (FOV) that corresponds to 70 m of the laser footprint at the Earth’s surface. Passive sensors have

much larger spatial resolution of up to several square kilometers. CALIOP can cover only 0.2% of the Earth's surface during one repeat cycle [*Kahn et al.*, 2008], thus making it difficult to find collocated data pairs between CALIOP and ground-based measurements [*Omar et al.*, 2013].

An alternative way for evaluating the accuracy CALIOP AOD is by comparing it with AOD from MODIS-Aqua. As part of the A-train satellite constellation, CALIPSO and Aqua satellites fly in close proximity. CALIPSO follows Aqua by 1-2 minutes providing nearly simultaneous and collocated observations. The expected error for CALIOP AOD is ±0.05 ± 40% over both land and ocean [*Winker et al.*, 2009; *Omar et al.*, 2013]. The MODIS AOD retrieval has less uncertainties, with expected errors of ±0.03 ± 5% over ocean and ±0.05 ± 15% over land [*Remer et al.*, 2005; *Levy et al.*, 2010]. *Kittaka et al.* [2011] reported that the CALIOP Version 2 product showed only a small global mean bias relative to MODIS Collection 5 for the period of June 2006 through August 2008, though the regional biases are large and vary with season. Global-mean AODs of CALIOP and MODIS over ocean for JJA (June to August) reported by *Kittaka et al.* [2011] are 0.076 and 0.083, respectively. *Oo and Holz* [2011] showed a mean AOD bias between MODIS and CALIOP of ~0.064 over the ocean using quality controlled and cloud screened data for

single aerosol layers. *Redemann et al.* [2012] found a RMS difference of 0.1 between CALIOP and MODIS AODs using quality-controlled and cloud screened data. However, none of these studies have compared AODs from the two sensors for different aerosol types.

In order to retrieve the aerosol extinction coefficient (or its column-integrated value, AOD) from CALIOP measurements, the aerosol type is determined *a priori* so that a type-specific lidar ratio (i.e., extinction-to-backscatter ratio) can be assigned to the aerosol layer. The lidar ratio is an essential parameter for aerosol extinction coefficient retrievals from elastic lidar measurements [*Fernald*, 1984]. Errors in the *a priori* prescription of this value can thus induce large errors in the retrieved AOD. Therefore, when validating CALIOP AOD using other instruments, errors associated with aerosol type or 'lidar ratio' should be considered. The validation of CALIOP AOD by segregating aerosol type can lead to an improvement of the accuracy of aerosol type classification and lidar ratio determination in CALIOP algorithm.

The goal of this study is to evaluate CALIOP AOD (Level 2 5-km Aerosol Product, Version 3.01) over ocean by comparing with collocated MODIS AOD (MYD04-L2 product, Collection 5.1). In order to figure out uncertainties in CALIOP AOD associated with aerosol type classification

and pre-determined lidar ratio, AODs from the two sensors are compared by considering aerosol subtypes classified by the CALIOP scene classification algorithms [*Omar et al.*, 2009; *Winker et al.*, 2009]. Potential sources for the discrepancies in AOD between the two sensors are discussed for each aerosol type.

2.2. Instruments and data

The A-Train constellation of satellites are Sun synchronous, near-polar orbiting satellites, which cover almost the whole globe (82°S - 82°N) from an altitude of ~700 km above the surface of the Earth and an orbital inclination of 98°. The A-train satellites cross the equator in ascending node at around 13:30 local solar time [*L'Ecuyer and Jiang*, 2010]. CALIPSO lags Aqua by one to two minutes. Thus, both satellites observe the same target within two minutes.

CALIOP uses a Nd:YAG laser that generates co-aligned pulses at 532 nm and 1064 nm, with a repetition frequency of 20.16 Hz producing 335 m of horizontal resolution along the ground track [*Winker et al.*, 2009]. Outgoing 532-nm pulses are linearly-polarized. Orthogonal polarizations of backscattered signals are measured to determine the linear

depolarization ratio, which provides information for determining the shape (spherical or nonspherical) of aerosol and cloud particles. The sampling vertical resolution of CALIOP for the 532 nm channel is 30 m from the surface to 8.2 km above mean sea level. The spatial resolutions of the CALIOP downlinked data throughout the atmosphere can be found in *Winker et al.* [*2009*].

CALIOP Level 2 algorithms consist of the following three major steps: (1) the selective iterative boundary locater (SIBYL) [*Vaughan et al.*, 2009], (2) the scene classification algorithm (SCA) [*Liu et al*., 2009; *Omar et al.*, 2009], and (3) the hybrid extinction retrieval algorithm (HERA) [*Winker et al.*, 2009, *Young and Vaughan*, 2009]. HERA is an iterative algorithm that retrieves aerosol extinction profiles for aerosol layers detected by SIBYL, using the lidar ratio determined a priori by SCA. The aerosol type classification is an essential step in CALIOP algorithm and has a direct impact on aerosol retrievals, since the lidar ratio is determined by aerosol type. The algorithm for the aerosol type classification is described in *Omar et al.* [2009].

MODIS measures radiance at 36 spectral bands in wavelengths ranging from 0.4 μm to 14.4 μm using calibrated reflectance data from

seven bands (0.47, 0.55, 0.66, 0.86, 1.24, 1.6 and 2.13 μm) to retrieve AOD. The spatial resolution is 250 m × 250 m for 0.66 and 0.86 μm, 500 m × 500 m for 0.47, 0.55, 1.24, 1.6, and 2.13 μm. During the MODIS retrieval, if all 20 × 20 pixels in a 10 × 10 km box are identified as "ocean", the ocean algorithm is implemented [*Remer et al.*, 2005]. After removing contaminated pixels, including cloud, sediment and glint masks, MODIS inversions attempt to minimize the difference between the observed spectral radiance in six MODIS channels and radiance pre-computed in a lookup table. The algorithm selects the best fit to the observed reflectance and reports AOD and other aerosol properties [*Levy et al.*, 2005; *Remer et al.*, 2005].

The data used in this study are CALIOP Level 2 aerosol layer and profile products (Version 3.01) and MODIS Level 2 aerosol product (Collection 5.1) over ocean, both from June 2006 to December 2010. 'Column_Optical_Depth_Aerosols_532' for CALIOP and 'Effective_Optical_Depth_Average_Ocean' at 550 nm for MODIS are used for the AOD comparison. CALIOP AODs in the Level 2 products are reported at a horizontal resolution of 5 km for Version 3. Horizontal resolution of MODIS AOD is 10 × 10 km at nadir. MODIS AODs over the land were not evaluated in this study because of higher uncertainty [*Remer*

et al., 2005; *Levy et al.*, 2010]. CALIOP provides data for both day and night, whereas MODIS AOD is available only for daytime. Therefore, comparisons of AOD between CALIOP and MODIS were made only for daytime data.

The uncertainty in CALIOP AOD can be caused by instrument calibration and normalization error, as well as errors in cloud-aerosol discrimination, layer boundary detection, multiple scattering assumption, and *a priori* lidar ratio [*Winker et al.*, 2009]. In many instances, the lidar ratio is one of the most significant sources of uncertainty in CALIOP AOD, with an uncertainty of 30-50%, depending on aerosol type [*Young et al.*, 2013]. Sensitivity tests to evaluate MODIS error sources were proposed by *Tanré et al.* [1997]. They report that the main sources of error in MODIS AOD are surface reflection, sensor calibration, contamination by glint, water-leaving radiance, and uncertainties involved in the lookup table such as aerosol size distribution, refractive index, and single scattering albedo.

AOD is reported at wavelengths of 532 nm and 550 nm for CALIOP and MODIS, respectively. Discrepancies in AOD due to different wavelengths can be approximated using an Ångström exponent (α) that

represents wavelength dependence of AOD. α is an indicator of effective aerosol particle size; $\alpha < 1$ indicates coarse-mode aerosols, such as dust and sea salt, and $\alpha \geq 2$ indicates fine-mode particles commonly associated with urban pollution and biomass burning [*Eck et al.*, 1999; *Schuster et al.*, 2006]. The difference between AOD at 532 nm and 550 nm increases as Ångström exponent increases and the typical difference is about 3% for the Ångström exponent of 1 and 6% for the Ångström exponent of 2. However, this difference is considered relatively small compared to uncertainties in AOD of both CALIOP [*Winker et al.*, 2009] and MODIS [*Remer et al.*, 2005], and, therefore, will be neglected in this study.

2.3. Data selection

The method used in this study to define spatial and temporal coincidence between CALIOP and MODIS for AOD comparison is nearly the same as that of *Kittaka et al.* [2011]. First, MODIS 10-km pixels whose centers are located less than 5 km from the CALIOP track are selected. Corresponding CALIOP data points located closer than 10 km from the center of the MODIS pixel were defined as collocated data points. Each selected MODIS pixel thus had three to five collocated CALIOP data

points. The collocated pairs used for the comparison are then MODIS pixel and the averaged value of these CALIOP data points. Figure 2.1 is a schematic diagram depicting a collocated MODIS pixel and CALIOP data points.

CALIOP AOD was obtained by vertical integration of aerosol extinction coefficient at 532 nm from the aerosol profile products. Since CALIOP identifies unique overlapping layers in the vertical, only AOD records with layers of single aerosol type throughout the column were used in the study. This was done to isolate specific aerosol types for unique one-to-one comparisons of single layer AOD with MODIS observations. ‘Feature_Classification_Flags’ of the CALIOP Level 2 layer products were used to determine the aerosol subtype. After filtering for single aerosol layers, approximately 20% of the CALIOP profiles were rejected.

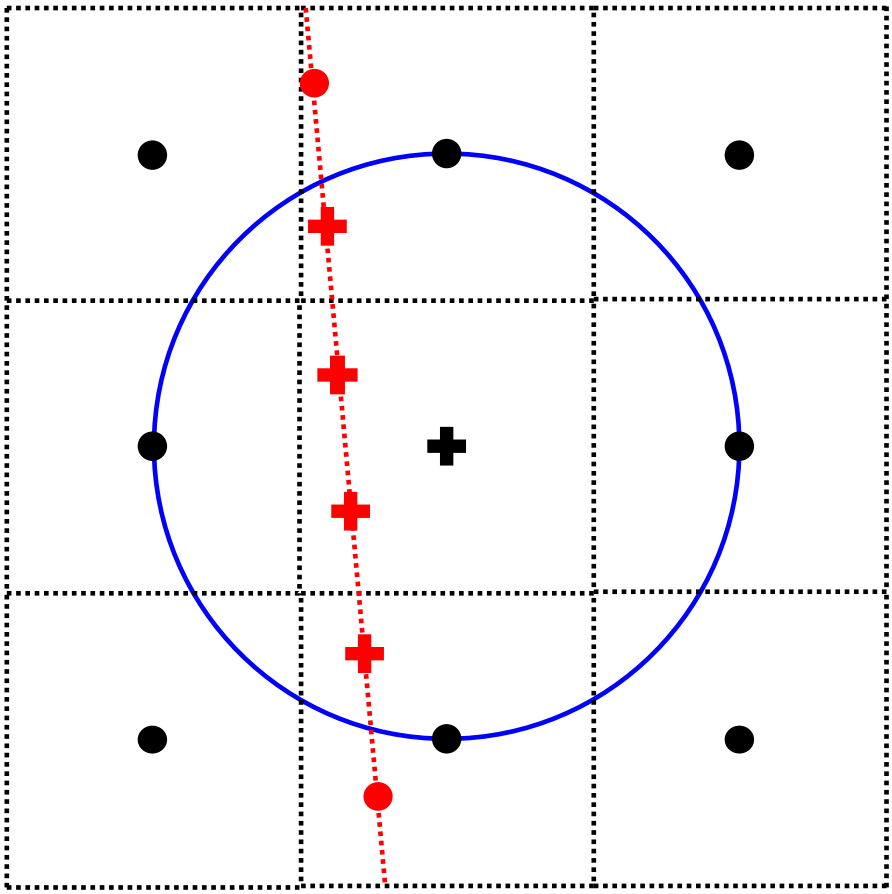

Figure 2.1. A schematic diagram representing collocated MODIS pixel (black crosshair) and CALIOP data points (red crosshair). Black dotted squares and red dotted line represent MODIS 10 × 10 km pixels and CALIPSO track, respectively. Black dots and crosses are the centers of MODIS pixels, and red dots and cross are CALIOP data points which have 5 km horizontal resolution. Blue circle shows the area covered within a radius of 10 km from the center of the MODIS pixel (black crosshair).

Cloud screening was independently applied for both CALIOP and MODIS data. CALIOP Level 2 data provides cloud optical depth (COD) and stratospheric optical depth (SOD). If any of these two values was not equal to zero, the collocated data pairs were not used. For the case of MODIS, “Cloud_Mask_QA” which represents cloud fraction is used to eliminate cloud contamination [*Ackerman et al.,* 1998]. The cloud fraction is determined using specific numerical thresholds of 1 km cloud mask pixels that meet certain criteria within the 10 × 10 km aerosol retrieval area. Only 10 × 10 km grid cells with less than 30% cloudy pixels were used in this study.

If optically-thick aerosol layers exist, the emitted laser sometimes cannot penetrate the layers, and becomes completely attenuated before reaching the earth’s surface. Such profiles are typically characterized by the failure of the lidar signal to detect the surface. Since in these cases, AODs from CALIOP are unreliable, fully-attenuated profiles are excluded. To remove these profiles, “Lidar_Surface_Elevation” of CALIOP Level 2 products, which represents an altitude of surface elevation detected by lidar return signal, was used. If CALIOP detects the Earth’s surface, then we assume that most of the layers in the atmosphere with an integrated attenuated backscatter above CALIOP’s detection threshold have also

been detected and included in the column AOD calculation. The profiles can be screened using a threshold integrated attenuated backscatter (e.g., 0.01 sr in *Kittaka et al.* [2011]) or the base altitude of the lowest layer (e.g., 250 m in *Campbell et al.* [2012, 2013]). These Kittaka and Campbell screening rubrics would reject only 2.6% and 7.8% of the collocated pairs used in this study, respectively. For biomass burning layers, however, 96.1% of our screened data are rejected by Campbell screening criteria because most of the smoke layers detected by CALIOP are elevated above 250 m. Contrary to this study, it should be noted that multiple aerosol types within a common layer column were included in *Campbell et al.* [2012, 2013].

The Extinction Quality Control (QC) flag and Cloud-Aerosol Discrimination (CAD) score of CALIOP Level 2 data files are also considered. Extinction QC is reported for each aerosol layer for which extinction was solved. If an aerosol layer is elevated, vertically isolated, and clear-air signals are detected above and below the layer, the extinction profile is solved using two-way transmittance [*Young and Vaughan*, 2009]. This is the so-called ‘constrained retrieval’. CALIOP algorithms employ an iterative solution to the lidar equation described in *Young and Vaughan* [2009] for unconstrained retrievals. However, sometimes the solutions for extinction do not converge with respect to the *a priori* lidar ratio selected.

In such cases, the CALIOP algorithm changes (by increasing or decreasing) the lidar ratio until the solution converges. In this study, the Extinction QC equals to 1 (constrained method using two-way transmittance) and 0 (unconstrained method without changing lidar ratio) were used. The sign of the CAD score, ranging between -100 (definitely aerosol) and 100 (definitely cloud), indicates confidence in the layer feature type. Positive values signify clouds, and negative values signify aerosols. CAD scores less than -80 (i.e., high confidence aerosol layers) are used for this study. 'Quality_Assurance_Ocean' is quality flag for MODIS ocean AOD discussed in *Hubanks* [2012]. No confidence MODIS ocean AODs denoted by QA flag 0 are rejected.

2.4. Results and discussion

Using the data selection method described above, nearly two million collocated data pairs were compared. Table 2.1 and Figure 2.2 show the results of the comparison for six different types of aerosol (clean marine, dust, polluted dust, polluted continental, biomass burning, and clean continental) classified by the CALIOP aerosol classification and lidar ratio selection algorithm [*Omar et al.*, 2009]. The mean AOD for all collocated

data pairs is 0.068 for CALIOP and 0.111 for MODIS, i.e., the mean MODIS AOD is 63% larger than CALIOP AOD. These mean values are not representative global mean AODs of the two sensors, because multiple layers with different aerosol types are not included. The difference reported in this study is larger than values reported in *Kittaka et al.* [2011], but closer to the biases reported by *Oo and Holz* [2011] and *Redemann et al.* [2012].

The discrepancies of AOD between the two sensors vary for the aerosol types reported by CALIOP. For most, mean MODIS AOD is higher than mean CALIOP AOD. For polluted continental and polluted dust, however, mean CALIOP AOD is higher. Large differences between MODIS and CALIOP were found for clean marine (mean MODIS AOD is 96% higher) and biomass burning (mean MODIS AOD 102% higher). A small bias and high correlation was found, though, for dust and polluted dust. *Schuster et al.* [2012] also reported a relatively large AOD bias for clean marine, biomass burning, and clean continental when comparing CALIOP and AERONET measurements. There are very few (less 0.031%) data pairs of the clean continental aerosol type. All of these are a result of uncertainties in determination of land and ocean borders for both CALIOP and MODIS, since the CALIOP aerosol type classification algorithm does

not allow clean continental aerosols over the ocean [*Omar et al.*, 2009]. We therefore did not consider the clean continental type for this study.

Table 2.1. Statistics of the comparison of CALIOP and MODIS AOD showing the mean ± standard deviation of the AOD, mean bias, relative(percent) bias, root-mean-square deviation (RMSD), correlation (R), and number of data pairs.

type	Mean±Standard Deviation		Mean bias	Relative bias (%)	RMSD	R	No. of data
	MODIS	CALIOP					
All	0.111±0.079	0.068±0.073	0.044	64	0.080	0.61	1808587
Clean Marine	0.110±0.064	0.056±0.038	0.053	95	0.072	0.65	1522590
Dust	0.236±0.179	0.209±0.217	0.027	12	0.139	0.78	49150
Polluted Continental	0.057±0.052	0.080±0.052	-0.023	-29	0.069	0.23	55295
Polluted Dust	0.105±0.098	0.123±0.132	-0.019	-15	0.107	0.62	173836
Biomass Burning	0.281±0.232	0.139±0.157	0.141	102	0.254	0.48	6614

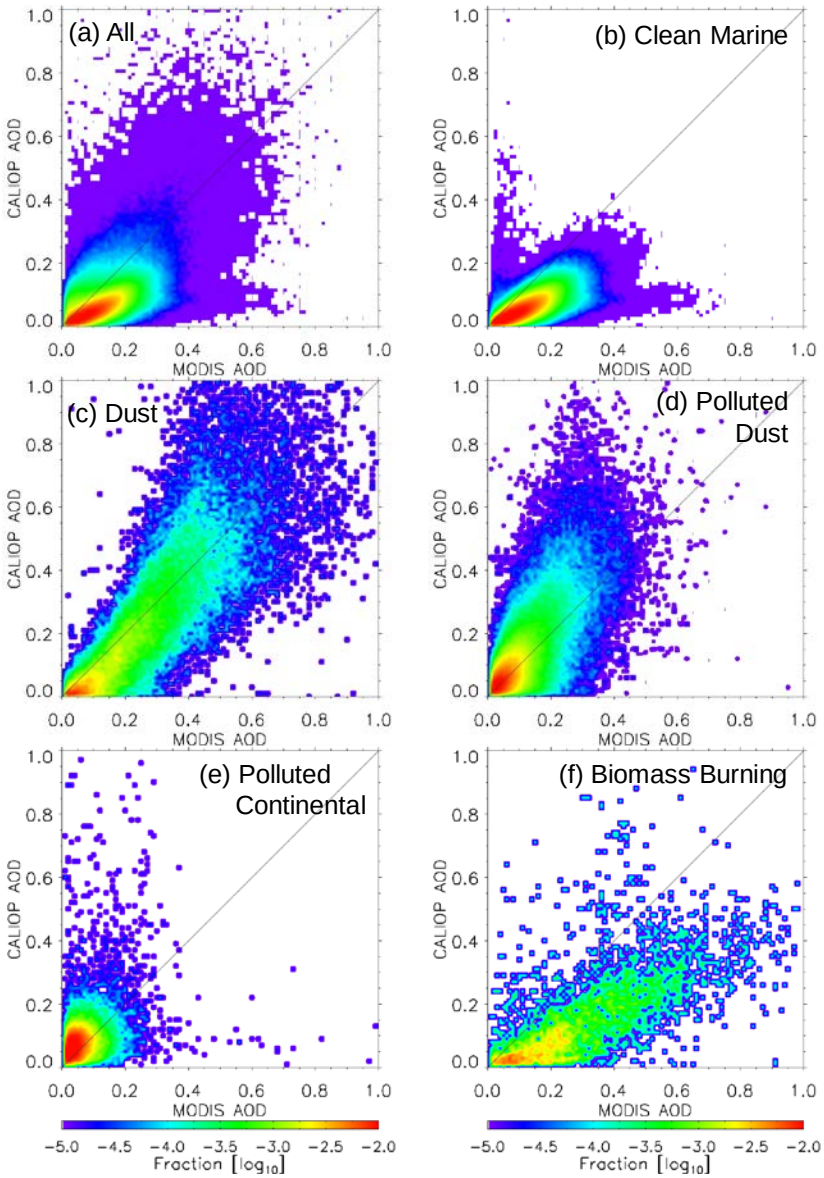

Figure 2.2. Frequency distributions of collocated CALIOP and MODIS AODs over ocean from June 2006 to December 2010 for single aerosol layers under a cloud-free condition: (a) all aerosol types, (b) clean marine, (c) dust, (d) polluted dust, (e) polluted continental, and (f) biomass burning aerosols.

2.4.1. Clean marine

While all other aerosol types are of continental origin, clean marine originates presumably in the ocean. It is the most dominant type of aerosol over the ocean, accounting for 84% of total aerosols observed (Table 2.1). A large number of these collocated data pairs occur over the remote oceans, whereas the occurrences of other aerosol types are mostly near shorelines.

The global distribution and meridional variation of AOD difference between the two instruments for clean marine is shown in Figures 2.3a and 2.3b, respectively. Differences are relatively large in the inter-tropical convergence zone (ITCZ) and sub-polar low region, and low in sub-tropical high region. Figure 2.4 shows the difference in the MODIS-CALIOP AOD and zonal mean wind speeds from NCEP/NCAR reanalysis data at sea surface level. The difference in AOD increases where surface wind is strong, especially for the Southern Hemisphere. Several studies have reported the enhancement of AOD under strong surface wind over remote oceans. *Anderson et al.* [2012] found a linear regression of τ_{bias} = 0.010 v – 0.024 after filtering the cloud fraction greater than 70%, where τ_{bias} is MODIS bias, and v is wind speed in m s^{-1}. *Smirnov et al.* [2012] showed that the slope of the linear regression between ship-based AOD

and wind speed (in m s^{-1}) is ~0.004-0.005. *O'Dowd et al.* [2010] reported a relation between the open ocean MODIS-derived AOD at 550nm and wind speed that follows a power-law, with the exponent ranging from 0.72 to 2.47 for a wind speed range of 2-18 m s^{-1}. In this study, the linear regressions between AOD and surface wind speed are τ_{CAL} = 0.003 v + 0.045 and τ_{MOD} = 0.008 v + 0.073, where v is wind speed (m s^{-1}), τ_{CAL} and τ_{MOD} are CALIOP and MODIS AOD, respectively, for the Southern Hemisphere. The zonal mean CALIOP and MODIS AODs have been averaged in 2.5 latitude degrees for comparison with the NCEP/NCAR reanalysis wind data.

CALIOP retrievals of extinction profile are not much affected by wind speed or surface reflectance/brightness, while the MODIS AOD retrieval is. Even though the MODIS algorithm takes into account sea surface reflectance under strong wind speed conditions by calculating the reflection of the sea surface from the rough ocean model [*Tanré et al.*, 1997], Figure 2.4 shows an overestimation of MODIS AOD caused by sea surface reflection over the rough ocean still exists. In the northern hemisphere, on the other hand, the difference of AOD and surface wind speed are not as strongly correlated. Although wind speeds in the Northern Hemisphere are relatively weak near the surface, the difference in AOD is

still large. We attribute this to the potential misclassification of continental aerosols as clean marine, thus resulting in lower values of CALIOP AOD due to offsets in their corresponding *a priori* lidar ratios.

The difference in clean marine AOD between the two sensors varies with geographical region (Figure 2.3b). Large differences occur along the coasts of South and East Asia and the Mid-Atlantic Ocean near Africa, where the transport of aerosol particles from the adjacent continents frequently occurs. In these regions, biomass burning and polluted continental are difficult to distinguish from clean marine using the two direct measurements CALIOP makes: attenuated backscatter and volume depolarization ratio. The CALIOP algorithm defines clean marine as optically thick layers consisting of spherical particles and polluted continental as optically thin layers with some non-spherical particles in the marine boundary layer [*Omar et al.*, 2009]. This classification might not be suitable for cases in the ocean close to aerosol source regions. Among the six aerosol types, clean marine has the smallest lidar ratio (20 sr), whereas biomass burning and polluted continental have the largest (70 sr). Therefore, misclassification of biomass burning or polluted continental as clean marine significantly depresses CALIOP AOD and increases the AOD difference between the two sensors.

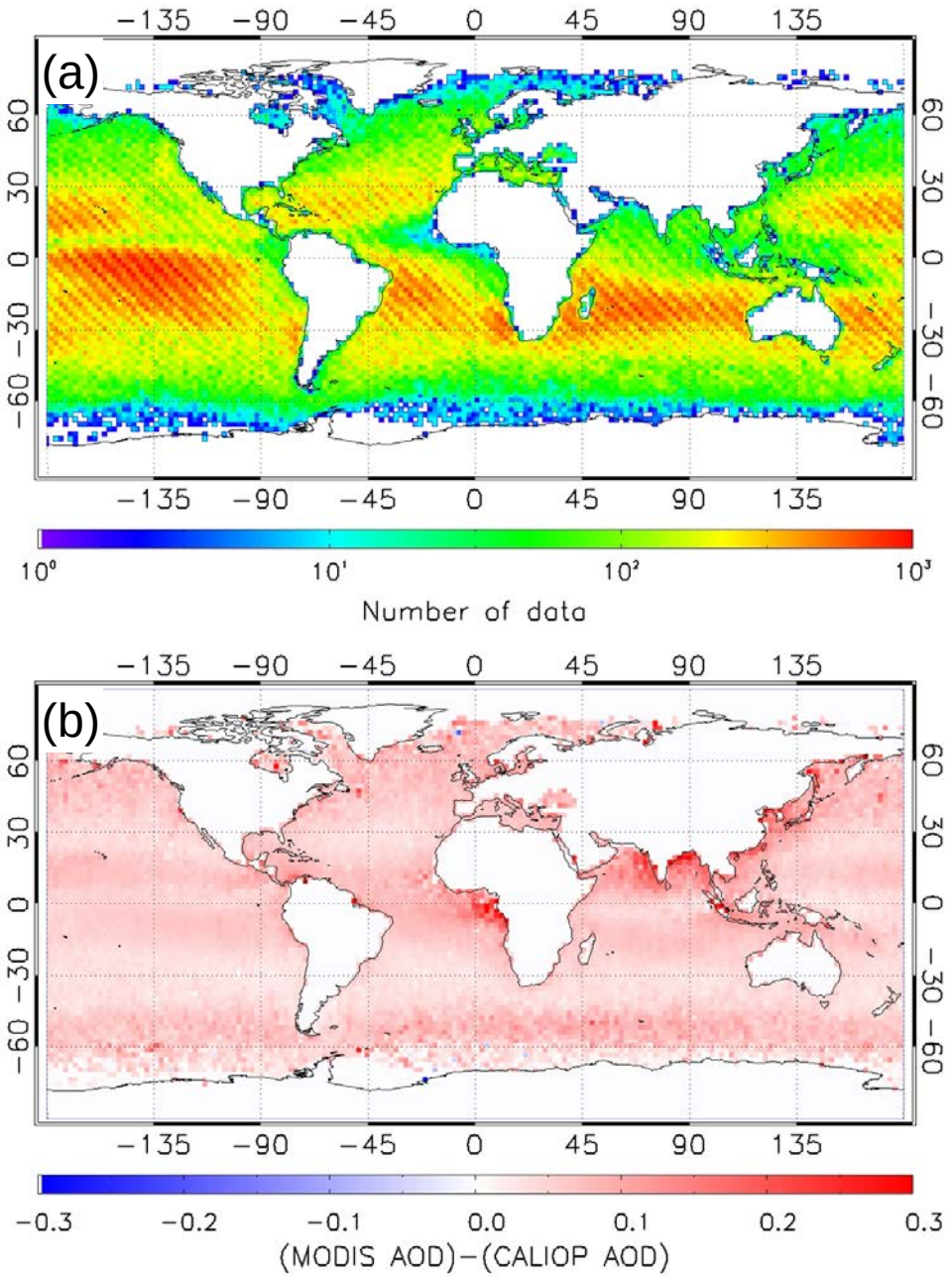

Figure 2.3. Global distribution of (a) the number of collocated data pairs and (b) difference between CALIOP and MODIS AODs for clean marine.

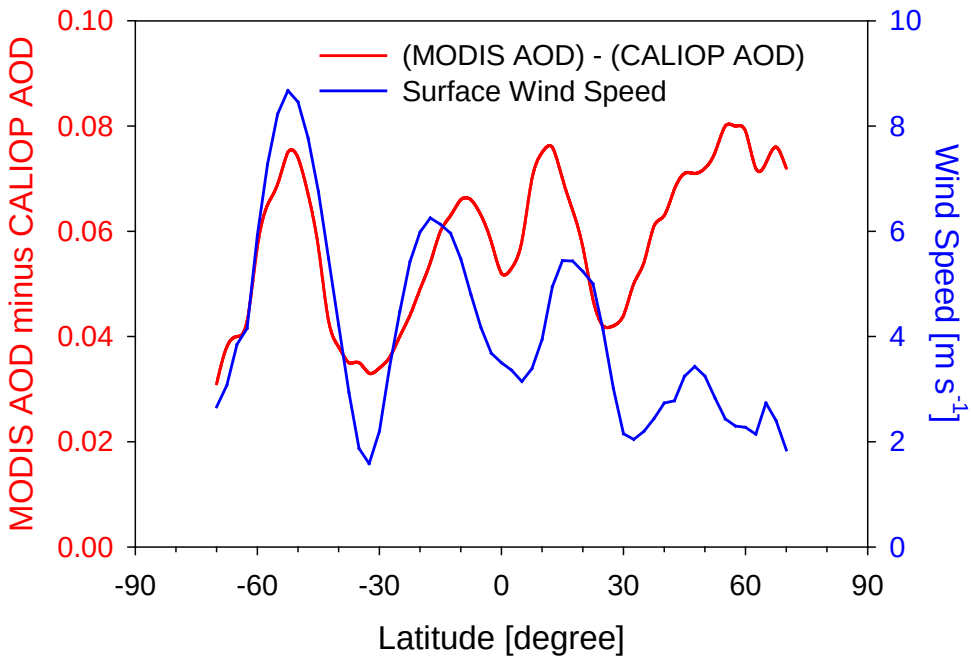

Figure 2.4. Zonal mean of AOD difference between CALIOP and MODIS and sea-level wind speed over oceans from June 2006 to December 2010.

2.4.2. Dust

Dust is predominantly non-spherical in shape with a relatively large depolarization ratio making its classification relatively unambiguous with respect to other common aerosol particles [e.g., *Freudenthaler et al.*, 2009; *Kai et al.*, 2008; *Sugimoto et al.*, 2002]. In general, the difference in dust AOD between the two instruments is smaller than the differences for other aerosol types (Table 2.1). Figure 2.2c also shows that dust AODs from the two sensors are better correlated than other aerosol types despite the large variance.

The global distribution of collocated dust data pairs is shown in Figure 2.5a. Dust appears more frequently near source regions, such as North Africa, Arabia, and East Asia, and AOD differences between the two sensors vary accordingly (Figure 2.5b). Mean MODIS AOD is larger than CALIOP AOD in East Asia, while the two mean AODs are comparable near the Saharan and Arabian Deserts. This variation in AOD difference implies that the optical properties of dust from Saharan and Arabian deserts are different from the optical properties of East Asian dust. Since CALIOP assumes that the lidar ratio for all dust is 40 sr, the difference in optical properties between East Asian and Saharan/Arabian dust has an impact on the accuracy CALIOP's AOD retrievals. Given the finding in

Figure 2.5, it is thus plausible, that the lidar ratio for East Asian dust is larger than the lidar ratio of Saharan and Arabian desert dust. The CALIOP algorithm lidar ratio for dust is comparable to *Voss et al.* [2001] for African dust (41 ± 8 sr) and *Cattrall et al.* [2005] for non-Asian desert dust (42 ± 4 sr). Several studies for the lidar ratio of Asian dust, however, report relatively larger values than Saharan dust: 42 - 55 sr by *Liu et al.* [2002], 50.4 ± 9.5 sr by *Murayama et al.* [2003], and 45.5 ± 8.6 sr by *Noh et al.* [2007]. Contrarily, *Schuster et al.* [2012] suggested a dust lidar ratio of 50-55 for Saharan dust after comparing CALIOP AODs with AERONET, and *Müller et al.* [2007] reported 55 ± 5 sr and 59 ± 11 sr for Saharan dust from Raman lidar measurements.

CALIOP algorithms classify dust aerosol when the estimated depolarization ratio (δ_v) is greater than 0.2, everywhere except for the polar regions [*Omar et al.*, 2009]. δ_v is an approximation of the particulate depolarization ratio (δ) defined by Eq. (9) in *Omar et al.* [2009]. δ, the depolarization due to only particles, is obtained after the retrieval of aerosol extinction profile. But for the retrieval, aerosol type, or the lidar ratio is required *a priori*. In order to determine the lidar ratio, therefore, δ_v is first estimated from the volume depolarization ratio, which is a sum of the depolarization due to particles and air molecules.

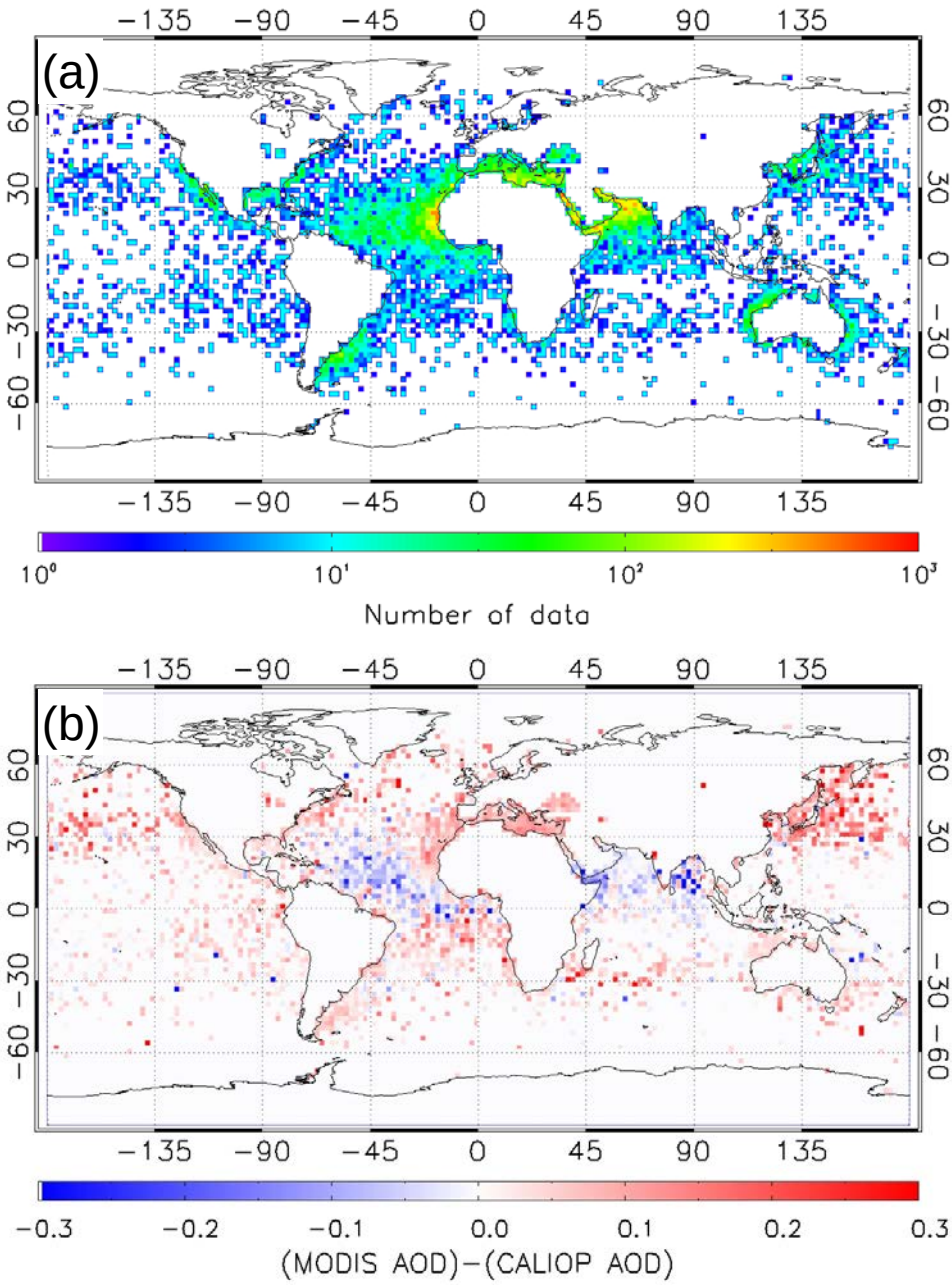

Figure 2.5. Same as Figure 2.3, except for dust.

To examine the relationship of the MODIS-CALIOP AOD differences and the depolarization ratio we define an extinction-normalized depolarization ratio, as a proxy for the particulate depolarization ratio obtained by following equation:

$$\bar{\delta} = \frac{\sum_{z_{base}}^{z_{top}} \sigma(z)\delta(z)}{\sum_{z_{base}}^{z_{top}} \sigma(z)} \quad \text{(EQ1)}$$

where z is the altitude with the resolution of 60 m; the subscripts “top” and “base” represent the top and the base height of the aerosol layer; and σ is the particulate extinction coefficient. Figure 2.6a shows frequency distributions of δ for dust, polluted dust, and clean marine.

δ is greater than 0.2 for most of the dust layers in Figure 2.6. However, for about 9% of the dust data used in this study, δ is less than 0.2. *Burton et al.* [2013] point out that in cases of strong attenuation and weak depolarization spurious classification of dust and polluted dust is likely.

Figure 2.6b shows the relation between the difference in AOD and $\bar{\delta}$ for dust, polluted dust and clean marine. While the differences of AOD for polluted dust and clean marine exhibit weak relations with $\bar{\delta}$, the difference of AOD for dust shows a very distinguishable dependence on $\bar{\delta}$.

When considering only collocated data pairs having $\bar{\delta}$ greater than 0.2 and assuming that the MODIS AOD and CALIOP classification of dust is correct, the increasing trend of the AOD difference with $\bar{\delta}$ implies that the lidar ratio of dust should increase as $\bar{\delta}$ increases.

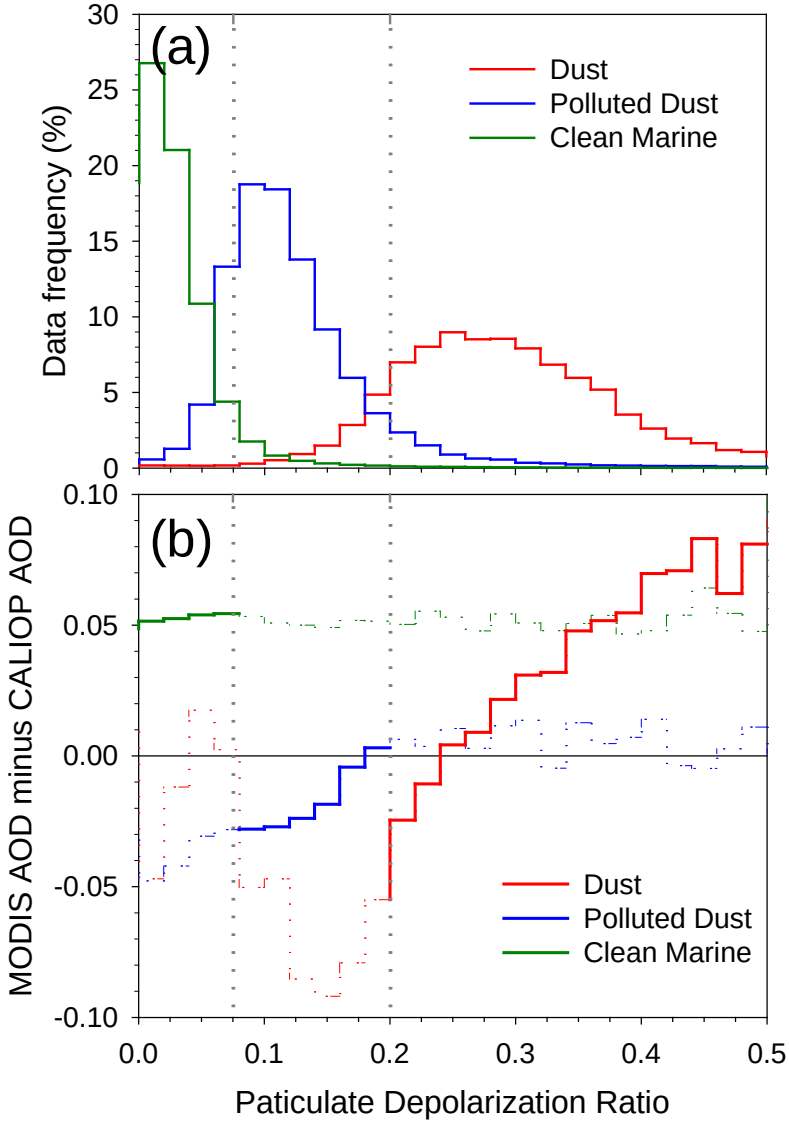

Figure 2.6. Variations in (a) data frequency and (b) AOD difference versus particulate depolarization ratio ($\overline{\boldsymbol{\delta}}$) for dust (red), polluted dust (blue), and clean marine (green). The criteria of depolarization ratio for the polluted dust (0.75) and dust (0.2) are shown in gray vertical dashed lines. For each type, the solid line denotes the region for which the algorithm threshold matches the $\overline{\boldsymbol{\delta}}$.

2.4.3. Polluted dust

Polluted dust is defined as dust mixed with biomass burning, and is identified when δ_v has the range between 0.075 and 0.2 regardless of elevation or region except for the poles [*Omar et al.*, 2009]. A lidar ratio of 55 sr is used in the CALIOP algorithms for polluted dust. A possible reason for higher CALIOP AOD compared to MODIS AOD for polluted dust is misclassification of aerosol type in CALIOP algorithm. If any aerosols which have lower lidar ratios than polluted dust, such as clean marine or dust are misclassified as polluted dust, CALIOP AOD will be larger than the true value. Since CALIOP aerosol classification does not include mixtures of dust and marine aerosols, it is possible for these mixtures to be classified as polluted dust as shown by *Burton et al.* [2013]. Such mixtures would have an effective lidar ratio between 20 and 40 sr, and therefore lower than the polluted dust ratio of 55 sr. Such a misclassification would therefore lead to a higher CALIOP AOD than the true value. Figure 2.7 shows global distributions of the number of collocated data points and difference between CALIOP and MODIS AODs for polluted dust. The number of data points increases near the continents where source regions of dust and biomass burning are close. The number is still relatively significant over remote oceans. As

mentioned above, polluted dust is identified using only δ_v over the ocean, which is only an approximation of the particulate depolarization. However, $\bar{\delta}$ is not exactly same as δ_v, and using δ_v instead of $\bar{\delta}$ can affect the classification of polluted dust, dust and clean marine aerosols. Figure 2.6a shows that 19.6% of polluted dust has $\bar{\delta}$ less than 0.075 or greater than 0.2, 11.2% of clean marine has $\bar{\delta}$ greater than 0.075 and 6.9% of dust has $\bar{\delta}$ less than 0.2.

Low SNR in the perpendicular 532 nm channel enhanced by high background solar radiation during daytime is one possible source for error in δ_v estimation affecting polluted dust classification. Figure 2.8 shows global distributions of the number of CALIOP data points of polluted dust for daytime and nighttime. The number of data points is high over the remote ocean for the daytime, whereas the number decreases as the distance from the source regions increases at night. This result implies that other aerosols (probably clean marine) could be misclassified as polluted dust over the ocean particularly during the daytime when the SNR is lower, which in turn would make CALIOP AOD higher than MODIS AOD on average.

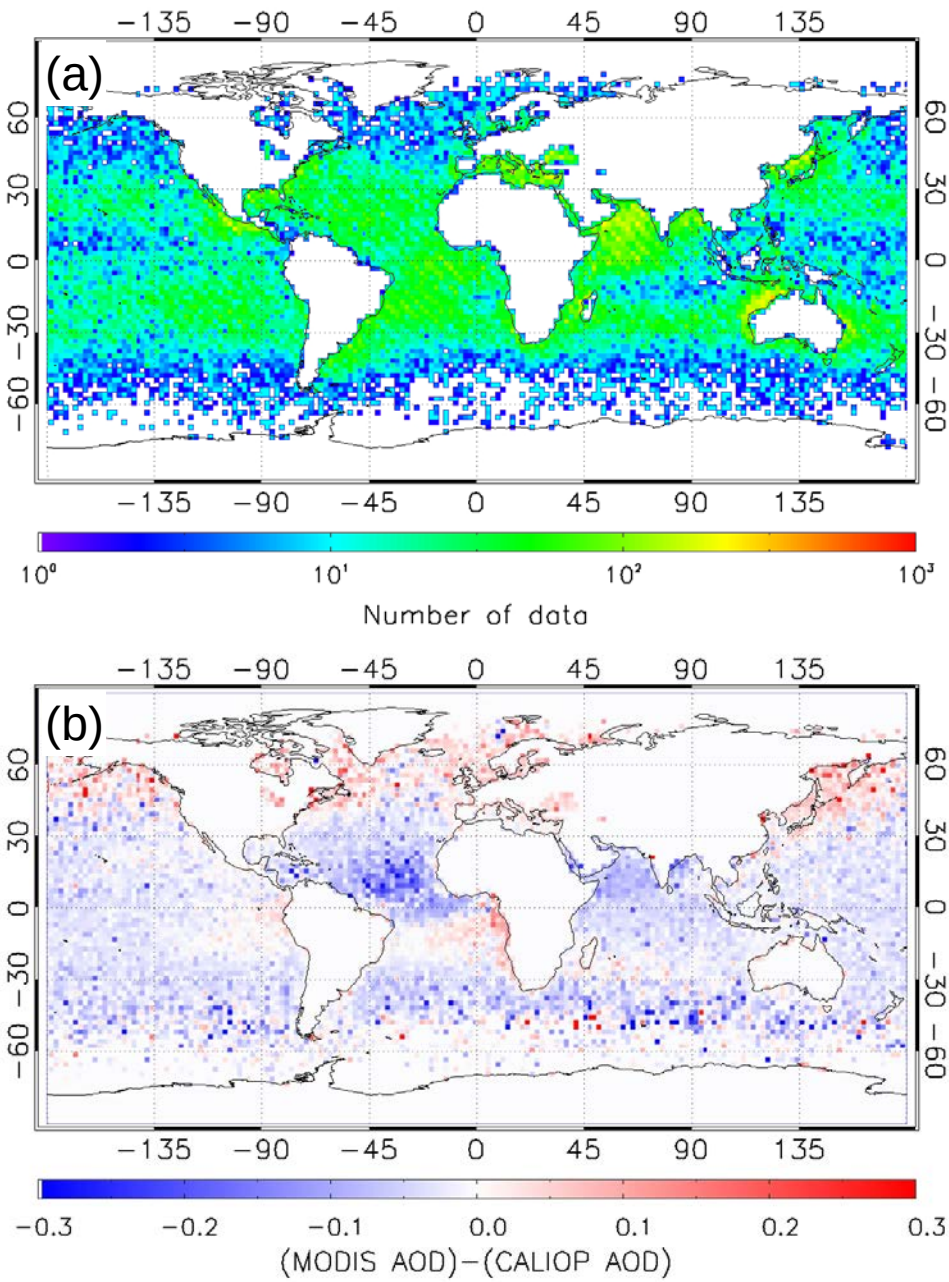

Figure 2.7. Same as Figure 2.3, except for polluted dust.

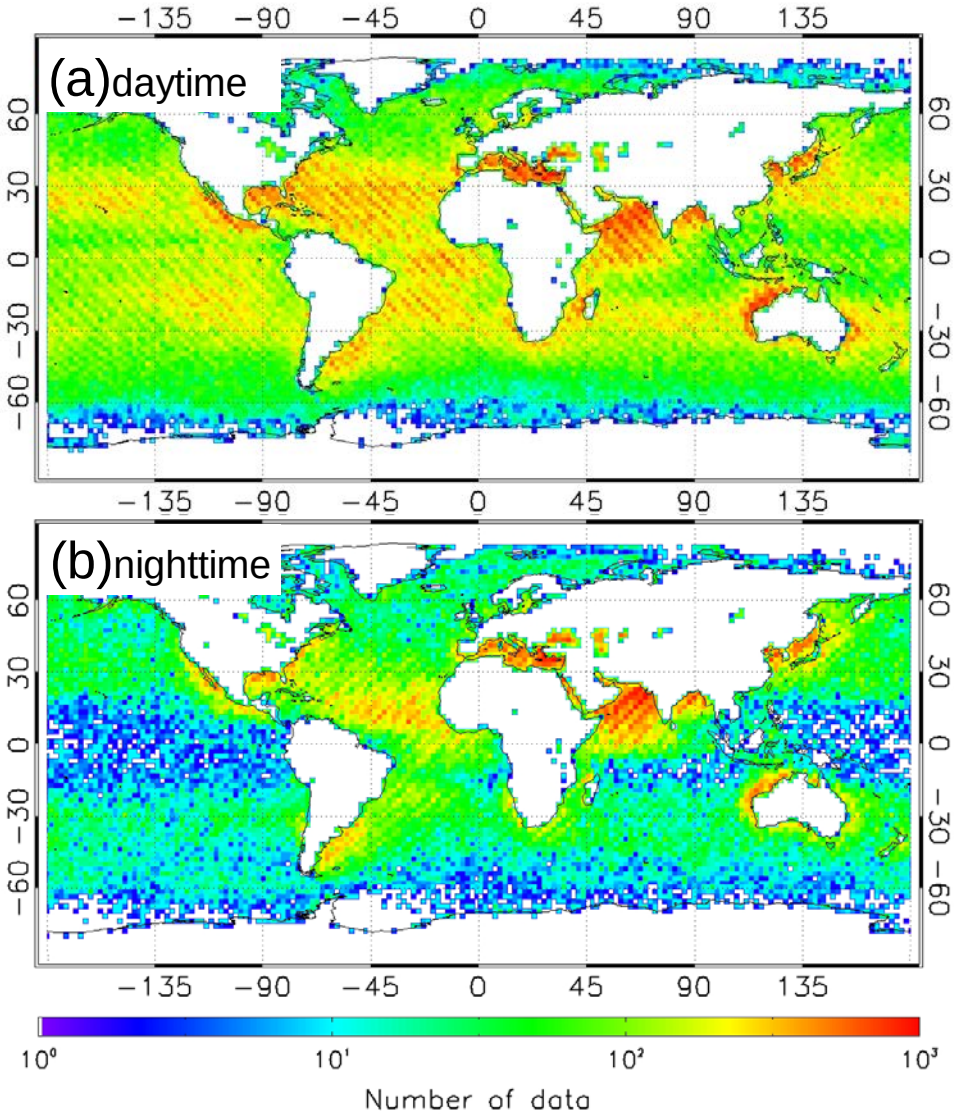

Figure 2.8. Global distribution of the number of CALIOP data points during (a) daytime and (b) nighttime for polluted dust.

2.4.4. Polluted continental

Omar et al. [2009] defined polluted continental as optically thin layers composed of mostly spherical particles with a layer-integrated attenuated backscatter at 532 nm (γ') less than 0.01 and δ_v greater than 0.05. Because optically-thin layers are classified as polluted continental, AODs for polluted continental over the ocean are even lower than those of clean marine (Table 1). As shown in Figure 6 of *Winker et al.* [2009], the retrieval error of MODIS AOD increases dramatically at AODs less than 0.1. Figure 2.2e shows that most of polluted continental AODs are less than 0.1 making the AOD comparison challenging.

Figure 2.9 shows the global distribution of numbers of collocated data pairs and differences of AOD between the two sensors for polluted continental over the ocean. Similar to polluted dust, the number of collocated data pairs for polluted continental is high not only along coastlines but also over remote ocean locations. Figure 2.10 also shows that the number of CALIOP data points for polluted continental over the remote ocean for daytime is high compared to that at nighttime, and implies a low SNR for γ' and δ_v during daytime is responsible for the misclassification of clean marine which is most common over remote oceans as polluted continental.

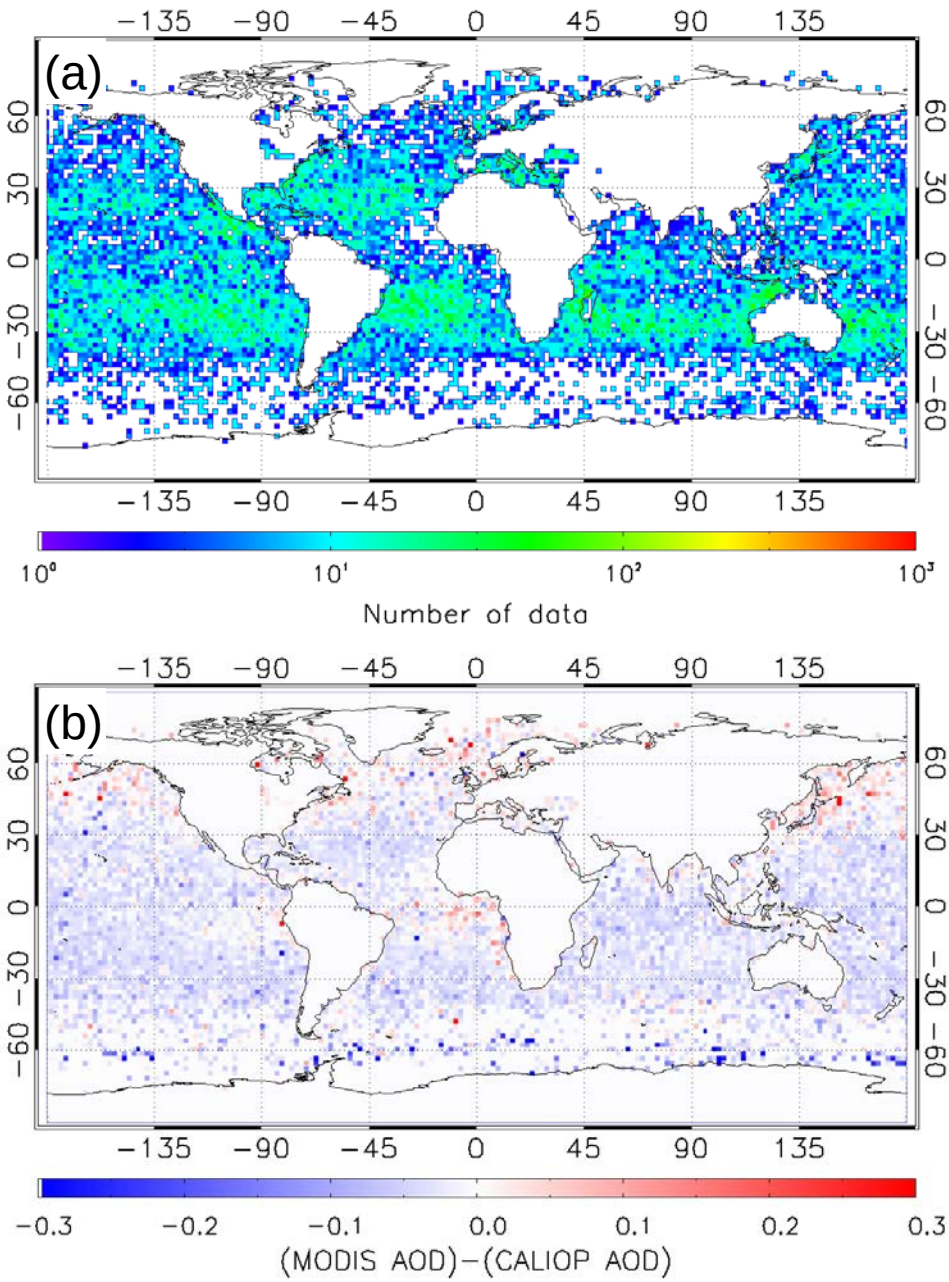

Figure 2.9. Same as Figure 2.3, except for polluted continental.

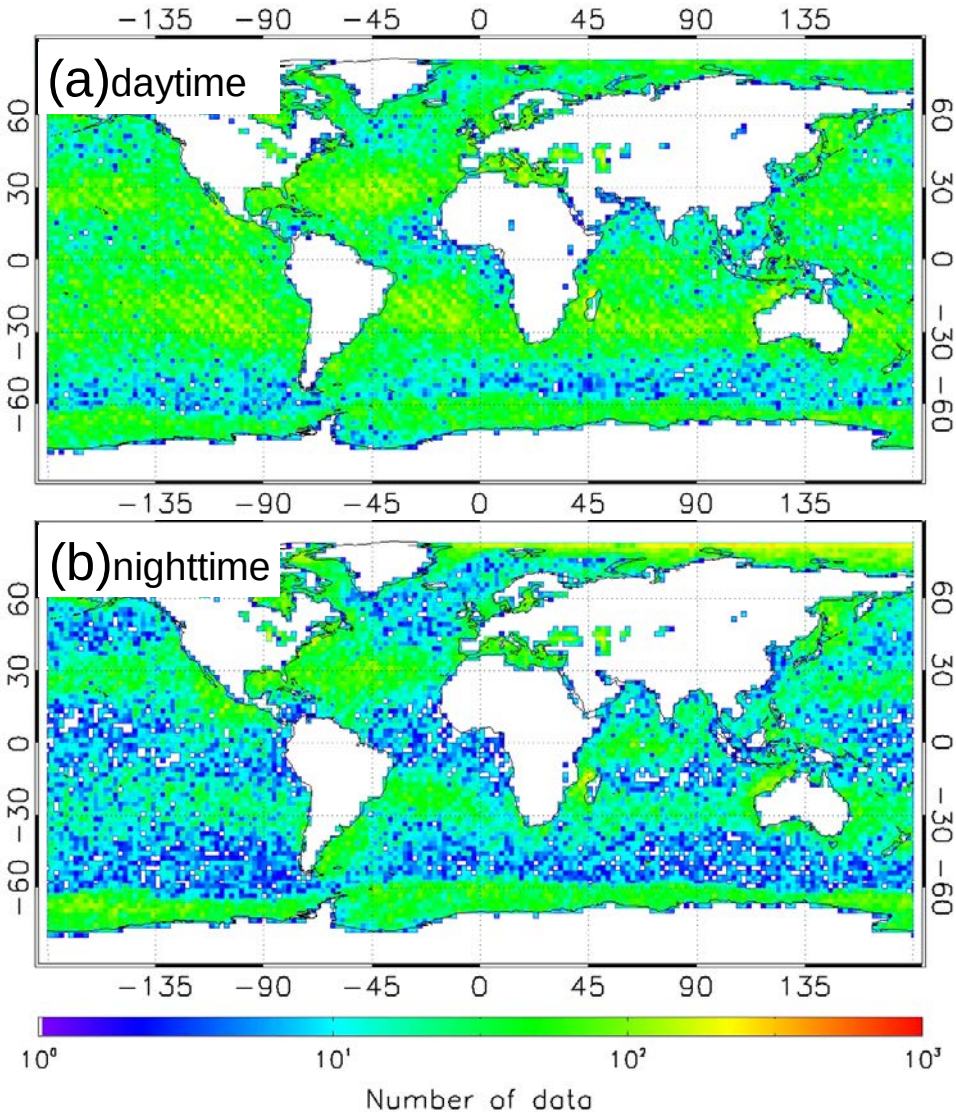

Figure 2.10. Same as Figure 2.8, except for polluted continental.

2.4.5. Biomass burning

Biomass burning, also referred to as smoke in the CALIOP algorithms, shows the largest difference of AOD between the two sensors. The mean AOD of MODIS (0.281 ± 0.232) is about twice that of the CALIOP AOD (0.139 ± 0.157). Collocated data pairs appear most frequently in the South Atlantic Ocean, west of Africa (Figure 2.11a), which is considered a primary global source region of biomass burning [*Duncan et al*., 2003]. CALIOP AOD is generally lower than MODIS AOD regardless of region (Figure 2.11b). The CALIOP lidar ratio for smoke is quite high at 70 sr and consistent with the values obtained by *Ansmann et al.* [2001], *Voss et al.* [2001], and *Cattrall et al.* [2005]. It is therefore unlikely that the low CALIOP AOD is a result of an underestimated smoke lidar ratio.

Biomass burning aerosols are buoyant at the source and thus more likely to be elevated above the marine boundary layer when transported over the ocean. In the CALIOP aerosol classification algorithms, all elevated non-dust aerosol layers over the ocean are identified as biomass burning [*Omar et al.*, 2009]. CALIOP, being a down-looking lidar system, readily detects the top height compared to the base height of a cloud or an aerosol layer. This is because the signal undergoes significant attenuation as it travels through optically ‘thick’ layers [*Vaughan et al.*, 2005; *Kim et*

al., 2011]. For most of the aerosol layers located near the surface, it is not necessary to find the base altitude as most often the layer reaches the surface. For the elevated layers, however, the base altitude is important in determining CALIOP AOD. Because biomass burning aerosols are more likely to be elevated and separated from the boundary layer, the correct location of the base height is crucial for AOD determination.

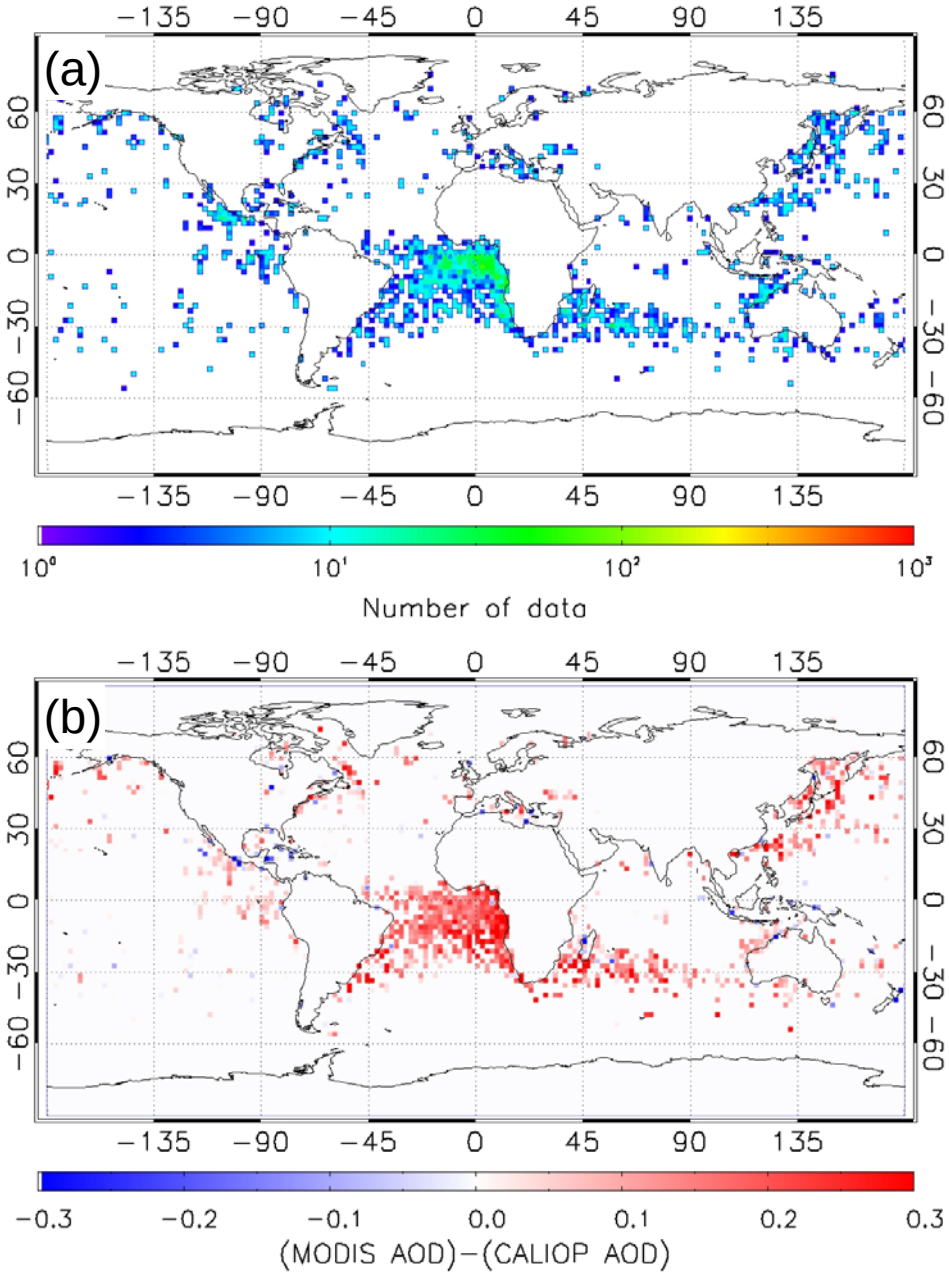

Figure 2.11. Same as Figure 2.3, except for biomass burning.

Figures 2.12 and 2.13 are examples of (a) the total attenuated backscatter at 532 nm for CALIOP Level 1B data, (b) aerosol extinction profile at 532 nm from Level 2 5-km profile data, and (c) column integrated AOD from CALIOP and MODIS for the collocated data pairs of biomass burning measured over the Southern Atlantic. In both figures, the layer top altitudes are easily distinguishable but the base altitudes determined by the CALIOP algorithms are quite variable and possibly uncertain. The base altitudes for the aerosol layer in Figure 2.12 are near 3-4 km and no other aerosol layers are detected below, whereas the base altitudes for Figure 2.13 extend to the surface. When comparing AOD for these two cases, a distinct contrast is found. The CALIOP AODs are similar or slightly larger than MODIS AOD for Figure 2.13c while MODIS AOD is nearly twice that of CALIOP AOD for Figure 2.12c. In this study, the mean layer base altitude for the collocated data pairs of biomass burning is 3.1 km. Also, 71.5% of the collocated data pairs have the base altitude higher than 2 km, which implies that the most of CALIOP AOD for biomass burning does not extend into the marine boundary layer.

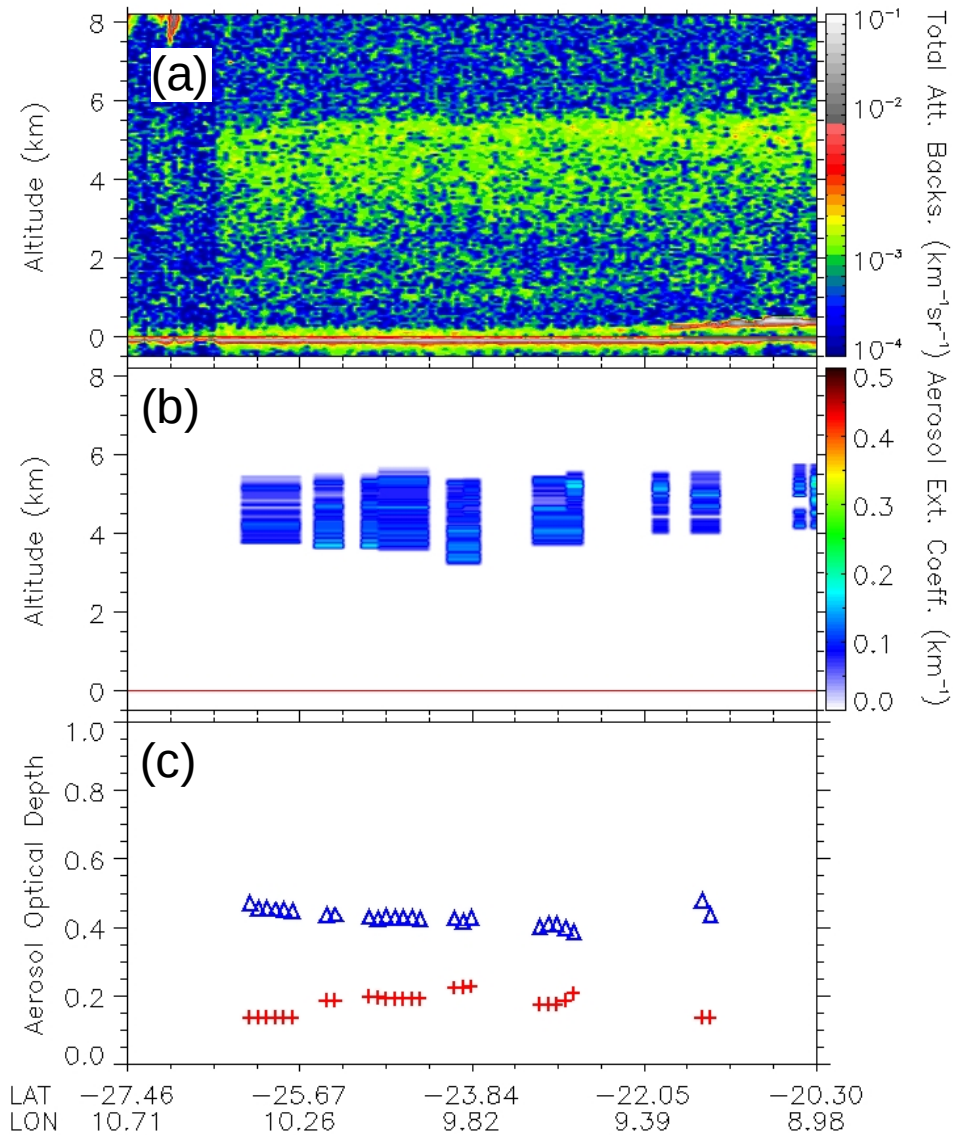

Figure 2.12. (a) CALIOP Level 1 total attenuated backscatter at 532 nm, (b) CALIOP Level 2 5-km aerosol extinction profile, and (c) column integrated AODs from CALIOP (red cross) and collocated MODIS AOD (blue triangle) for the biomass burning aerosols from 13:19 UTC to 13:21 UTC, October 6, 2010.

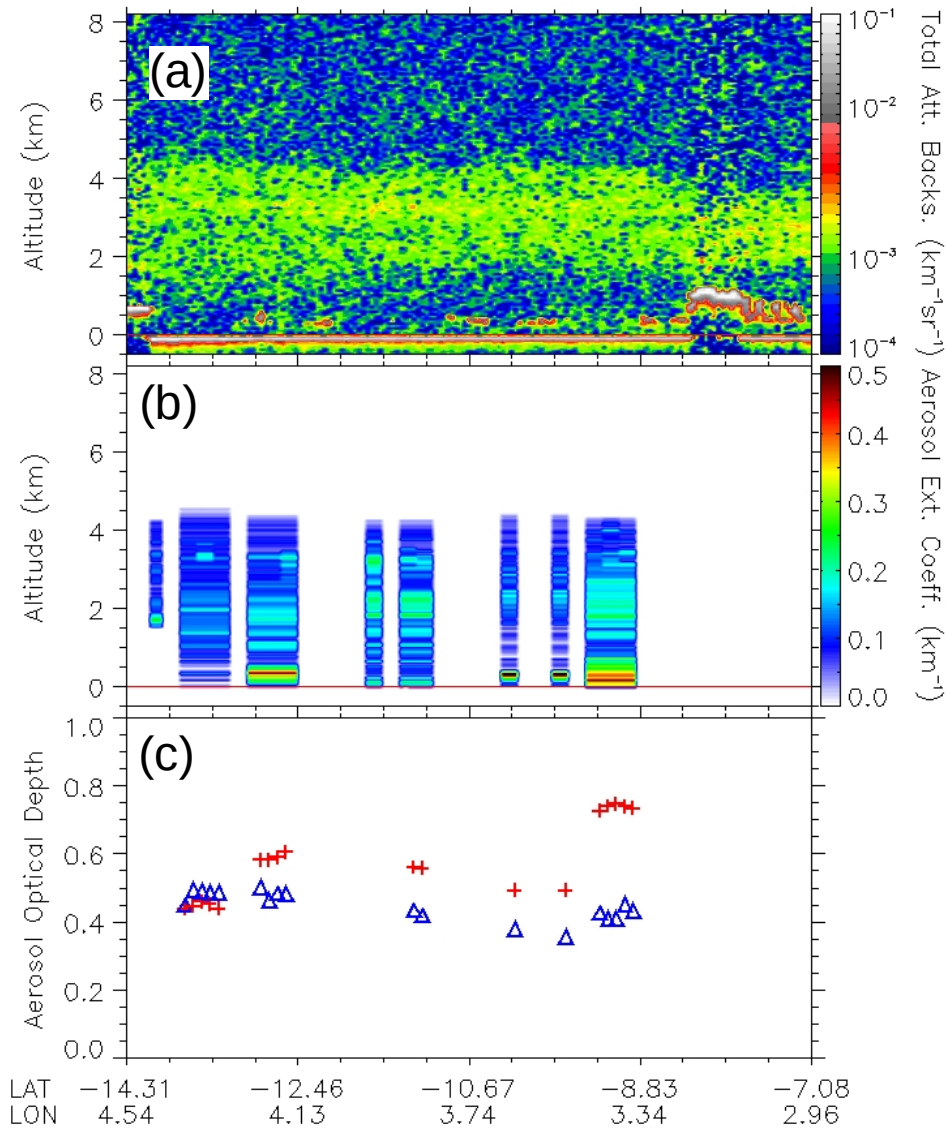

Figure 2.13. Same as Figure 2.12, except from 13:34 UTC to 13:36 UTC, October 4, 2010.

Figure 2.14 shows aerosol extinction profiles from CALIOP Level 2 Aerosol Profile product (blue) and retrieved in this study using same retrieval algorithm with *Young and Vaughan* [2009] from CALIOP Level 1 product (red). This profile comes from the center of Figure 2.12, from -24.15° to -24.69° in latitude. For that region, CALIOP Level 2 product does not report aerosol layers blow 3.5 km from the surface. Our retrieval matches relatively well with CALIOP L2 products for detected aerosol layers from 3.5 km to 5.8 km. However, our retrieval shows that aerosol extinction is still high enough below the detected aerosol layer. Thus, AOD increases from 0.19 to 0.40. As shown in this figure, surface reflection is not fully removed in our retrieval. If we remove aerosol extinction near the surface (below 300 m), AOD is found to be 0.34 which is still higher than AOD from CALIOP Level 2 product.

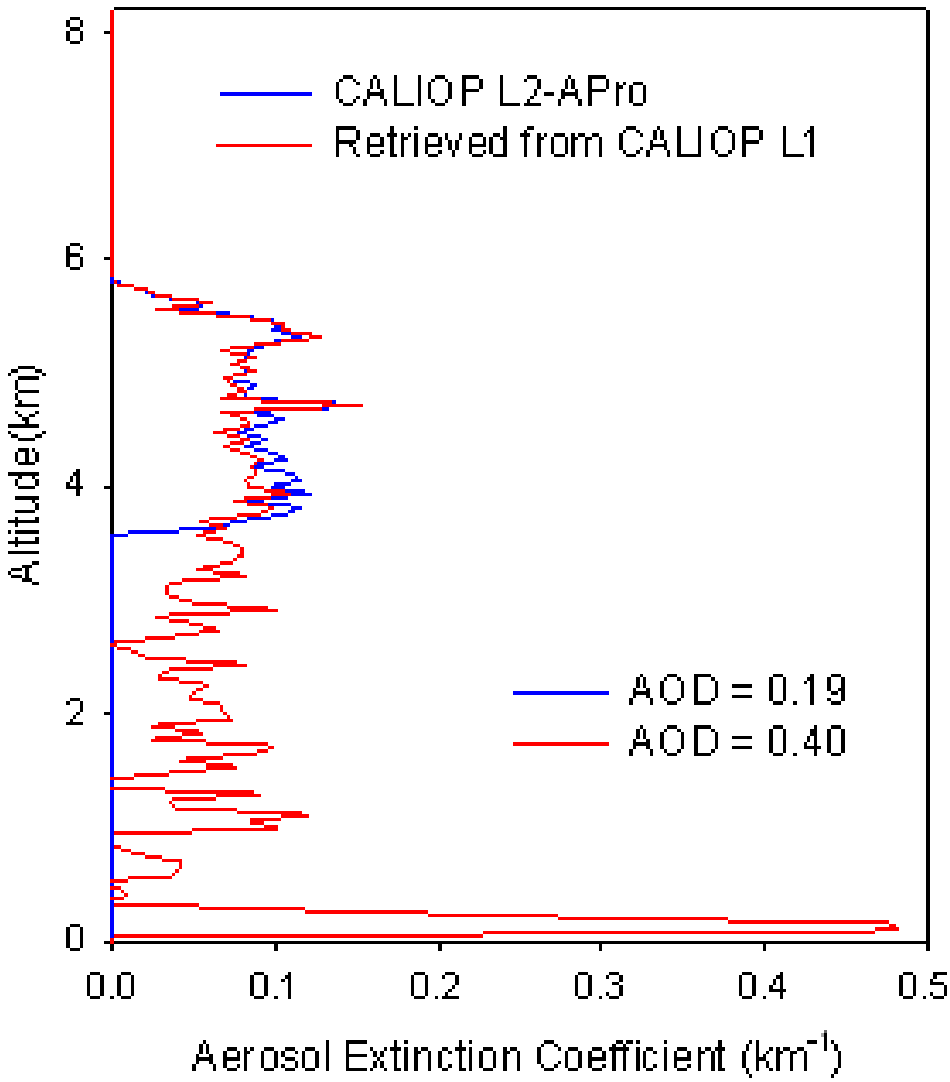

Figure 2.14. Aerosol extinction profiles from CALIOP 5-km Level 2 Aerosol Profile Product (blue) and retrieved in this study from CALIOP 333-m Level 1 product using same retrieval algorithm with Young and Vaughan [2009] from the top of the layer to the surface level (red). The aerosol extinction profiles correspond to the center of Figure 2.12, from -24.15° to -24.69° in latitude.

2.5. Summary

Nearly two million collocated AOD data pairs have been compared over oceans for cloud-free conditions using CALIOP Level 2 aerosol layer and profile products (Version 3.01) and MODIS Level 2 aerosol product (Collection 5.1) from June 2006 to December 2010. MODIS 10-km pixel and CALIOP profiles closer than 10 km from MODIS pixel are chosen as a collocated data pair. In order to consider errors associated with aerosol type classification and pre-determined lidar ratio, CALIOP AODs with layers of a single aerosol type throughout the column were selected for the comparison. The mean MODIS AOD is 63% larger than that of CALIOP AOD for all aerosol types. When considering aerosol types defined in CALIOP algorithm, the differences in AOD between the two sensors show some dependence on the type of aerosol. MODIS AOD is higher than CALIOP AOD for most aerosol types except for polluted dust and polluted continental.

AOD differences between MODIS and CALIOP for clean marine (relative bias of 96%) show latitude dependency, which is related to the surface wind speed, especially for the southern hemisphere. Because CALIOP AOD is not affected by surface conditions, the latitudinal variation in the AOD difference is likely due to surface related retrieval

errors of MODIS AOD. A strong surface wind brightens the ocean and thus can contribute to the higher MODIS AOD.

Dust AOD from CALIOP and MODIS are in good agreement with a relative bias of 13%. However, they show distinct regional variations. MODIS AOD is much higher than CALIOP AOD for the Asian dust, while MODIS AOD is almost similar or sometimes lower for the dust from Saharan and Arabian deserts. The AOD difference for dust also shows strong dependence on extinction-normalized particulate depolarization ratio ($\bar{\delta}$). The increasing trend of the AOD difference with $\bar{\delta}$ implies that the lidar ratio for dust should increase as $\bar{\delta}$ increases, if the MODIS AOD is correct.

Mean AOD of CALIOP is larger than that of MODIS for polluted dust (relative bias of -15%) and polluted continental (relative bias of -29%). It is possible that the lidar ratios for these aerosols are overestimated or that some other aerosols with smaller lidar ratio are misclassified if MODIS AOD is assumed to be correct. The large number of collocated data pairs for polluted dust and polluted continental over the remote ocean, far from their source region, may be an indication that other aerosols such as clean marine are being misclassified as polluted dust and polluted continental.

A large difference in AOD (102%) between CALIOP and MODIS was found for biomass burning. A reason for the low CALIOP AOD is due to the errors in determining the layer base altitude. By definition in the CALIOP algorithms, biomass burning aerosol layers are all elevated. It is therefore critical to determine the base altitude correctly in order to account for all aerosols in the column. This can be a challenge for satellite based down-looking lidar systems especially in the presence of highly attenuating smoke layers frequently encountered near biomass burning source regions. In this study, most of the biomass burning layers do not extend into the boundary layer which may have led to the underestimation of the CALIOP AOD.

This study has shown several areas where both the CALIOP and MODIS algorithms can be improved. It is possible that MODIS retrievals are affected by sea surface wind speeds in the Southern Hemisphere and the algorithms might benefit from updated surface models and dynamic wind fields to account for ocean surface reflectance. The CALIOP algorithms can increase the accuracy of the Asian dust AODs by adopting regionally variable dust lidar ratios. Additionally, an examination of the layer base altitude for smoke layers and comparison with independent measurements to determine what corrections if any to the calculation of

the AOD for smoke are warranted. As the study has shown, the effect of the daytime SNR on the depolarization ratio has important consequences for the aerosol classification scheme. While there are no easy solutions to some of the findings of this study CALIPSO team is working on several fronts to mitigate some of these shortcomings in the upcoming algorithm release.

CHAPTER 3.
EVALUATION OF CALIOP LIDAR RATIO USING AOD CONSTRAINED METHOD

3.1. Introduction

CALIOP data products are available in three “levels” that reflect the degree of processing involved [*King et al.*, 2004]. Level 1 data products include the calibrated attenuated backscatter profiles at the two wavelengths (532 nm and 1064 nm) along with various ancillary atmospheric and navigational data. The fundamental sampling resolution of CALIOP is 30 m vertical and 335 m horizontal. The laser pulse repetition frequency of 20.16 Hz produces footprints every 333 m along the ground [*Winker et al.*, 2009], which corresponds to the horizontal resolution of CALIOP Level 1 Products. The vertical resolution of CALIOP Level 1 Products is 30 m from -0.5 to 8.2 km and averaged vertically above an altitude of 8.2 km [*Winker et al.*, 2009]. CALIOP Level 2 Products are created from the Level 1 Products. Primary Level 2 data products from the lidar are the location of atmospheric regions that

contains particulate matter (clouds and aerosols), the identification of these particles according to type. CALIOP Level 2 Products consist of “Layer Product” and “Profile Product”. The Layer Products provide the spatial and optical characteristics of each feature found, and include quantities such as layer base and top altitudes, integrated attenuated backscatter, layer-integrated volume depolarization ratio, and optical depth. The Profile Products report profiles of particle extinction, backscatter, and additional profile information (e.g., particulate depolarization ratios) derived from these fundamental products. The horizontal resolution of CALIOP Aerosol Level 2 Products is 5 km and the vertical resolution of CALIOP Aerosol Level 2 Profile Products is 60 m from -0.5 km to 20.2 km. CALIPSO Level 3 Aerosol Product reports monthly mean profiles of aerosol optical properties on a uniform spatial grid. It is intended to be a tropospheric product, so data are only reported below altitudes of 12 km.

The CALIOP level 2 algorithms retrieve the aerosol extinction profiles from the CALIOP Level 1 Products. To retrieve aerosol extinction profile from lidar measurements, the lidar equation should be solved. *Klett* [1985] or *Fernald* [1984] methods are typically used especially for the ground-based lidar. These methods adopt an analytic solution for the lidar equation assuming aerosol free atmosphere. Then, aerosol extinction

profiles are retrieved for each level to the ground. One of the biggest advantages of these methods is that the solution is very stable for ground-based lidar system. Also, the calibration constant of the lidar equation is eliminated during the retrieval. However, these methods are commonly unstable for down-looking lidar systems such as space-borne and air-borne lidar systems. The CALIOP level 2 algorithm uses a numerical solution to retrieve aerosol extinction profiles [*Young and Vaughan*, 2009].

To solve the lidar equation using analytic or numerical solutions from elastic lidar measurements, $\boldsymbol{S_{aer}}$ should be determined and it is frequently either assumed or inferred from additional measurements. In the CALIOP algorithm, $\boldsymbol{S_{aer}}$ is determined by aerosol type classification based on the cluster analysis of a multiyear (1993-2002) AEROENT dataset [*Omar et al.*, 2005]. $\boldsymbol{S_{aer}}$ is considered to be constant over certain intervals within each backscatter profile, as determined by the layer detection and scene classification algorithms. However, a pre-determined $\boldsymbol{S_{aer}}$ has large uncertainty, higher than 30% [*Omar et al.*, 2009].

As denoted in *Winker et al*. [2013], uncertainty in $\boldsymbol{S_{aer}}$ is the largest source of uncertainty in the CALIOP AOD. Current CALIOP level 2 algorithm uses pre-determined $\boldsymbol{S_{aer}}$ for classified aerosol types. However,

not only using single values of $\boldsymbol{S_{aer}}$ for each aerosol type but also aerosol classification algorithm could be sources of uncertainties in aerosol extinction retrieval. In this study, aerosol extinction profiles are retrieved from CALIOP Level 1 Products using independently measured AOD from AERONET or MODIS-Aqua as a constraint without assuming aerosol type or $\boldsymbol{S_{aer}}$. By comparing the retrieved $\boldsymbol{S_{aer}}$ with that value of CALIOP Level 2 algorithm, the uncertainties of currently used $\boldsymbol{S_{aer}}$ in CALIOP algorithm was evaluated, especially for dust aerosol which is considered as the most accurately classified among CALIOP Level 2 aerosol subtypes.

3.2. Methodology

3.2.1. Aerosol extinction retrieval

In order to retrieve aerosol extinction coefficients from the measurements of elastic backscatter lidar, the lidar equation [EQ2] should be solved.

$$P(z) = \frac{C}{z^2}[\beta_{aer}(z) + \beta_{mol}(z)]e^{-2\int_0^z[\sigma_{aer}(r)+\sigma_{mol}(r)]dr} \qquad \text{[EQ 2]}$$

Here, $P(z)$ is the returned lidar signal from the altitude z, C is the constant including all range-independent parameters, β_{aer} and β_{mol} are the volume aerosol backscatter coefficient of aerosols and molecules, σ_{aer} and σ_{mol} represent the volume aerosol extinction coefficients of aerosol and molecules, respectively.

Normally, β_{aer} and β_{mol} are calculated using air temperature and pressure profiles for the ‘Standard Atmosphere’ or using data from radio sonde profiling. The CALIOP Level 2 product provides ‘Molecular Number Density’ which is obtained from the ancillary meteorological data

provided by the GMAO (http://gmao.gsfc.nasa.gov/ operations/). The calibration constant (C) in [EQ 2] can be calculated or eliminated by assuming aerosol free atmosphere. However, even if the vertical information of molecules (β_{mol}, σ_{mol}) and the calibration constant (C) are known, [EQ 2] cannot be solved because it still has two unknowns: aerosol extinction and backscatter coefficients. To solve this ill-posed equation, we should know $\boldsymbol{S_{aer}}$ which represents the ratio between aerosol backscatter and extinction coefficients as follows.

$$S_{aer}(z) = \frac{\beta_{aer}(z)}{\sigma_{aer}(z)} \qquad \text{[EQ 3]}$$

To derive analytic solution of [EQ 2], *Sasano et al.* (1985) used normalized total extinction coefficient y(z) defined as

$$\mathrm{y}(z) = \sigma_{aer}(z) + \frac{S_{aer}(z)}{S_{mol}}\sigma_{mol}(z). \qquad \text{[EQ 4]}$$

Here, $\boldsymbol{S_{mol}}$ is molecular lidar ratio which is not dependent on height. Then we can obtain following equation by substituting above equation for [EQ 2] and taking the logarithm and differentiating them with z.

$$\frac{d\ln\left(S_{aer}(z)P(z)z^2 e^{-2\left[\frac{S_{aer}}{S_{mol}}-1\right]\int_0^z \sigma_{mol}(r)dr}\right)}{dz} = \frac{1}{\mathrm{y}(z)}\frac{d\mathrm{y}(z)}{dz} - 2\mathrm{y}(z) \qquad \text{[EQ 5]}$$

[EQ 5] is known as Bernoulli's differential equation and has following solution [*Klett*, 1981; *Fernald*, 1984, *Sasano et al.*, 1985].

$$\sigma_{aer}(z) + \frac{S_{aer}}{S_{mol}}\sigma_{mol}(z) = \qquad \text{[EQ 6]}$$

$$\frac{S_{aer}P(z)z^2 e^{-2\left[\frac{S_{aer}}{S_{mol}}-1\right]\int_{z_0}^z \sigma_{mol}(r)dr}}{\frac{S_{mol}P(z_0){z_0}^2}{\sigma_{mol}(z_0)} - 2\int_{z_0}^z S_{aer}P(r)r^2 e^{-2\left[\frac{S_{aer}}{S_{mol}}-1\right]\int_{z_0}^r \sigma_{mol}(r`)dr`}dr}$$

where, z_0 is reference altitude where the aerosol extinction is assumed to be zero. In this equation $\boldsymbol{S_{aer}}$ is assumed constant with altitude.

The analytic solution described above is widely used for ground-based lidar measurements due to its stableness. For the down-looking lidar system such as CALIOP, however, the integration of [EQ 6] is performed in forward direction. Thus, the denominator sometimes can be infinitesimal and [EQ 6] becomes unstable. For this reason, CALIOP level 2 algorithm uses an iterative solution [*Young and Vaughan*, 2009]. [EQ 2] can be rewired for down-looking lidar systems as follows.

$$P'(z) = \frac{P(z)z^2}{C} = [\beta_{aer}(z) + \beta_{mol}(z)]T_{aer}^2(0,z)T_{mol}^2(0,z) \qquad \text{[EQ 7]}$$

Here, $P'(z)$ is range corrected lidar signal, T_{aer}^2 and T_{mol}^2 are two-way transmittance for aerosol and air molecules, respectively. To solve [EQ 7], the "renormalized" attenuated backscatter is calculated using the renormalization factor defined as follows.

$$R_N(z_N) = T^2_{aer}(0, z_N)T^2_{mol}(0, z_N). \qquad \text{[EQ 7]}$$

Thus, [EQ 7] can be rewritten as

$$P'_N(z) = [\beta_{aer}(z) + \beta_{mol}(z)]T^2_{aer}(z_N, z)T^2_{mol}(z_N, z) \qquad \text{[EQ 8]}$$

Solving for the particulate backscattering coefficient at range z, we have

$$\beta_{aer}(z) = \frac{P'_N(z)}{T^2_{aer}(z_N,z)T^2_{mol}(z_N,z)} - \beta_{mol}(z). \qquad \text{[EQ 9]}$$

In [EQ 9], however, $T^2_{aer}(z_N, z)$ is also a function of $\beta_{aer}(z)$. Therefore, we have to find a solution to an equation of the form $x = F(x)$. Equations of this form are commonly solved using fixed-point iteration algorithms and CALIOP level 2 algorithm uses a Newtonian (Newton-Raphson) method iteration. In this method, successive estimates, *k*, of the particulate

backscatter at any range, z, from the lidar are obtained from the following formula:

$$\beta_{aer,k+1}(z) = \beta_{aer,k}(z) - \frac{f[\beta_{aer,k}(z)]}{f'[\beta_{aer,k}(z)]}. \qquad \text{[EQ 10]}$$

Here, $f\left[\beta_{aer,k}(z)\right]$ is

$$f\left[\beta_{aer,k}(z)\right] = \frac{P'_N(z)}{T^2_{mol}(z_N, z)} \exp\left[2\int_{z_N}^{z} \sigma_{aer}(r)dr\right] - \beta_{mol}(z) - \beta_{aer,k}(z)$$

[EQ 11]

and $f'\left[\beta_{aer,k}(z)\right]$ is the derivative of $f\left[\beta_{aer,k}(z)\right]$ with respect to $\beta_{aer}(z)$ at $\beta_{aer,k}(z)$,

$$f'\left[\beta_{aer,k}(z)\right] = \frac{S_{aer}\,\delta z\,P'_N(z)}{T^2_{mol}(z_N,z)} \exp\left[2\int_{z_N}^{z} \sigma_{aer}(r)dr\right] - 1 \qquad \text{[EQ 12]}$$

where δz is the range increment at range z. The retrieved profile of $\beta_{aer}(z)$ may diverge from the correct values if incorrect estimates of the lidar ratio, multiple scattering function (assumed 1 for aerosols), or correction for the attenuation of overlying features are used. When the solution diverges, the CALIOP level 2 algorithm adjust the lidar ratio to prevent divergence in features.

3.2.2. Lidar ratio determination

Aerosol extinction profiles can be retrieved from lidar measurements by solving lidar equation as described in previous section. To solve this equation, however, $\boldsymbol{S_{aer}}$ should be known. It is normally assumed or inferred from order independent observations. In this study, AOD from independently measured from AERONET or MODIS-Aqua are used as a constraint to determine $\boldsymbol{S_{aer}}$. Figure 3.1 shows a schematic flow chart of the algorithm used in this study.

Aerosol extinction profiles are firstly retrieved using $\boldsymbol{S_{aer}}$ of 10 sr or any arbitrary value. By integrating aerosol extinction profile vertically, we can obtain AOD from CALIOP measurement. Then, the CALIOP-derived AOD is compared with MODIS AOD. If the difference of AOD between

two sensors is larger than 0.5%, $\boldsymbol{S_{aer}}$ is adjusted and aerosol extinction profile is calculated again. Final $\boldsymbol{S_{aer}}$ and aerosol extinction profile is determined when the difference of AOD between two sensors is less than 0.5%.

As mentioned in section 2.3, $\boldsymbol{S_{aer}}$ is assumed as constant with altitude which means this algorithm produce vertically averaged values of $\boldsymbol{S_{aer}}$. This assumption can cause error in aerosol vertical structure, but vertically integrated aerosol loading (AOD) is not changed. For the single aerosol layers, this assumption is acceptable. For the multi-layers with different aerosol types, however, this assumption causes the errors in aerosol extinction profiles [*Sasano et al.*, 1985]. In this study, in order to minimize this uncertainty, only single aerosol layers are considered to determine $\boldsymbol{S_{aer}}$.

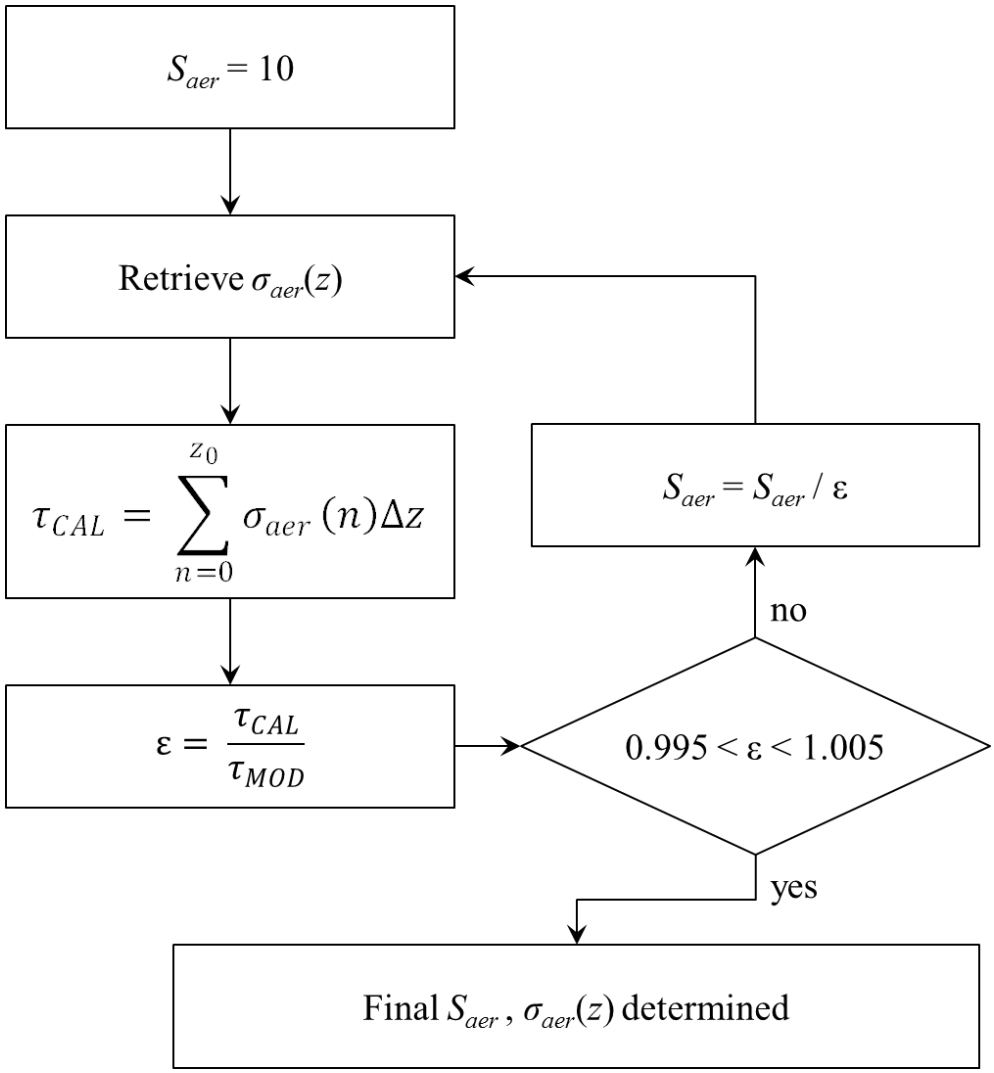

Figure 3.1. Flow chart of the algorithm for determination of the lidar ratio and extinction profile. τ_{CAL} and τ_{MOD} are the AOD from CALIOP and MODIS.

3.3. Determination of lidar ratio from Ground-based Lidar and sky radiometer Measurements

The method described above was successfully applied to determine $\boldsymbol{S_{aer}}$ using 4-year measurements of elastic-backscatter lidar and sky radiometer at Seoul National University of Seoul, Korea. AOD from sky radiometer was adjusted from 500 nm to 532 nm using Ångstöm exponent.

Figure 3.2 shows the seasonal variation of $\boldsymbol{S_{aer}}$, Ångstöm exponent, total depolarization ratio and AOD. Here, Ångstöm exponent and AOD are obtained from sky radiometer and depolarization ratio(*DR*) is vertically integrated values defined as follows.

$$DR = \frac{\sum_{n=0}^{z_0} \delta(n)\sigma_{aer}(n)}{\sum_{n=0}^{z_0} \sigma_{aer}(n)} \qquad \text{[EQ 13]}$$

where, $\delta(n)$ and $\sigma_{aer}(n)$ are total depolarization ratio and aerosol extinction coefficient for nth layer. Aerosol depolarization ratio for dust often exceeds 0.3 and total depolarization ratio is a little bit lower. But the integrated total depolarization ratio used in this study is much less than that of dust layer because it is weighted mean values for the whole layers.

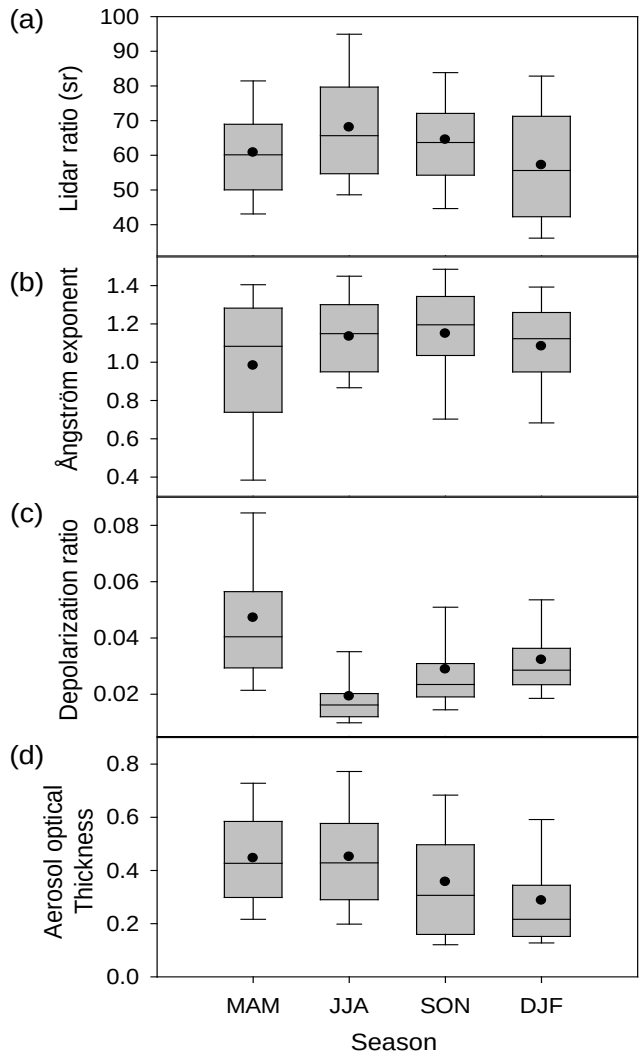

Figure 3.2. Seasonal variation of (a) lidar ratio, (b) Ångström exponent, (c) integrated total depolarization ratio and (d) aerosol optical thickness at Seoul, Korea. Top and bottom of boxes and whiskers represent 75th, 25th, 95th and 5th percentile, respectively. Lines in the boxes are median values and dots represent mean values. Lidar ratio and depolarization ratio are at 532 nm, and Ångström exponent is determined from AOD at five wave length (400, 500, 675, 870, and 1020 nm).

The mean lidar ratio (with standard deviation) based on 4 years of measurements is found to be 61.7±16.5 sr, and has the range of 20 – 110 sr. Relatively weak seasonal variations are noted with a maximum in JJA (68.1±16.8 sr) and a minimum in DJF (57.2±17.9 sr). The impact of Asian dust was clearly noticeable in MAM (spring) through the low values of Ångstöm exponent and high values of depolarization ratio.

From these four-year data, $\boldsymbol{S_{aer}}$ values for some dominant aerosol types are analyzed. Pollution aerosols and dust aerosols can be distinguishable using Ångstöm exponent which provides information about aerosol size [*Jeong and Li*, 2005; *Jung et al.*, 2010]. In this study, dust and pollution aerosols are defined when the Ångstöm exponent belongs to minimum 10% (<0.6) and maximum 10% (>1.4), respectively. Clean or background aerosol is also considered when the AOD belongs to minimum 10% (<0.2). The lidar ratios for clean, dust, and polluted conditions are estimated to be 45.0±9.5 sr, 51.7±13.7 sr, and 62.2±13.2 sr, respectively (Figure 3.3). While the lidar ratio for the polluted condition appears to be consistent with previous studies [e.g., *Ansmann et al.*, 2001; *Cattrall et al.*, 2005; *Barnaba and Gobbi*, 2004], clean conditions tend to have larger ratios, compared to previous estimates and currently used values in CALIOP algorithm [e.g., *Ansmann et al.*, 2001; *Voss et al.*, 2001;

Liu et al., 2002; *Catrall et al.*, 2005; *Muller et al.*, 2007; *Omar et al.*, 2009].

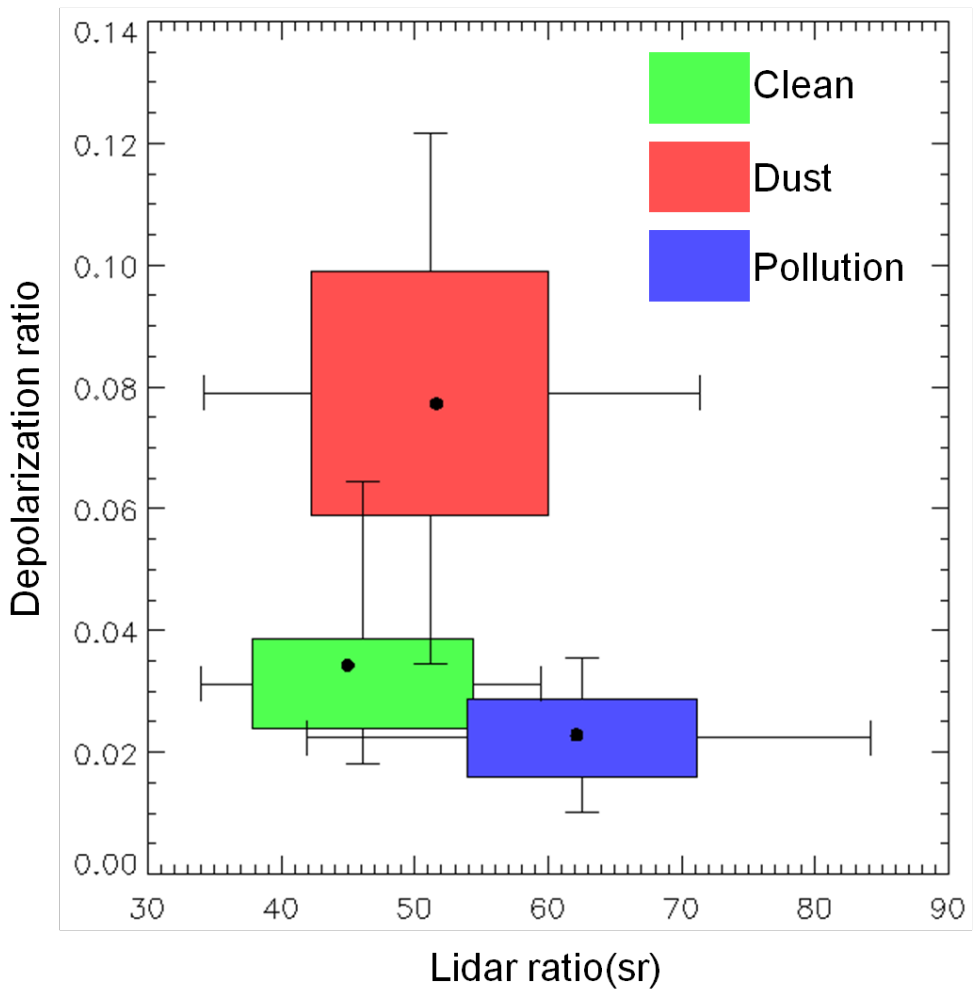

Figure 3.3. Box plots of lidar ratio versus integrated total depolarization ratio at 532 nm for different aerosol types. The boxes represent 25 and 75 percentile and whiskers are 5 and 95 percentile.

Lidar ratios are also retrieved using ground-based lidar and AERONET sun/sky radiometer during Distributed Regional Aerosol Gridded Observation Networks (DRAGON) Northeast Asia Campaign 2012. DRAGON NE Asia Campaign was held in Korea and Japan from March to May 2012, composed by NASA AERONET. During the campaign, lidars from the National Institute for Environmental Studies (NIES) of Japan and AERONET sun/sky radiometers were collocated and operated together at six observatories (Seoul, Gosan, Fukue, Osaka, Chiba, and Tsukuba). In this study, lidar ratio is retrieved for Seoul and Osaka where stable measurements were performed for both lidar and sun/sky radiometer during whole campaign period.

Figure 3.4 shows frequency distributions of lidar ratios at Seoul and Osaka during the campaign. Mean (and standard deviation) lidar ratios at Seoul and Osaka were retrieved as 65.41±21.42 sr and 65.04±20.62 sr, respectively. Mean lidar ratios from two observatories are almost same and comparable to the lidar ratio for pollution [e.g., *Ansmann et al.,* 2001; *Cattrall et al.,* 2005; *Barnaba and Gobbi*, 2004], which implies that the dominant aerosol type in those cities during the campaign is polluted aerosol. One difference between the two cities is that the lidar ratios in Seoul have broader range than Osaka.

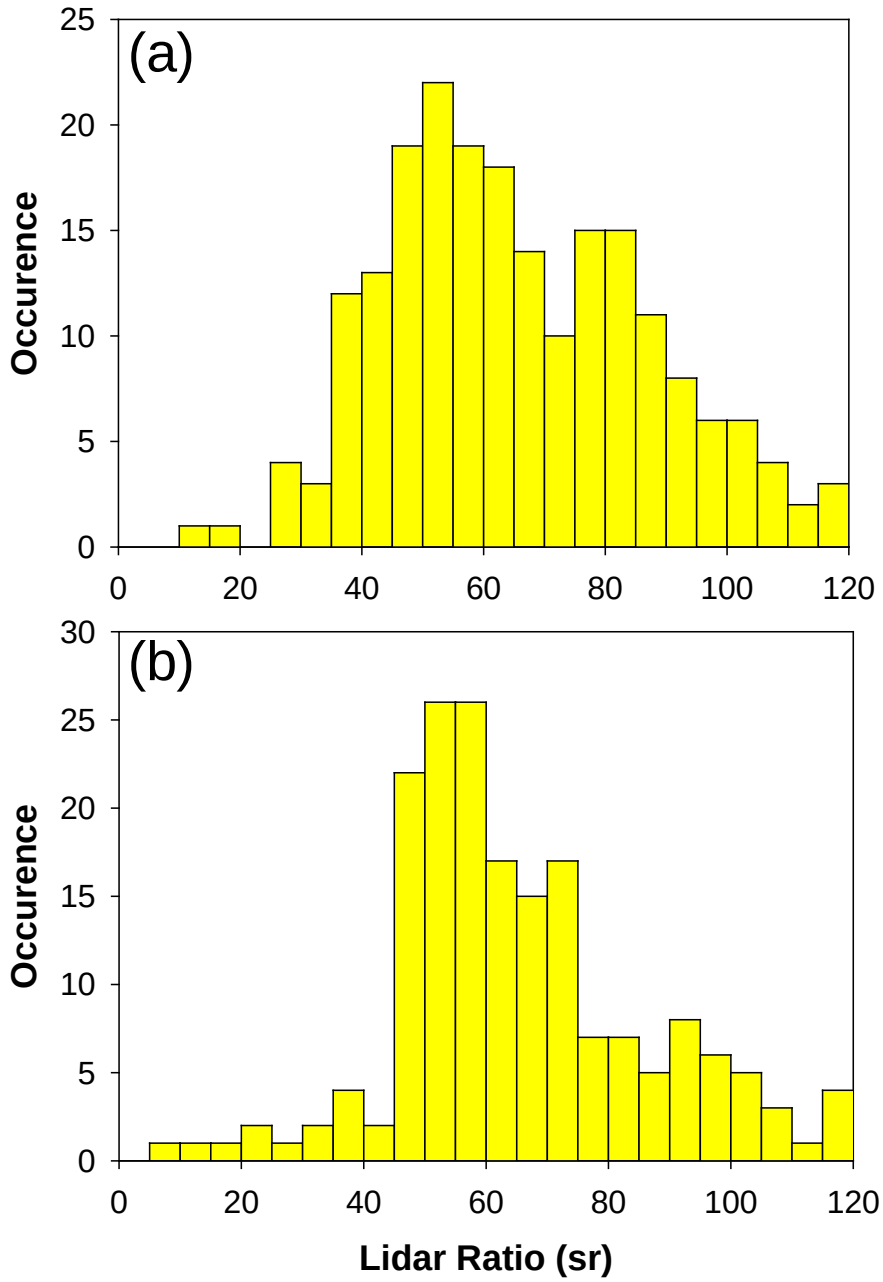

Figure 3.4. Occurrence distribution of lidar ratios retrieved from NIES lidar measurements using collocated AOD as a constraint in (a) Seoul and (b) Osaka during DRAGON NE-Asia Campaign from March to May 2013.

Figure 3.5 and 3.6 are results from lidar and AERONET for dust event during the campaign from April 27 to April 29. Depolarization ratio was small and Ångström exponent was large in Seoul on April 26 (Figure 3.5). This implies that the small and spherical-shaped polluted aerosols were dominant on this day. Then, depolarization ratio increased and Ångström exponent decreased on April 27, which indicates dust plume arrived. Lidar ratios during dust event were retrieved to 40-60 sr (48.02±9.38 sr) which is higher than CALIOP (40 sr). Dust plume passed over Korea and reached Osaka on April 28 (Figure 3.6). Depolarization ratio was increased to ~0.15, but not much large as observed in Seoul. Lidar ratios for dust plume in Osaka are 50~80 sr which are much larger than Seoul. Higher lidar ratios in Osaka than Seoul for dust are due to mixing with polluted aerosols during transport from Korea to Japan. Relatively lower depolarization ratio in Osaka compared to Seoul also shows that dust plume is mixed with spherical-shaped aerosols.

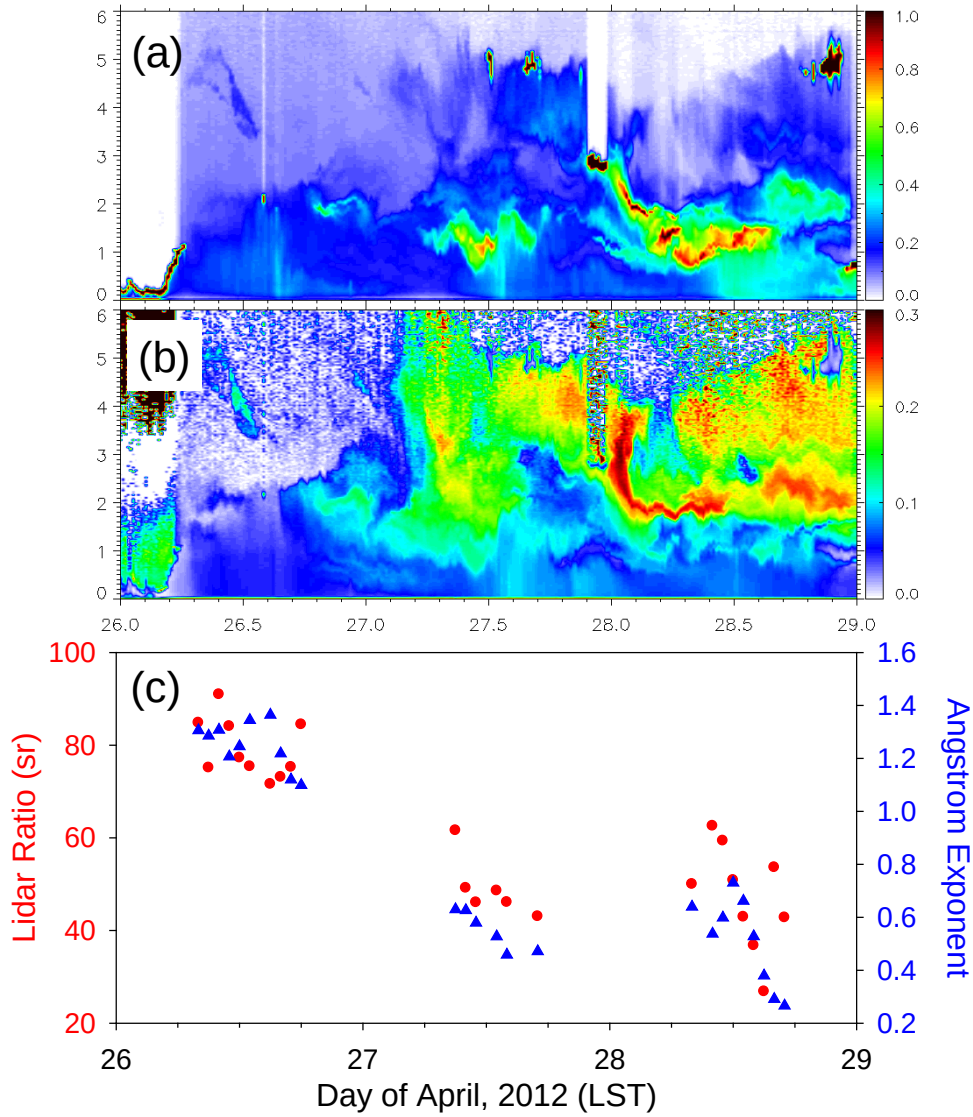

Figure 3.5. (a) Total attenuated backscatter, (b) depolarization ratio, (c) lidar ratios and Ångström exponent from lidar and AERONET measurements in Seoul from 26 to 28 April 2013.

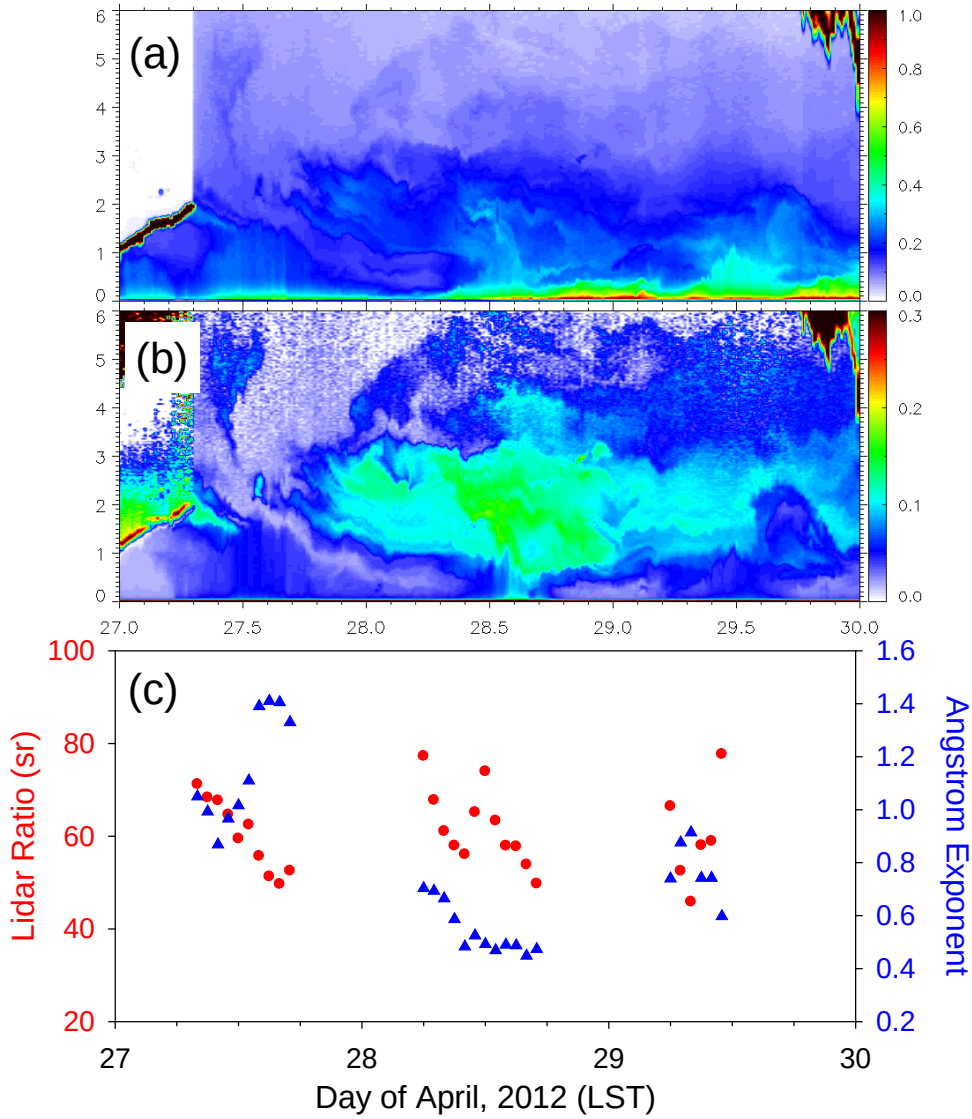

Figure 3.6. Same as Figure 3.5, but in Osaka from 27 to 29 April 2013.

3.4. Determination of lidar ratio from CALIOP and AERONET measurements

Retrieving aerosol extinction from CALIOP is quite different from ground-based lidars as explained in Section 3.2. An iteration method, same as CALIOP level 2 algorithm [*Young and Vaughan*, 2009], was used in this study. To assess the performance of retrieval algorithm, AODs retrieved in this study (AOD_Ret) from CALIOP Level 1 Product were compared AODs from CALIOP Level 2 Product (AOD_CAL). Figure 3.7 is a scatter plot of AOD_Ret and AOD_CAL. 4464 CALIOP profiles for dust aerosol were retrieved in 2010. As mentioned above, CALIOP Level 1 Product has horizontal resolution of 333 m, whereas the horizontal resolution of CALIOP Level 2 Product is 5 km. Thus, fifteen CALIOP Level 1 profiles are averaged to retrieve the aerosol extinction coefficient. To remove surface returns in of CALIOP Level 1 profiles, lidar signals below the surface level were assumed to be zero. Since CALIOP level 2 algorithm retrieves aerosol extinction coefficient only for the detected aerosol layers, the retrieval was performed for same layers.

The linear regression shows that retrieval algorithm used in this study performs properly with the correlation coefficient of 0.975. Only few profiles have large difference between AOD_Ret and AOD_CAL. Most of

these cases are related with failure in separating surface returns.

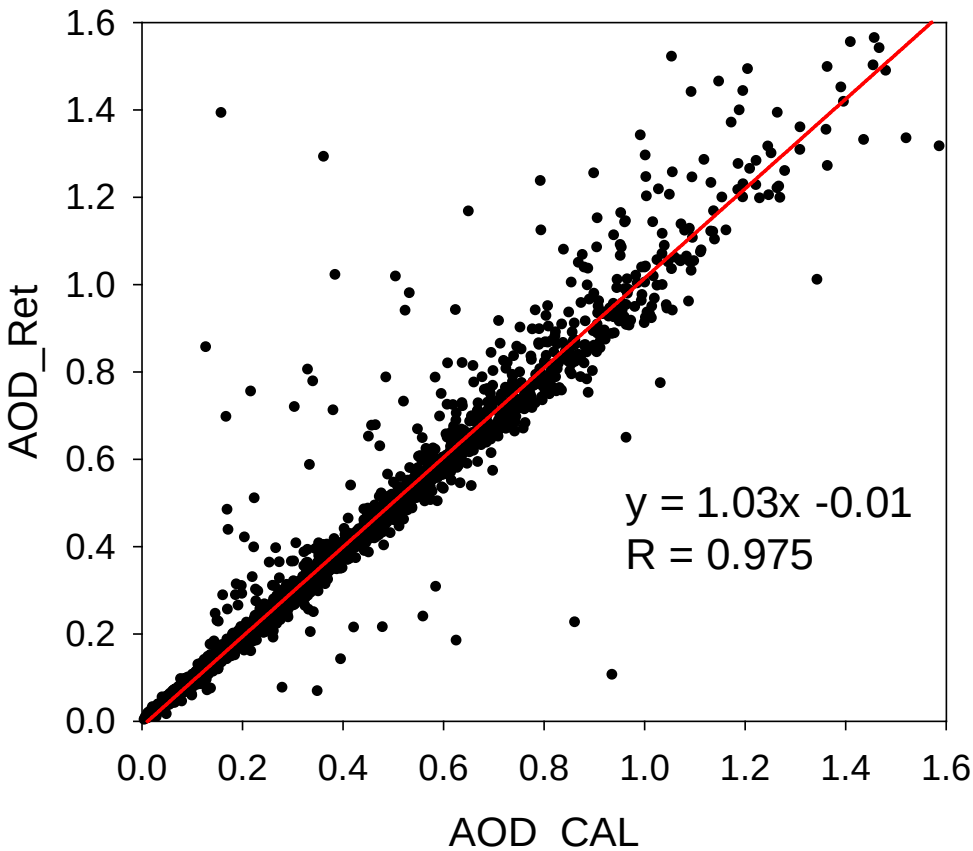

Figure 3.7. Scatter plot of AOD retrieved in this study (AOD_Ret) and CALIOP Level 2 Product (AOD_CAL) for dust aerosols in 2010. Red line represents a linear regression of the data. 4644 profiles have used.

Using the method described in Section 3.2, lidar ratios were retrieved from CALIOP Level 1 Product using AERONET AOD as a constraint for Saharan dust. 15 AERONET sites were chosen where CALIPSO satellite passes nearby. CALIOP profiles within 10 km from AERONET site were selected and AERONET AODs measured within 15 minutes from CALIPSO closest overpass time were averaged. Figure 3.8(a) shows a distribution of retrieved lidar ratio for Saharan dust. The mean (and standard deviation) retrieved lidar ratio was 50.5±19.5 sr. For dust aerosols classified in CALIOP algorithm, the mean lidar ratio decreased to 47.5±16.5 sr (Figure 3.8b). But this value is still larger than currently used lidar ratio for dust in CALIOP algorithm [*Omar et al.*, 2009].

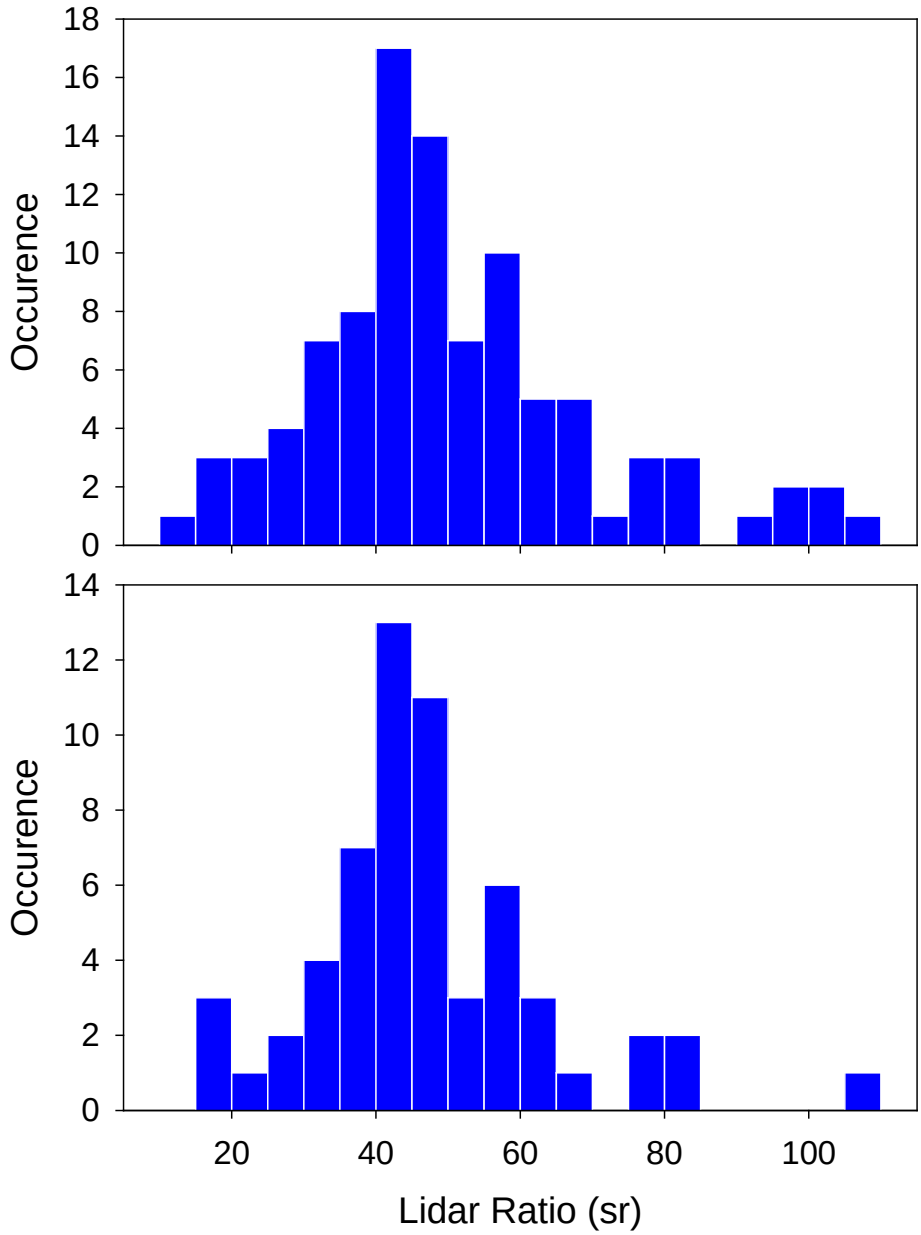

Figure 3.8. Number distribution of retrieved lidar ratios from CALIOP Level 1 Products over near-Saharan AERONET sites for (a) whole retrieved results and for (b) dust aerosols classified in CALIOP algorithm.

3.5. Determination of lidar ratio from CALIOP and MODIS measurements

Aerosol lidar ratio and extinction coefficient are retrieved from CALIOP measurements using MODIS-Aqua AOD as a constraint. CALIOP Level 1 ValStage1 data (Version 3.01) and MODIS-Aqua Level 2 aerosol data (MYD04-L2) are used from January to December 2010. For both instruments, cloud screened and quality assured data over the ocean are used.

Figure 3.9 and 3.10 are examples of CALIOP vertical profiles and retrieved aerosol optical properties. Figure 3.9 shows a typical case of marine boundary aerosol layer. Aerosols are detected from surface to 1~2 km above the surface and most of them classified as clean marine (Figure 3.9d). MODIS AOD is larger than CALIOP AOD for most profiles (Figure 3.9e). Two main differences in aerosol extinction retrieval between AOD constrained method (Figure 3.9c) and CALIOP Level 2 Profile Product (Figure 3.9b) are lidar ratio and retrieving range. In this study, aerosol extinction retrieved for whole profile from the surface to 8.2 km using adjusted lidar ratio, whereas CALIOP Level 2 algorithm retrieves only for detected aerosol layer with pre-determined lidar ratio. Figure 3.9(f) shows

CALIOP lidar ratios have single value of 20 sr for clean marine aerosol, but retrieved lidar ratios have range from 10 sr to 40 sr.

Dust and polluted dust plumes are observed in Figure 3.10. MODIS AOD is generally larger than CALIOP AOD for clean marine aerosols as shown in Figure 3.9. On the other hand, AODs from the two sensors are relatively well matched for dust and polluted dust aerosols (0°-5°N in Figure 3.9). Retrieved liar ratios for dust and polluted dust are relatively larger than clean marine with the range from 20 sr to 60 sr (Figure 3.9f).

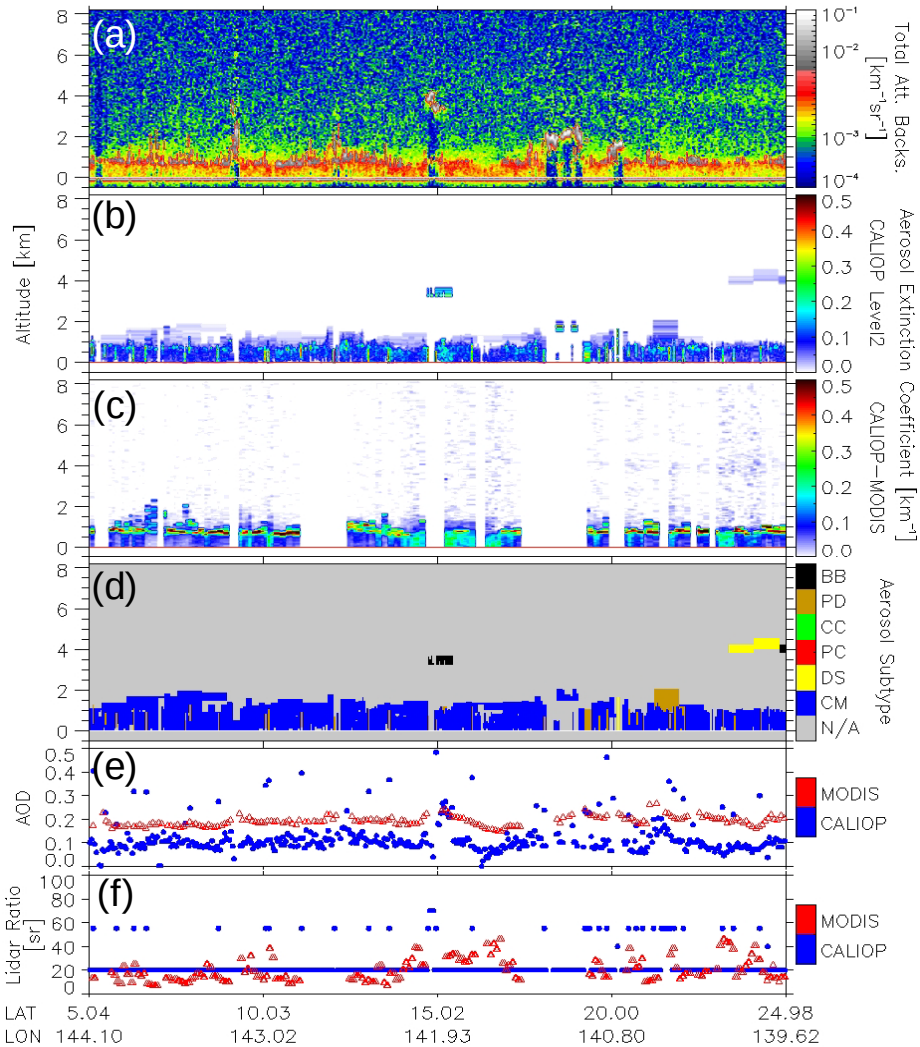

Figure 3.9. (a) Total attenuated backscatter, (b) aerosol extinction from CALIOP Level 2 Product, (c) aerosol extinction retrieved in this study, (d) aerosol subtype (e) aerosol optical depth from MODIS (red triangle) and CALIOP Level 2 Product (blue circle), and (f) lidar ratios for dominant aerosol subtype in CALIOP Level 2 Product (blue circle) and retrieved in this study using MODIS AOD as a constraint (red triangle) observed on 15 March 2010 ~04UTC over Western Pacific.

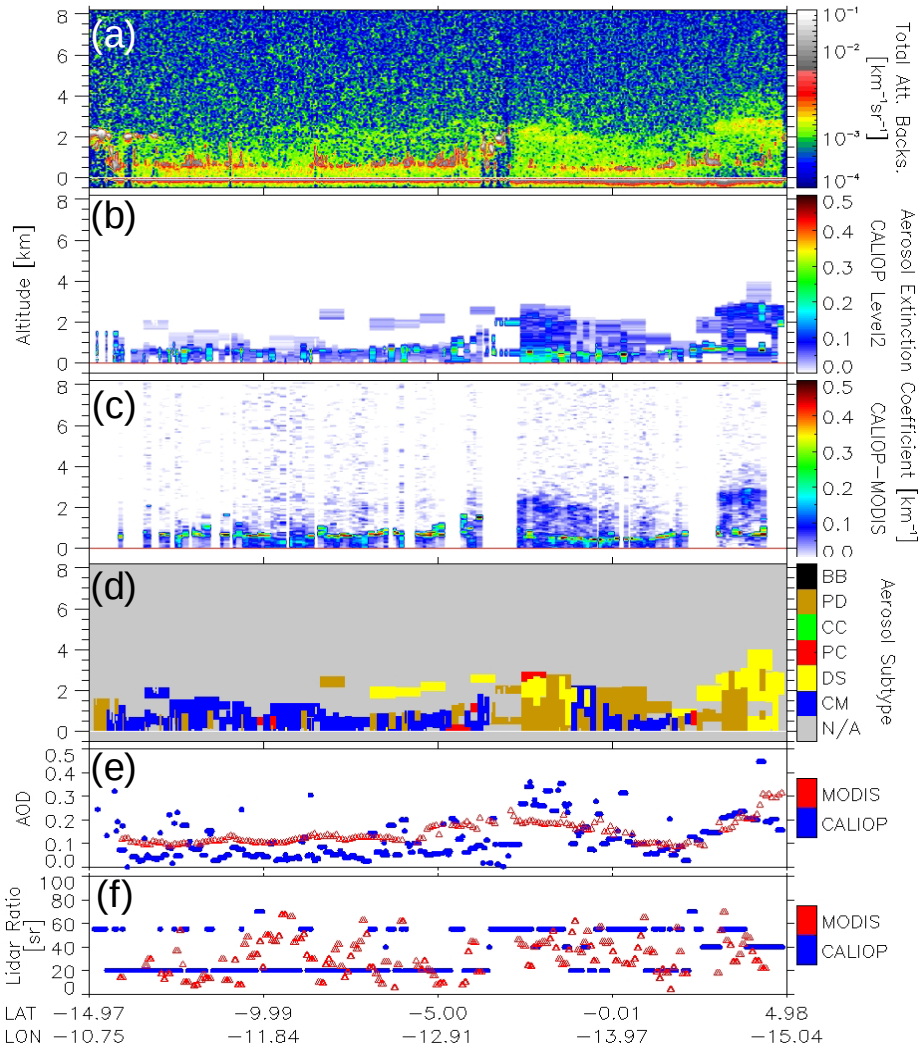

Figure 3.10. Same as Figure 3.9, but observed on 16 March 2010 ~14UTC over Mid Atlantic.

Figure 3.11 and 3.12 show frequency distributions of retrieved lidar ratios using AOD constrained method. Mean value of the retrieved lidar ratios for clean marine (25.66±23.68 sr) is slightly larger than 20 sr which is currently used in CALIOP algorithm (Figure 3.11a). However, its distribution with the median of 20.40 sr, in Figure 3.11(a), shows that currently used lidar ratio (20 ar) and aerosol type classification for clean marine aerosol in CALIOP algorithm is acceptable in spite of large standard deviation.

The mean lidar ratio retrieved from CALIOP and MODIS measurements using AOD constrained method for dust aerosol (46.32±14.44 sr) shows very similar values, shown in Section 3.3 and 3.4, which implies currently used lidar ratio for dust in CALIOP algorithm need to be increased (Figure 3.11b). Especially for Asian dust (110°E - 180°E, 20°N – 50°N), the lidar ratios are retrieved much larger. This result also suggests that the lidar ratios for dust have regional variation as mentioned in Section 2.4.2.

The mean retrieved lidar ratios for polluted dust, biomass burning, and polluted continental aerosols are 47.41±19.57 sr, 59.15±20.69 sr, and 56.91±24.12 sr, respectively, 14-19% less than those values in CALIOP

algorithm (Figure 3.12). The mean lidar ratio for biomass burning was expected to be larger than 70 sr, which is used in CALIOP algorithm, because MODIS AOD is much larger than CALIOP AOD for biomass burning as shown in Section 2.4.5. In this study, however, unlike CALIOP Level 2 algorithm, aerosol extinction retrieval is performed from 8.2 km to the surface not from the layer top altitude to the layer base altitude. As a result, CALIOP AOD can increase compared to CALIOP Level 2 product and the mean lidar ratio can be retrieved less than 70 sr for biomass burning aerosol. This result shows that CALIOP AOD for biomass burning would be larger when the retrieval is performed for whole profile. Thus error in layer detection is a significant source of uncertainty in CALIOP AOD for biomass burning.

Currently used lidar ratios in CALIOP algorithm for polluted dust, polluted continental, and biomass burning aerosols are consistent with other previous studies [e.g., *Ansmann et al.*, 2001; *Voss et al.*, 2001; *Catrall et al.*, 2005]. Therefore, discrepancies in lidar ratios between CALIOP algorithm and this study for those aerosols are thought be due to errors in aerosol type classification rather than errors in lidar ratio itself.

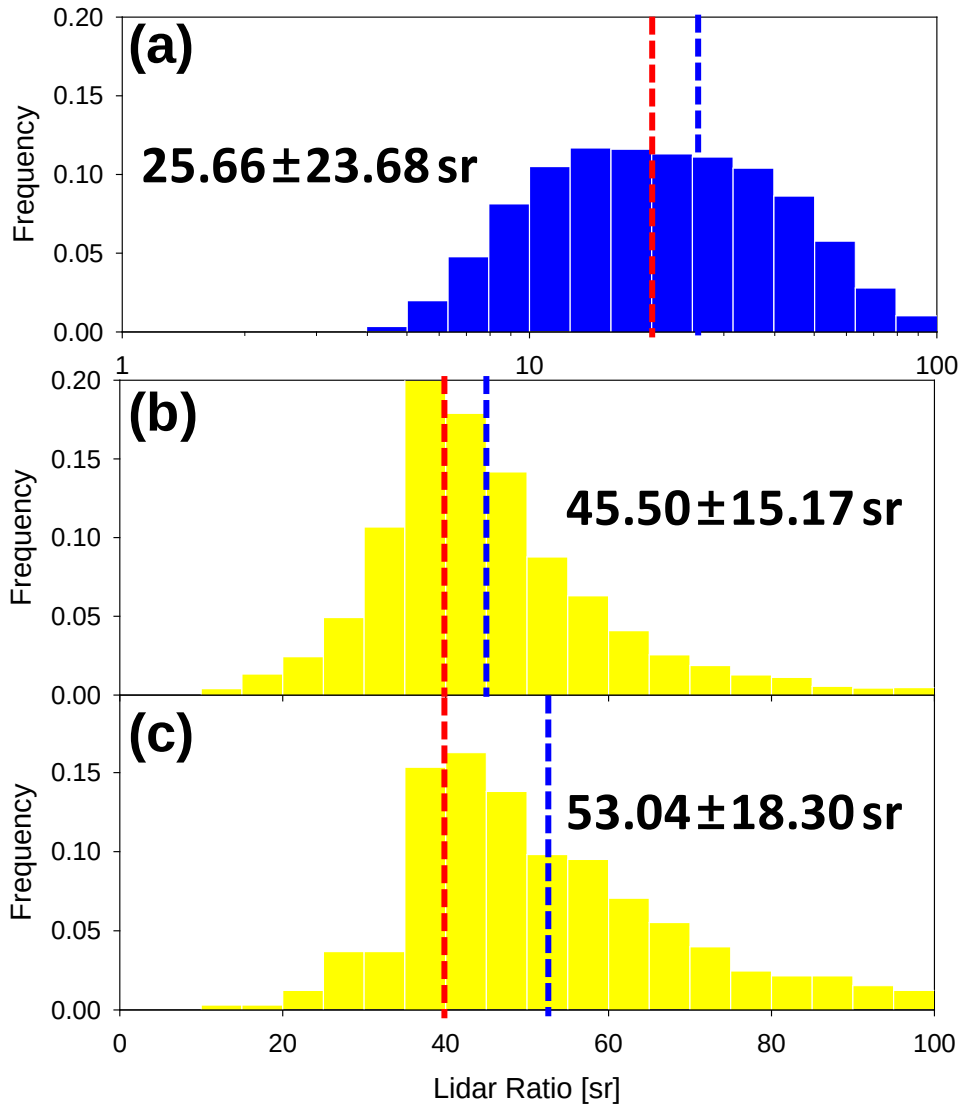

Figure 3.11. Frequency distributions of retrieved lidar ratios from CALIOP and MODIS measurements using AOD constrained method for (a) clean marine (log scale), (b) dust, and (c) Asian dust aerosols. Red and blue dashed lines represent currently used lidar ratios in CALIOP algorithm and mean values retrieved in this study, respectively. Mean (and standard deviation) lidar ratios are also shown.

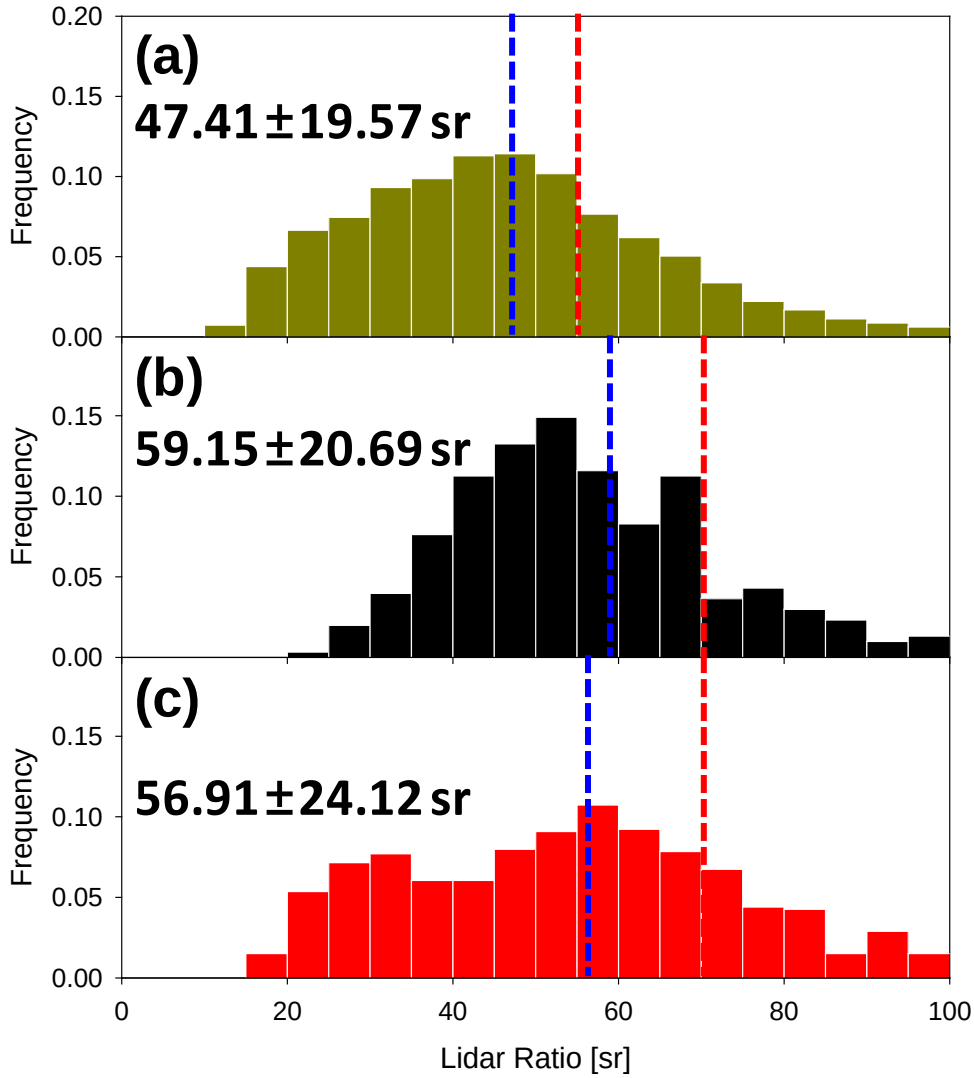

Figure 3.12. Same as Figure 3.11 but for (a) polluted dust, (b) biomass burning, and (c) polluted continental aerosols.

3.6. Summary

Aerosol extinction profile can be retrieved from lidar measurement by solving lidar equation. The Raman lidar technique [*Ansmann et al.*, 1990] and the high spectral resolution lidar (HSRL) technique [*Shipley et al.*, 1983] can derive aerosol extinction profiles needless to assume the S_{aer} by separating aerosol returns from molecular returns. However, the elastic backscatter lidar, which is most commonly used lidar system, cannot derive aerosol extinction directly from the measurement. In order to retrieve aerosol extinction from elastic backscatter lidar, $\boldsymbol{S_{aer}}$ should be determined and it is frequently either assumed or inferred from additional measurements.

Because uncertainty in S_{aer} is the largest source of uncertainty in the CALIOP AOD, it is desirable to improve S_{aer} values used in CALIOP algorithm to retrieve accurate AOD (or aerosol extinction). Current CALIOP level 2 algorithm uses pre-determined $\boldsymbol{S_{aer}}$ for classified aerosol types. However, not only using single values of $\boldsymbol{S_{aer}}$ for each aerosol type but also aerosol classification algorithm could be sources of uncertainties in aerosol extinction retrieval. In this study, to improve currently used $\boldsymbol{S_{aer}}$ in CALIOP level 2 algorithm, $\boldsymbol{S_{aer}}$ is determined

from CALIOP by using AOD from AERONET and MODIS-Aqua as a constraint without any assumption.

Using 4-year measurements (2006-2010) of elastic-backscatter lidar and SKYNET sun/sky radiometer at Seoul National University of Seoul, Korea, mean lidar ratio is estimated to be 61.7±16.5 sr. Lidar ratios are also retrieved using ground-based lidar and AERONET sun/sky radiometer during Distributed Regional Aerosol Gridded Observation Networks (DRAGON) Northeast Asia Campaign 2012. Mean lidar ratios at Seoul and Osaka were retrieved as 65.41±21.42 sr and 65.04±20.62 sr, respectively. Mean lidar ratios from Seoul and Osaka, which are metropolitan cities in East Asia, are almost same and comparable to the lidar ratio for pollution used in CALIOP algorithm (70 sr).

Dust aerosol is easily recognized from depolarization ratio measurements due to its non-spherical shape. *Burton et al.* [2013] reported that aerosol type classification for dust is the most accurate in CALIOP algorithm. For this reason, lidar ratios are retrieved mainly focused on dust aerosol and compared other studies and CALIOP Level 2 Product. The lidar ratio for dust conditions are estimated to be 51.7±13.7 sr using 4-year measurements of elastic-backscatter lidar and SKYNET sun/sky

radiometer at Seoul National University of Seoul, Korea. During DRAGON 2012 NE Asia campaign, lidar ratio for dust event on 27-28 April 2012 in Seoul is retrieved as 48.02±9.38 sr from elastic-backscatter lidar and AERONET sun/sky radiometer. From a synergy of CALIOP and AERONET, lidar ratio for Saharan/Arabian dust is derived to be 47.45±16.52 sr. Lastly, using CALIOP and MODIS measurements together, dust lidar ratio is retrieved as 45.50±15.17 sr. All the lidar ratios for dust aerosol retrieved in this study using AOD constrained method show larger values than currently used lidar ratio for dust in CALIOP algorithm (40 sr), which suggests that dust lidar ratio in CALIOP algorithm is underestimated and needs to be increased. Moreover, the retrieved lidar ratio for Asian dust (110°E - 180°E, 20°N – 50°N) appears as 53.04±18.30 sr, which is much larger than global mean of dust lidar ratio (45.50±15.17 sr). This result implies that the lidar ratios for dust have regional variation.

CHAPTER 4.
SUMMARY AND FURTHERWORKS

Aerosol extinction profile is one of the most important parameter to estimate aerosol radiative forcing, especially when calculating atmospheric heating by aerosol. CALIOP is a very useful instrument that provides aerosol vertical profiles over the glove. However, current CALIOP-derived AOD (or aerosol extinction) has large uncertainty compared to other passive sensors. The expected error for CALIOP AOD is ±0.05 ± 40% over both land and ocean [*Winker et al.*, 2009; *Omar et al.*, 2013], whereas the MODIS AOD retrieval has less uncertainties, with expected errors of ±0.03 ± 5% over ocean and ±0.05 ± 15% over land [*Remer et al.*, 2005; *Levy et al.*, 2010].

In order to retrieve the aerosol extinction coefficient (or AOD) from CALIOP measurements, the aerosol type is determined *a priori* so that a type-specific lidar ratio can be assigned to the aerosol layer. The lidar ratio is an essential parameter for aerosol extinction coefficient retrievals from elastic lidar measurements [*Fernald*, 1984]. Errors in the *a priori* prescription of this value can thus induce large errors in the retrieved AOD.

Therefore, when validating CALIOP AOD using other instruments, errors associated with aerosol type or ‘lidar ratio’ should be considered. The validation of CALIOP AOD by segregating aerosol type can lead to an improvement of the accuracy of aerosol type classification and lidar ratio determination in CALIOP algorithm.

Nearly two million collocated AOD data pairs over oceans from CALIOP and MODIS from June 2006 to December 2010 have been compared to evaluate the CALIOP AODs in this study. The mean MODIS AOD is 61% larger than that of CALIOP AOD. When considering aerosol types defined in CALIOP algorithm, the differences in AOD between the two sensors show some dependence on the type of aerosol. MODIS AOD is higher than CALIOP AOD for most aerosol types except for polluted dust and polluted continental.

The AOD comparison between CALIOP and MODIS shows that the CALIOP algorithms can increase the accuracy of the Asian dust AODs by adopting regionally variable dust lidar ratios. Additionally, an examination of the layer base altitude for smoke layers and comparing with independent measurements to determine what corrections if any to the calculation of the AOD for smoke are warranted. As the study has shown,

the effect of the daytime SNR on the depolarization ratio has important consequences for the aerosol classification scheme.

It is desirable to improve lidar ratios used in CALIOP algorithm to retrieve accurate AOD (or aerosol extinction) because the lidar ratio is a crucial source of uncertainties in CALIOP aerosol retrieval. In this study, lidar ratios were retrieved from CALIOP measurements using independently measured AOD from AERONET and MODIS as a constraint. By comparing retrieved lidar ratios with pre-determined lidar ratios in CALIOP algorithm for each aerosol type, the accuracy of currently used lidar ratio in CALIOP algorithm will be assessed and the algorithm for determining lidar ratio and classifying aerosol types will be improved.

Lidar ratios for dust are retrieved as 51.7±13.7 sr and 48.02±9.38 sr from ground-based elastic lidar and sun/sky radiometer measurements. The CALIOP-derived lidar ratio for dusts using AODs from AERONET and MODIS are found to be 47.45±16.52 sr and 46.32±14.44 sr, respectively. These results are larger than currently used lidar ratio for dust in CALIOP algorithm (40 sr), which suggests that currently used lidar ratio for dust in CALIOP algorithm needs to be increased. Moreover,

retrieved lidar ratio for Asian dust is estimated to be 53.04±18.30 sr from a synergy of CALIOP and MODIS, which is much larger than other regions. This result implies that the lidar ratios for dust have regional variation.

Although aerosol lidar ratios used in CALIOP algorithm have relatively large uncertainty (lager then 30% as shown in *Young et al.*. [2013]), their mean values are consistent with other previous studies (e.g., *Ansmann et al.*, [2001], *Voss et al.*, [2001], *Catrall et al.*, [2005]). Thus, in order to produce more accurate AOD and aerosol extinction from CALIOP measurements, it is reliable to improve the aerosol type classification in CALIOP algorithm, except for dust aerosol which is classified accurately compared to other types. Several results reported in this study can provide suggestions to improve aerosol type classification in CALIOP algorithm.

REFERENCES

Ackerman, S. A., K. I. Strabala, W. P. Menzel, R. A. Frey, C. C. Moeller, and L. E. Gumley, 1998: Discriminating clear sky from clouds with MODIS, *J. Geophys. Res.*, 103(D24), 32141–32157, doi:10.1029/1998JD200032.

Anderson, J. C., J. Wang, J. Zeng, M. Petrenko, G. G. Leptoukh, and C. Ichoku, 2012: Accuracy assessment of Aqua-MODIS aerosol optical depth over coastal regions: importance of quality flag and sea surface wind speed, *Atmos. Meas. Tech. Discuss.*, 5, 5205-5243, doi:10.5194/amtd-5-5205-2012.

Ansmann, A., F. Wagner, D. Althausen, D. Müller, A. Herber, and U. Wandinger, 2001: European pollution outbreaks during ACE 2: Lofted aerosol plumes observed with Raman lidar at the Portuguese coast, *Journal of Geophysical Research*, **106**, 20725–20733, doi:10.1029/2000JD000091.

Barnaba, F., and G. P. Gobbi, 2004: Modeling the aerosol extinction versus backscatter relationship for lidar applications: Maritime and continental conditions, *J. Atmos. Oceanic Technol.*, **21**, 428–442.

Boucher, O., D. Randall, P. Artaxo, C. Bretherton, G. Feingold, P. Forster, V.-M. Kerminen, Y. Kondo, H. Liao, U. Lohmann, P. Rasch, S. K. Satheesh, S. Sherwood, B. Stevens and X. Y. Zhang, 2013: Clouds and Aerosols. In: Climate Change 2013: The Physical Science Basis. Contribution of Working Group I to the Fifth Assessment Report of the Intergovernmental Panel on Climate Change [Stocker, T. F.,D. Qin, G.-K. Plattner, M. Tignor, S. K. Allen, J. Boschung, A. Nauels, Y. Xia, V. Bex and P. M. Midgley (eds.)]. *Cambridge University Press, Cambridge*, United Kingdom and New York, NY, USA, in press.

Bréon, F-M., A. Vermeulen, and J. Descloitres, 2011: An evaluation of satellite aerosol products against sunphotometer measurements, *Remote Sens. Environ.*, 115, 3102-3111, doi:10.1016/j.rse.2011.06.017.

Burton, S. P., R. A. Ferrare, M. A. Vaughan, A. H. Omar, R. R. Rogers, C. A. Hostetler, and J. W. Hair, 2013: Aerosol classification from airborne HSRL and comparisons with the CALIPSO vertical feature mask, *Atmos. Meas. Tech. Discuss.*, 6, 1815-1858, doi:10.5194/amtd-6-1815-2013.

Burton, S. P., R. A. Ferrare, C. A. Hostetler, J. W. Hair, C. Kittaka, M. A. Vaughan, M. D. Obland, R. R. Rogers, A. L. Cook, D. B. Harper, and L. A. Remer, 2010: Using airborne high spectral resolution lidar data to evaluate combined active plus passive retrievals of aerosol extinction profiles, *Journal of Geophysical Research*, **115**, D00H15, doi:10.1029/2009JD012130.

Campbell, J. R., J. L. Tackett, J. S. Reid, J. Zhang, C. A. Curtis, E. J. Hyer, W. R. Sessions, D. L. Westphal, J. M. Prospero, E. J. Welton, A. H. Omar, M. A. Vaughan, and D. M. Winker, 2012: Evaluating nighttime CALIOP 0.532 μm aerosol optical depth and extinction coefficient retrievals, *Atmos. Meas. Tech.*, 5, 2143-2160, doi:10.5194/amt-5-2143-2012.

Campbell, J. R., J. S. Reid, D. L. Westphal, J. L. Zhang, J. L. Tackett, B. N. Chew, E. J. Welton, A. Shimizu, N. Sugimoto, K. Aoki, and D. M. Winker, 2013: Characterizing the vertical profile of aerosol particle extinction and linear depolarization over Southeast Asia and the Maritime Continent: The 2007-2009 view from CALIOP, *Atmos. Res.*, 122, 520-543.

Cattrall, C., J. Reagan, K. Thome, and O. Dubovik, 2005: Variability of aerosol and spectral lidar and backscatter and extinction ratios of key aerosol types derived from selected Aerosol Robotic Network locations, *J. Geophys. Res.*, 110, D10S11, doi:10.1029/2004JD005124.

Chazette, P., J.-C. Raut, F. Dulac, S. Berthier, S.-W. Kim, P. Royer, J. Sanak, S. Loaec, and H. Grigaut-Desbrosses, 2010: Simultaneous observations of lower tropospheric continental aerosols with a ground-based, an airborne, and the spaceborne CALIOP lidar systems, *J. Geophys. Res.*, 115, D00H31, doi:10.1029/2009JD012341.

Doherty, Sarah J., Theodore L. Anderson, and Robert J. Charlson, 1999: Measurement of the Lidar Ratio for Atmospheric Aerosols with a 180° Backscatter Nephelometer, *Applied Optics*, **38**, 1823-1832.

Dubovik, O., A. Sinyuk, T. Lapyonok, B. N. Holben, M. Mishchenko, P. Yang, T. F. Eck, H. Volten, O. Munoz, B. Veihelmann, van der Zander, M Sorokin, and I. Slutsker, 2006: Application of spheroid models to account for aerosol particle nonsphericity in remote sensing of desert dust, *Journal of Geophysical Research*, **111**, D11208, doi:10.1029/2005JD006619.

Duncan, B. N., R. V. Martin, A. C. Staudt, R. Yevich, and J. A. Logan, 2003: Interannual and seasonal variability of biomass burning emissions constrained by satellite observations, *J. Geophys. Res.*, 108(D2), 4100, doi:10.1029/2002JD002378.

Eck, T., B. N. Holben, J. Reid, O. Dubovik, A. Smirnov, N. O'Neill, I. Slutsker, and S. Kinne, 1999: Wavelength dependence of the optical depth of biomass burning, urban, and desert dust aerosols, *J. Geophys. Res.*, 104(D24), 31333– 31349.

Fernald, F. G., 1984: Analysis of atmospheric lidar observations: some comments, *Applied Optics*, **23**, 652-653.

Freudenthaler, V., M. Esselborn, M. Wiegner, B. Heese, M. Tesche, A. Ansmann, D. Muller, D. Althausen, M. Wirth, A. Fix, G. Ehret, P. Knippertz, C. Toledano, J. Gasteiger, M. Garhammer, and M. Seefeldner, 2009: Depolarization ratio profiling at several wavelengths in pure Saharan dust during SAMUM 2006, *Tellus B*, 61, 165–179. doi: 10.1111/j.1600-0889.2008.00396.

Hansen, J.E., M. Sato and R. Ruedy, 1997: Radiative forcing and climate response. *Journal of Geophysical Research*, **102**, 6831-6864, 1997.

Huang, J., Q. Fu, J. Su, Q. Tang, P. Minnis, Y. Hu, Y. Yi, and Q. Zhao, 2009: Taklimakan dust aerosol radiative heating derived from CALIPSO observations using the Fu-Liou radiation model with CERES constraints, *Atmospheric Chemistry and Physics*, **9**, 4011–4021.

Hubanks, P. A., 2012: MODIS Atmosphere QA Plan for Collection 005 and 051, 63 pp., available at: http://modis-atmos.gsfc.nasa.gov/_docs/QA_Plan_2012_01_12.pdf.

Jeong, Myeong-jae and Zhanqing Li, 2005: Quality, compatibility, and synergy analyses of global aerosol products derived from the advanced very high resolution radiometer and Total Ozone Mapping Spectrometer, Journal of Geophysical Research, 110, D10S08, doi:10.1029/2004JD004647.

Jung, J.,, Y. J. Kim, K. Y. Lee, M. G.-Cayetano, T. Batmunkh, J.-H. Koo, and J. Kim, 2010: Spectral optical properties of long-range transport Asian dust and pollution aerosols over Northeast Asia in 2007 and 2008, Atmospheric Chemistry and Physics, 10, 5391–5408, doi:10.5194/acp-10-5391-2010.

Kacenelenbogen, M., M. A. Vaughan, J. Redemann, R. M. Hoff, R. R. Rogers, R. A. Ferrare, P. B. Russell, C. A. Hostetler, J. W. Hair, and B. N. Holben, 2011: An accuracy assessment of the CALIOP/CALIPSO version 2/version 3 daytime aerosol extinction product based on a detailed multi-sensor, multi-platform case study, *Atmos. Chem. Phys.*, 11, 3981-4000, doi:10.5194/acpd-10-27967-2010.

Kahn, R. A., Y. Chen, D. L. Nelson, F.-Y. Leung, Q. Li, D. J. Diner, and J. A. Logan, 2008: Wildfire smoke injection heights: Two perspectives from space, *Geophysical Research Letters*, **35**, L04809, doi:10.1029/2007GL032165.

Kai, K., Y. Nagata, N. Tsunematsu, T. Matsumura, H.-S. KIM, T. Matsumoto, S. Hu, H. Zhou, M. Abo, and T. Nagai, 2008: The Structure of the dust layer over the Taklimakan Desert during the dust storm in April 2002 as observed using a depolarization lidar, *J. Meteor. Soc. Japan*, 86, 1-16.

Kaufman, Y. J., J. M. Haywood, P. V. Hobbs, W. Hart, R. Kleidman, and B. Schmid, 2003: Remote sensing of vertical distributions of smoke

aerosol off the coast of Africa, *Geophysical Research Letters*, **30(16)**, 1831, doi:10.1029/2003GL017068.

Kim, S.-W., S. Berthier, P. Chazette, J.-C. Raut, F. Dulac, and S.-C. Yoon, 2008: Validation of aerosol and cloud layer structures from the space-borne lidar CALIOP using Seoul National University ground-based lidar, *Atmos. Chem. Phys.*, 8, 3705-3720.

Kim, S.-W., E.-S. Chung, S.-C. Yoon, B.-J. Sohn, and N. Sugimoto, 2011: Intercomparisons of cloud-top and cloud-base heights from ground-based Lidar, CloudSat and CALIPSO measurements, *Int. J. Remote Sens.*, 32, 1179-1197, doi:10.1080/01431160903527439.

King, M., J. Closs, S. Spangler, R. Greenstone, S. Wharton, and M. Myers, 2004: *EOS Data Products Handbook.* Vol. 1. EOS Project Science Office, NASA Goddard Space Flight Center, Greenbelt, MD, 260 pp. [Available from EOS Project Science Office, Code 900, NASA Goddard Space Flight Center, Greenbelt, MD 20771; or online at http://eospso.gsfc.nasa.gov/ftp_docs/data_products_1.pdf.]

Kittaka, C., D. M. Winker, M. A. Vaughan, A. Omar, and L. A. Remer, 2010: Intercomparison of CALIOP and MODIS aerosol optical

depth retrievals, *Atmospheric Measurement Techniques*, **4**, 131–141, doi:10.5194/amt-4-131-2011

Klett, J. D., 1981: Stable analytical inversion solution for processing lidar returns, *Applied Optics*, **20(2)**, 211-220.

L'Ecuyer, T. S., and J. H. Jiang, 2010: Touring the atmosphere aboard the A-Train, *Phys. Today*, 63(7), 36–41, doi:10.1063/1.3463626.

Léon, J.-F., D. Tanré, J. Pelon, Y. J. Kaufman, J. M. Haywood, and B. Chatenet, 2003: Profiling of a Saharan dust outbreak based on a synergy between active and passive remote sensing, *Journal of Geophysical Research*, **108(D18)**, 8575, doi:10.1029/2002JD002774.

Levy, R. C., L. A. Remer, J. V. Martins, Y. J. Kaufman, A. Plana-Fattori, J. Redemann, and B. Wenny, 2005: Evaluation of the MODIS aerosol retrievals over ocean and land during CLAMS, *J. Atmos. Sci.*, 62(4), 974-992.

Levy, R. C., L. A. Remer, R. G. Kleidman, S. Mattoo, C. Ichoku, R. Kahn, and T. F. Eck, 2010: Global evaluation of the Collection 5 MODIS dark-target aerosol products over land, *Atmos. Chem. Phys.*, 10, 10399–10420, doi:10.5194/acp-10-10399-2010.

Liu, Z., N. Sugimoto, and T. Murayama, 2002: Extinction-To-Backscatter Ratio of Asian Dust Observed With High-Spectral-Resolution Lidar and Raman Lidar, *App. Opt.*, 41, 2760-2767.

Liu, Z. Y., M. Vaughan, D. Winker, C. Kittaka, B. Getzewich, R. Kuehn, A. Omar, K. Powell, C. Trepte, and C. Hostetler, 2009: The CALIPSO lidar cloud and aerosol discrimination: Version 2 algorithm and initial assessment of performance, *J. Atmos. Ocean. Tech.*, 26, 1198–1213.

McPherson, C. J., J. A. Reagan, J. Schafer, D. Giles, R. Ferrare, J. Hair, and C. Hostetler, 2010: AERONET, airborne HSRL, and CALIPSO aerosol retrievals compared and combined: A case study, *Journal of Geophysical Research*, **115**, D00H21, doi:10.1029/2009JD012389.

Mielonen, T., A. Arola, M. Komppula, J. Kukkonen, J. Koskinen, G. de Leeuw, and K. E. J. Lehtinen, 2009: Comparison of CALIOP Level 2 aerosol subtypes to aerosol types derived from AERONET inversion data, *Geophys. Res. Lett.*, 36, L18804, doi:10.1029/2009GL039609.

Misra, Amit, S. N. Tripathi, D. S. Kaul, Ellsworth J. Welton, 2012: Study of MPLNET-Derived Aerosol Climatology over Kanpur, India, and Validation of CALIPSO Level 2 Version 3 Backscatter and Extinction Products, *J. Atmos. Oceanic Technol.*, 29, 1285-1294.

Müller, D., F. Wagner, D. Althausen, U. Wandinger, and A. Ansmann, 2000: Physical properties of the Indian aerosol plume derived from six-wavelength lidar observations on 25 March 1999 of the Indian Ocean Experiment, *Geophys. Res. Lett.*, **27**, 1403–1406.

Murayama, T., S. Masonis, J. Redemann, T. L. Anderson, B. Schmid, J. M. Livingston, P. B. Russell, B. Huebert, S. G. Howell, C. S. McNaughton, A. Clarke, M. Abo, A. Shimizu, N. Sugimoto, M. Yabuki, H. Kuze, S. Fukagawa, K. Maxwell-Meier, R. J. Weber, D. A. Orsini, B. Blomquist, A. Bandy, and D. Thornton, 2003: An intercomparison of lidar-derived aerosol optical properties with airborne measurements near Tokyo during ACE-Asia, *J. Geophys. Res.*, 108(D23), 8651, doi:10.1029/2002JD003259.

Noh, Y. M., Y. J. Kim, B. C. Choi, and T. Murayama, 2007: Aerosol lidar ratio characteristics measured by a multi-wavelength Raman lidar system at Anmyeon Island, Korea, *Atmos. Res.*, 86, 76-87, doi:10.1016/j.atmosres.2007.03.006.

O'Dowd, C., C. Scannell, J. Mulcahy, and S. G. Jennings, 2010: Wind speed influences on marine aerosol optical depth, *Adv. Meteorol.*, 2010, 830846, doi:10.1155/2010/830846.

Omar A. H., D. M. Winker, C. Kittaka, M. A. Vaughan, Z. Lou, Y. Hu, C. R. Trepte, R. R. Rogers, R. A. Ferrare, K-P Lee, R. E. Kuehn, and Chris A. Hostetler, 2009: The CALIPSO Automated Aerosol Classification and Lidar Ratio Selection Algorithm, *Journal of Atmospheric and Oceanic Technology*, **26**, 1994–2014, doi: 10.1175/2009JTECHA1231.1.

Omar, A. H., J.-G. Won, D. M. Winker, S.-C. Yoon, O. Dubovik, and M. P. McCormick, 2005: Development of global aerosol models using cluster analysis of Aerosol Robotic Network (AERONET) measurements. *Journal of Geophysical Research*, **110**, D10S14, doi:10.1029/2004JD004874.

Omar, A. H., D. M. Winker, J. L. Tackett, D. M. Giles, J. Kar, Z. Liu, M. A. Vaughan, K. A. Powell, and C. R. Trepte, 2013: CALIOP and AERONET aerosol optical depth comparisons: One size fits none, *J. Geophys. Res.*, 118, 1-19, doi:10.1002/jgrd.50330.

Oo, M., R. Holz, 2011: Improving the CALIOP aerosol optical depth using combined MODIS-CALIOP observations and CALIOP integrated attenuated total color ratio, *Journal of Geophysical Research*, **116**, D14201, doi:10.1029/ 2010JD014894

Ramana, M. V., V. Ramanathan, Y. Feng, S-C. Yoon, S-W. Kim, G. R.

Carmichael and J. J. Schauer, 2010: Warming influenced by the ratio of black carbon to sulphate and the black-carbon source, *Nature Geoscience*, **3**, 542–545, doi:10.1038/ngeo918.

Ramanathan, V., M. V. Ramana, G. Roberts, D. Kim, C. Corrigan, C. Chung, and D. Winker, 2007: Warming trends in Asia amplified by brown cloud solar absorption, *Nature*, **448**, 575–578, doi:10.1038/nature06019.

Remer, L. A., Y. J. Kaufman, D. DTanr´e, S. Mattoo, D.A. Chu, J. V. Martins, R.-R. Li, C. Cichoku, R. C. Levy, R. G. Kleidman, T. F. Eck, E. Vermote, and B. N. Holben, 2005: The MODIS Aerosol Algorithm, Products, and Validation, *Journal of Atmospheric Science*, **62**, 947–973.

Sasano, Y., E. V. Browell, and S. Ismail, 1985: Error caused by using a constant extinction/backscattering ratio in the lidar solution, *Applied Optics*, **24**, 3929-3932.

Schuster, G. L., O. Dubovik, and B. N. Holben, 2006: Angstrom exponent and bimodal aerosol size distributions, *J. Geophys. Res.*, 111, D07207, doi:10.1029/2005JD006328.

Schuster, G. L., M. Vaughan, D. MacDonnell, W. Su, D. Winker, O. Dubovik, T. Lapyonok, and C. Trepte, 2012: Comparison of CALIPSO aerosol optical depth retrievals to AERONET measurements, and a climatology for the lidar ratio of dust, *Atmos. Chem. Phys.*, 12, 7431-7452, doi:10.5194/acp-12-7431-2012, 2012.

Shipley, S. T., D. H. Tracy, E. W. Eloranta, J. T. Tauger, J. T. Sroga, F. L. Roesler, and J. A. Weinman, 1983: High spectral resolution lidar to measure optical scattering properties of atmospheric aerosols. 1: Theory and instrumentation, *Applied Optics*, **22**, 3716-3724.

Smirnov, A., A. M. Sayer, B. N. Holben, N. C. Hsu, S. M. Sakerin, A. Macke, N. B. Nelson, Y. Courcoux, T. J. Smyth, P. Croot, P. K. Quinn, J. Sciare, S. K. Gulev, S. Piketh, R. Losno, S. Kinne, and V. F. Radionov, 2012: Effect of wind speed on aerosol optical depth over remote oceans, based on data from the Maritime Aerosol Network, *Atmos. Meas. Tech.*, 5, 377-388, doi:10.5194/amt-5-377-2012.

Sugimoto, N., I. Matsui, A. Shimizu, I. Uno, K. Asai, T. Endoh, and T. Nakajima, 2002: Observation of dust and anthropogenic aerosol plumes in the Northwest Pacific with a two-wavelength polarization

lidar on board the research vessel Mirai, *Geophys. Res. Lett.*, 29(19), 1901, doi:10.1029/2002GL015112.

Tanré, D., Y. J. Kaufman, M. Herman, and S. Mattoo, 1997: Remote sensing of aerosol properties over oceans using the MODIS/EOS spectral radiances, *J. Geophys. Res.*, 102, 16971–16988.

Vaughan, M. A., D. M. Winker, and K. A. Powell, 2005: CALIOP algorithm theoretical basis document— Part 2: Feature Detection and Layer Properties Algorithms, Release 1.01, PC-SCI-202, *NASA Langley Research Center*, Hampton, VA, 87pp.

Vaughan, M. A, K. A. Powell, R. E. Kuehn, S. A. Young, D. M. Winker, C. A. Hostetler, W. H. Hunt, Z. Liu, M. J. McGill, and B. J. Getzewich, 2009: Fully Automated Detection of Cloud and Aerosol Layers in the CALIPSO Lidar Measurements, *Journal of Atmospheric and Oceanic Technology*, **26**, 2034–2050, doi: 10.1175/2009JTECHA1228.1.

Voss, K. J., E. J. Welton, P. K. Quinn, J. Johnson, A. M. Thompson, and H. R. Gordon, 2001: Lidar measurements during Aerosols99, *J. of Geophys. Res.*, 106, 20821–20831, doi:10.1029/2001JD900217.

Welton, E. J., Voss, K. J., Gordon, H. R., Maring, H., Smirnov, A., Holben, B., Schmid, B., Livingston, J. M., Russell, P. B., Durkee, P. A., Formenti, P. and Andreae, M. O., 2000: Ground-based lidar measurements of aerosols during ACE-2: instrument description, results, and comparisons with other ground-based and airborne measurements. *Tellus B*, **52**, 636–651, doi:10.1034/j.1600-0889.2000.00025.

Winker, D. M., J. Pelon, and M. P. McCormick, 2003: The CALIPSO mission: Spaceborne lidar for observations of aerosols and clouds. Lidar Remote Sensing for Industry and Environment Monitoring III, U. N. Singh, T. Itabe, and Z. Liu, Eds., *International Society for Optical Engineering (SPIE Proceedings, Vol. 4893)*, doi:10.1117/12.466539.

Winker, D. M., M. A. Vaughan, A. Omar, Y. Hu, K. A. Powell, Z. Liu, W. H. Hunt, and S. A. Young, 2009: Overview of the CALIPSO Mission and CALIOP Data Processing Algorithms, *Journal of Atmospheric and Oceanic Technology*, **26**, 2310–2323, doi: 10.1175/2009JTECHA1281.1.

Winker, D. M., W. H. Hunt, and M. J. McGill, 2007, Initial performance assessment of CALIOP, *Geophysical Research Letters*, **34**, L19803, doi:10.1029/ 2007GL030135

Won, J.-G., S.-C. Yoon, S.-W. Kim, A. Jefferson, E. G. Dutton, and B. Holben, 2004: Estimation of direct radiative forcing of Asian dust aerosols with Sun/sky radiometer and lidar measurements at Gosan, Korea, *Journal of the Meteorological Society Japan*, **82**, 115–130.

Young, S. A., M. A. Vaughan, 2009: The Retrieval of Profiles of Particulate Extinction from Cloud-Aerosol Lidar Infrared Pathfinder Satellite Observations (CALIPSO) Data: Algorithm Description. *Journal of Atmospheric and Oceanic Technology*, **26**, 1105–1119, doi: 10.1175/2008JTECHA1221.1.

Young, S. A., M. A. Vaughan, R. E. Kuehn, D. M. Winker, 2013: The Retrieval of Profiles of Particulate Extinction from Cloud–Aerosol Lidar and Infrared Pathfinder Satellite Observations (CALIPSO) Data: Uncertainty and Error Sensitivity Analyses. *J. Atmos. Oceanic Technol.*, **30**, 395–428, doi: http://dx.doi.org/10.1175/JTECH-D-12-00046.1

국문초록

CALIOP (the Cloud-Aerosol Lidar with Orthogonal Polarization)은 CALIPSO (the Cloud-Aerosol Lidar and Infrared Pathfinder Satellite Observation) 위성에 탑재된 라이다로 전구에 걸쳐 대기의 연직 분포를 관측하는 유용한 기기이다. 그러나 CALIOP 에서 제공하는 에어로졸 광학두께 (AOD; aerosol optical depth)는 기존의 다른 위성 관측 결과에 비해 정확도가 낮은 것이 현실이다. CALIOP AOD 의 정확도를 평가하고 오차 발생 원인을 분석하기 위해 MODIS AOD 자료와 비교•검증을 수행하였다. 비교•검증에는 MODIS AOD 의 정확도가 높은 해양 자료만을 사용하였으며 2006 년 6 월부터 2010 년 12 월까지의 자료를 이용하여 CALIOP 에서 구분된 여섯 종류의 에어로졸 (clean marine, dust, polluted dust, polluted continental, biomass burning)로 나누어 분석하였다. 550 nm 에서의 MODIS AOD 는 평균 0.111 ± 0.079 로 CALIOP AOD (0.068 ± 0.073) 보다 약 63% 높게 나타났다. Clean marine 의 경우, MODIS AOD 가 0.110 ± 0.064 로 CALIOP AOD (0.056 ± 0.038)보다 거의 두 배 가까이 높게 나타났으며 위도에 따라 두 기기의 AOD 차이가 변하는 모습을

보였다. 이는 해수면 풍속이 강할 때, 지표면 알베도 (albedo)가 증가하여 MODIS AOD 가 과대모의 되기 때문으로 판단된다. Dust 에어로졸의 AOD 차이는 다른 에어로졸에 비해 적게 나타났지만 지역에 따른 변화가 뚜렷하게 나타났다. 또한, 에어로졸에 편광소멸도가 증가함에 따라 두 기기의 AOD 차이가 증가하는 모습도 확인할 수 있었다. Polluted dust 와 polluted continental 에어로졸은 CALIOP AOD 가 각각 15%와 29% 크게 나타났다. 특히, 두 종류의 에어로졸은 육지에서 유입되는 에어로졸이 거의 없을 것으로 예상되는 먼 바다에서도 관측 빈도가 높아 clean marine 에어로졸이 잘못 구분될 수 있음을 추측해 볼 수 있었다. Biomass burning 에어로졸은 CALIOP 알고리즘에서 상층에 떠 있는 에어로졸로 정의되어 하층의 에어로졸을 감지하지 못하는 사례가 많았으며 이로 인해 CALIOP AOD 가 매우 낮게 산출되는 것을 확인하였다.

현재 CALIOP Level 2 알고리즘은 에어로졸 종류에 따라 미리 정해진 라이다 상수 (lidar ratio)를 사용하여 에어로졸 소산계수를 산출하고 있다. 그러나 에어로졸 종류를 구분하고 구분된 에어로졸에 따라 단일한 라이다 상수 값을 사용하기 때문에 CALIOP AOD 에 오차가 발생할 수 있다. 본 연구에서는 라이다로부터 에어로졸 소산계수 및 AOD 를 산출하는데 가장

큰 오차의 원인인 라이다 상수를 가정하지 않고 MODIS 나 AERONET 등의 관측으로 얻은 AOD 값을 이용하여 직접 구하였다. 서울대학교에서 지상 라이다와 SKYNET 선/스카이 레디오미터로 2006 년부터 2010 년까지 관측 결과를 이용하여 라이다 상수를 산출한 결과 평균 61.7±16.5 sr 로 나타났다. 또한, 2012 년 3-5 월 한반도와 일본에서 수행된 DRAGON 캠페인 기간 동안 AERONET 과 라이다의 공동관측 결과를 이용하여 서울과 오사카에서 캠페인 기간 라이다 상수를 계산한 결과, 각각 65.41±21.42 sr, 65.04±20.62 sr 로 나타났다. 이러한 결과는 기존의 선행연구에서 보고한 오염물질의 라이다 상수 및 현재 CALIOP 에서 사용하고 있는 polluted continental 의 라이다 상수인 70 sr 과 비슷한 결과이다.

Dust 에어로졸은 현재 CALIOP 알고리즘 상에서 에어로졸 종류 구분의 정확도가 상대적으로 가장 정확한 것으로 보고되고 있다 [*Burton et al.,* 2013]. 따라서 본 연구에서는 dust 에 초점을 맞추어 라이다 상수를 직접 산출하고 현재 CALIOP 알고리즘에서 사용 중인 40 sr 과 비교하여 보았다. 서울에서 2006 년부터 2010 년까지 황사 사례에서의 라이다 상수를 산출한 결과는 51.7±13.7 sr 로 나타났다. 2012 년 DRAGON 캠페인 기간 황사가 발생했던 2012 년 4 월 27-28 일

서울에서의 라이다 상수는 48.02±9.38 sr 로 비슷한 값을 보였다. CALIOP 과 AERONET 자료를 이용하여 사하라 사막 지역의 dust 에 대해 라이다 상수를 산출한 결과는 47.45±16.52 sr 로 나타났으며 CALIOP 과 MODIS 자료로부터 산출된 dust 의 라이다 상수는 45.50±15.17 sr 이었다. 특히, CALIOP 과 MODIS 자료를 이용하여 동아시아 지역에서의 dust 라이다 상수 산출 결과는 53.04±18.30 sr 로 전구 평균 보다 높은 값을 보였다. 이와 같이 dust 의 라이다 상수는 40 sr 보다 모두 높은 값을 보여 현재 CALIOP 알고리즘에서 사용하고 있는 값보다 큰 값을 사용할 필요가 있음을 보여준다. 또한, 동아시아에서는 더욱 큰 값을 보여 지역에 따라 다른 값을 사용할 필요성이 있음을 알 수 있었다.

주요어: CALIOP, 에어로졸 광학두께, 에어로졸 종류, 라이다 상수, MODIS

학 번: 2005-20504

Thesis for a Ph.D. Degree

Assessment of aerosol optical depth and estimation of lidar ratio from CALIOP measurements

CALIOP 에어로졸 광학 두께의 검증과 라이다 상수 산정에 관한 연구

Man-Hae Kim

February 2014

School of Earth and Environmental Sciences

Graduated School

Seoul National University

Assessment of aerosol optical depth and estimation of lidar ratio from CALIOP measurements

by

Man-Hae Kim

Dissertation Submitted to the Faculty of Graduated School of Seoul National University in Partial Fulfillment of the Requirement for the Degree of Doctor of Philosophy

Degree Awarded:

February 2014

Advisory Committee:

Professor	Byung-Ju Sohn,	Chair
Professor	Soon-Chang Yoon,	Advisor
Professor	Young-Sung Ghim	
Professor	Jhoon Kim	
Professor	Sang-Woo Kim	

이학박사학위논문

CALIOP 에어로졸 광학 두께의 검증과 라이다 상수 산정에 관한 연구

Assessment of aerosol optical depth and estimation of lidar ratio from CALIOP measurements

2014년 2월

서울대학교 대학원

지구환경과학부

김 만 해

ABSTRACT

Assessment of aerosol optical depth and estimation of lidar ratio from CALIOP measurements

Man-Hae Kim

School of Earth and Environmental Sciences

The Graduated School

Seoul National University

The Cloud-Aerosol Lidar with Orthogonal Polarization (CALIOP) is a space-borne lidar system onboard the Cloud-Aerosol Lidar and Infrared Pathfinder Satellite Observation (CALIPSO) satellite. CALIOP is a unique instrument that can provide aerosol extinction profile and AOD on a global scale for both day and night. However, the uncertainty in CALIOP AOD is relatively high compared to other passive sensors. In order to assess the uncertainty in CALIOP AOD and investigate potential sources of uncertainty, CALIOP AOD was compared with MODIS-Aqua (hereafter referred to MODIS) AOD over ocean by separating aerosol type

defined in CALIOP level 2 algorithm. Such comparisons have been performed for five different aerosol subtypes classified by CALIOP algorithm, namely clean marine, dust, polluted dust, polluted continental, and biomass burning, over the ocean from June 2006 to December 2010. MODIS AOD at 550 nm (0.111 ± 0.079) for the collocated data pairs is about 63% higher than CALIOP AOD at 532nm (0.068 ± 0.073). For clean marine, MODIS AOD (0.110 ± 0.064) is almost twice the CALIOPAOD (0.056 ± 0.038), and the difference between the AOD values has a strong latitude dependence likely related to the surface wind speed over the ocean. The difference in AOD for dust (13%) is observed to be the lowest among the five aerosol types under consideration, but it shows a slight regional variation. The discrepancy of AOD for dust also shows strong dependency on the layer mean of the particulate depolarization ratio. CALIOP AOD is higher than MODIS AOD for both polluted dust and polluted continental by 15% and 29%, respectively, for most of the ocean. One of the possible reasons for the difference is the misclassification of clean marine (or marine + dust) as polluted dust and polluted continental in the CALIOP algorithm. For biomass burning, uncertainty in the layer base altitude is thought to be one of the main reasons for the lower value of CALIOP AOD.

Current CALIOP level 2 algorithm uses pre-determined $\boldsymbol{S_{aer}}$ for classified aerosol types. However, not only using single values of $\boldsymbol{S_{aer}}$ for each aerosol type but also aerosol classification algorithm could be sources of uncertainties in aerosol extinction retrieval. In this study, to improve currently used $\boldsymbol{S_{aer}}$ in CALIOP level 2 algorithm, $\boldsymbol{S_{aer}}$ is determined from CALIOP by using AOD from AERONET and MODIS-Aqua as a constraint without any assumption. Using 4-year measurements (2006-2010) of elastic-backscatter lidar and SKYNET sun/sky radiometer at Seoul National University of Seoul, Korea, mean lidar ratio is estimated to be 61.7±16.5 sr. Lidar ratios are also retrieved using ground-based lidar and AERONET sun/sky radiometer during Distributed Regional Aerosol Gridded Observation Networks (DRAGON) Northeast Asia Campaign 2012. Mean lidar ratios at Seoul and Osaka were retrieved as 65.41±21.42 sr and 65.04±20.62 sr, respectively. Mean lidar ratios from Seoul and Osaka, which are metropolitan cities in East Asia, are almost same and comparable to the lidar ratio for pollution used in CALIOP algorithm.

Dust aerosol is easily recognized from depolarization ratio measurements due to its non-spherical shape. *Burton et al.* [2013] reported that aerosol type classification for dust is the most accurate in CALIOP algorithm. For this reason, lidar ratios are retrieved mainly focused on dust

aerosol and compared other studies and CALIOP Level 2 Product. The lidar ratio for dust conditions are estimated to be 51.7±13.7 sr using 4-year measurements of elastic-backscatter lidar and SKYNET sun/sky radiometer at Seoul National University of Seoul, Korea. During DRAGON 2012 NE Asia campaign, lidar ratio for dust event on 27-28 April 2012 in Seoul is retrieved as 48.02±9.38 sr from elastic-backscatter lidar and AERONET sun/sky radiometer. From a synergy of CALIOP and AERONET, lidar ratio for Saharan/Arabian dust is derived to be 47.45±16.52 sr. Lastly, using CALIOP and MODIS measurements together, dust lidar ratio is retrieved as 45.50±15.17 sr. Especially, the mean lidar ratio for Asian dust is estimated much larger as 53.04±18.30 sr. All the lidar ratios for dust aerosol retrieved in this study using AOD constrained method show larger values than currently used lidar ratio for dust in CALIOP algorithm (40 sr), which suggests that dust lidar ratio in CALIOP algorithm is underestimated and needs to be increased.

Keywords: CALIOP, aerosol optical depth, aerosol type, lidar ratio, MODIS

Student Number: 2005-20504

TABLE OF CONTENTS

LIST OF FIGURES

LIST OF TABLES

CHAPTER 1. INTRODUTION

1.1. Background and motivation

1.1.1. The importance of aerosol vertical distribution on radiative forcing

Aerosols continue to contribute one of the largest uncertainties to estimate and interpret of the Earth's changing energy budget. Aerosol-climate feedbacks occur mainly through changes in the source strength of natural aerosols or changes in the sink efficiency of natural and anthropogenic aerosols; a limited number of modelling studies have bracketed the feedback parameter within ±0.2 W m^{-2} $°C^{-1}$ with low confidence [*Boucher et al.*, 2013]. The impact of aerosols on Earth' radiation budget mainly depends on their optical properties and horizontal/vertical distribution. The vertical distribution of aerosols, especially light-absorbing aerosol, is very important because they can modify the radiative heating in the atmosphere [e.g., *Won et al.*, 2004; *Ramanathan et al.*, 2007; *Ramana et al.*, 2010].

Lidar (light detection and ranging) is a useful instrument, which can provide vertical distribution of aerosols to estimate aerosol direct radiative

forcing and atmospheric heating rate. In June 2006, the Cloud-Aerosol Lidar and Infrared Pathfinder Satellite Observation (CALIPSO) satellite which contains space-borne lidar system, the Cloud-Aerosol Lidar with Orthogonal Polarization (CALIOP), has been launched [*Winker et al.*, 2003; *Vaughan et al.*, 2009]. Therefore, it is a great opportunity for us to estimate aerosol direct radiative forcing and atmospheric heating rate using CALIOP measurements on a global scale. *Huang et al.* [2009] used CALIOP data to estimate dust aerosol radiative forcing and atmospheric heating rate over the Taklimakan Desert in Northwestern China. On a global scale, however, the estimation of aerosol radiative forcing using observed aerosol profile data is still insufficient.

1.1.2. Aerosol extinction retrieval from CALIOP measurements

CALIOP is a space-borne lidar system onboard CALIPSO. CALIOP is an elastic lidar system having three channels: two channels measuring orthogonally polarized components of backscatter at 532 nm and one measuring total backscatter at 1064 nm. The CALIOP data products are divided into level 1, level 2 and level 3. The CALIOP level 1 product is calibrated, range-corrected lidar signal and the CALIOP level 2 aerosol product is intended product for use by science community, including

aerosol extinction profiles and other optical properties. The CALIOP level 3 aerosol product reports monthly mean profiles of aerosol optical properties on a uniform spatial grid. The CALIOP level 2 extinction retrieval algorithm has three steps. First, it detects cloud and aerosol layers from level 1 dataset. Then it classifies detected layers by type using several indicators such as backscatter intensity, depolarization ratio, surface (region) type. The last step of the algorithm is performing extinction retrievals for the layers which are determined at step 1 [*Winker et al.*, 2009; *Omar et al.*, 2009; *Young and Vaughan*, 2009]. The CALIOP data flow within the level 2 data processing system is shown in Figure 1.1.

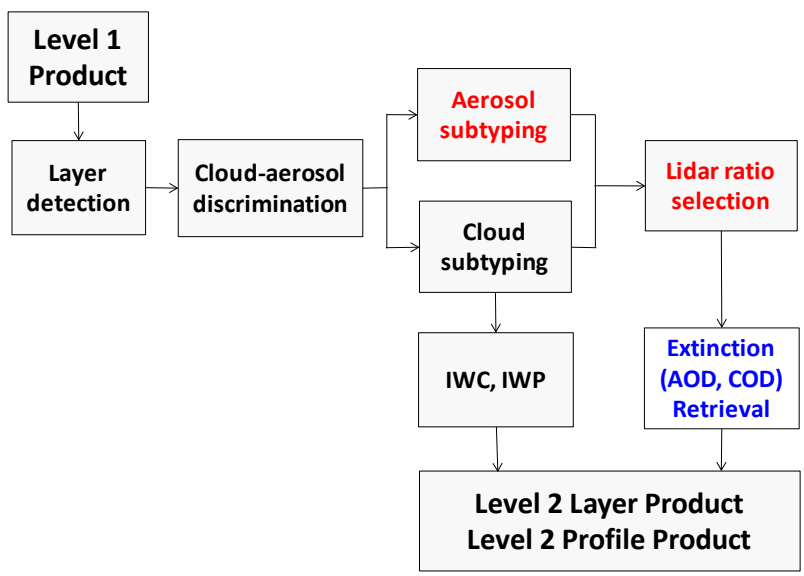

Figure 1.1. A schematic diagram of the CALIOP operational data process to produce the level 2 products (http://www-calipso.larc.nasa.gov/).

The expected error for CALIOP aerosol optical depth (AOD) is ± (0.05 + 40%) over both land and ocean [*Winker et al.*, 2009; *Omar et al.*, 2013]. The relative error of CALIOP AOD is quite large compared to the expected error for MODIS (Moderate Resolution Imaging Spectroradiometer) AOD of ± (0.05 + 15%) over land and ± (0.03 + 5%) over ocean [Remer et al., 2005]. The main sources of uncertainties in the CALIOP extinction retrieval are errors in (1) instrument calibration, (2) feature detection, (3) identification of feature types, (4) multiple-scattering function, and (5) specification of the corresponding lidar ratios [*Winker et al.*, 2009; *Omar et al.*, 2013; *Young et al.*, 2013]. Because values for lidar ratios can vary over a large range, even for a particular feature type, lidar ratio is the largest source of uncertainty in the retrievals [*Young et al.*, 2013]. Omar et al. [2009] declared that the goal is to constrain the uncertainty in the lidar ratio to no more than 30%. However, the uncertainties in the lidar ratio are known to be larger than 30%. The currently used lidar ratios in CALIOP algorithm for each aerosol type and their uncertainties are shown in Table 1.1. Moreover, errors in identification of feature types are directly related with uncertainty in the lidar ratio, thus an effect of the lidar ratios on the accuracy of CALIOP AOD is significant.

Table 1.1. Lidar ratios for the aerosol types identified in the version 3 CALIOP algorithm, together with the one standard deviation uncertainties and relative uncertainties [*Young et al.*, 2013].

type	Lidar ratio (sr)	Uncertainty (sr)	Relative uncertainty (%)
Clean Marine	20.0	6.0	30
Dust	40.0	20.0	50
Clean Continental	35.0	15.8	45
Polluted Continental	70.0	24.5	35
Polluted Dust	55.0	22.0	40
Biomass Burning	70.0	28.0	40

1.1.3. Determination of aerosol lidar ratio (S_{aer}) for the elastic lidar

Elastic backscatter lidars are commonly used to derive the aerosol extinction profile using lidar equation [*Klett*, 1981; *Fernald*, 1984]. However, the lidar equation has two unknown variables; aerosol extinction and backscatter coefficients. To solve ill-posed problem of the elastic lidar equation, the aerosol extinction-to-backscatter ratio or aerosol lidar ratio (hereafter, referred to as $\boldsymbol{S_{aer}}$) should be determined. $\boldsymbol{S_{aer}}$ is a key parameter, which is a function of aerosol physical and chemical properties such as aerosol size, shape, refractive index and chemical composition. It is frequently either assumed or inferred from additional measurements.

Various techniques have been implemented to avoid the assumption of $\boldsymbol{S_{aer}}$. The Raman lidar technique [*Ansmann et al.*, 1990] and the high spectral resolution lidar (HSRL) technique [*Shipley et al.*, 1983] can derive aerosol extinction profiles needless to assume the $\boldsymbol{S_{aer}}$ by separating aerosol returns from molecular returns. The elastic lidar, however, cannot measure or derive the aerosol $\boldsymbol{S_{aer}}$ by itself. So, additional measurements are needed to determine $\boldsymbol{S_{aer}}$ for the elastic lidar. *Doherty et al.* [1999] calculate $\boldsymbol{S_{aer}}$ from in-situ measurements. They used modified Nephelometer to measure aerosol scattering coefficient and 180° backscatter coefficient and particle soot absorption

photometer (PSAP) to obtain aerosol absorption coefficient. *Dubovik et al.* [2006] and *McPherson et al.* [2010] used aerosol phase function, and other aerosol optical properties from AERONET (Aerosol Robotic Network) sun/sky radiometer measurements to derive $\boldsymbol{S_{aer}}$. *Kaufman et al.* [2003] and *Leon et al.* [2003] used similar way to calculate $\boldsymbol{S_{aer}}$, but they used aerosol models with one fine and one coarse mode and MODIS (Moderate Resolution Imaging Spectroradiometer) measurements instead of AERONET. The CALIPSO lidar ratio selection algorithm also uses aerosol models [*Omar et al.*, 2009], which based on cluster analysis of a multiyear AERONET dataset [*Omar et al.*, 2005].

Welton et al. [2000] used an independently measured AOD with MPL (Micro Pulse Lidar) measurement to determine $\boldsymbol{S_{aer}}$. They used AOD as a constraint to produce the aerosol extinction profiles. The advantage of this technique is that information of $\boldsymbol{S_{aer}}$ is not required. The similar technique was used by *Burton et al.* [2010]. They retrieved aerosol extinction profiles from CALIPSO lidar measurements using MODIS derived AOD as a constraint to determine $\boldsymbol{S_{aer}}$ and evaluated this result by comparing with coincident measurement of airborne HSRL. The comparison of 37 profiles shows that the resulting retrievals agree well with HSRL measurements within $\pm 20\%$.

1.2. Objectives of this study

CALIOP is a unique instrument that can provide aerosol extinction profile and AOD on a global scale for both day and night. However, the uncertainty in CALIOP AOD is relatively high compared to other passive sensors such as MODIS, POLDER (Polarization and Directionality of the Earth's Reflectances), MERIS (Medium Resolution Imaging Spectrometer), and SEVIRI (Spinning Enhanced Visible and Infrared Imager). In order to assess the uncertainty in CALIOP AOD and investigate potential sources of uncertainty, CALIOP AOD was compared with MODIS-Aqua (hereafter referred to MODIS) AOD over ocean by separating aerosol type defined in CALIOP level 2 algorithm. MODIS AOD was chosen because expected error over ocean (± 0.03 ± 5%) is much less than the expected error for CALIOP AOD (± 0.05 ± 40%). Moreover, as part of the A-train satellite constellation, CALIPSO and Aqua can provide numerous collocated datasets to compare with. AOD from CALIOP Version 3.01 Aerosol Profile Products has been compared with AOD from MODIS-Aqua Collection 5.1 MYD04-L2 data over the ocean by considering aerosol subtypes classified by the CALIOP scene classification algorithms [*Omar et al.,* 2009; Winker et al., 2009].

Potential sources for the discrepancies in AOD between the two sensors are discussed for each aerosol type.

Because uncertainty in S_{aer} is the largest source of uncertainty in the CALIOP AOD, It is desirable to improve S_{aer} values used in CALIOP algorithm to retrieve accurate AOD (or aerosol extinction). Current CALIOP level 2 algorithm uses pre-determined $\boldsymbol{S_{aer}}$ for classified aerosol types. However, not only using single values of $\boldsymbol{S_{aer}}$ for each aerosol type but also aerosol classification algorithm could be sources of uncertainties in aerosol extinction retrieval. In this study, to improve currently used $\boldsymbol{S_{aer}}$ in CALIOP level 2 algorithm, $\boldsymbol{S_{aer}}$ is determined from CALIOP by using AOD from AERONET and MODIS-Aqua as a constraint without any assumption. Then, the characteristics of $\boldsymbol{S_{aer}}$ will be discussed for each aerosol type.

CHAPTER 2.
ASSESSMENT OF CALIOP AOD BY COMPARING WITH MODIS

2.1. Introduction

CALIOP onboard CALIPSO satellite is a space-borne lidar system that can measure the vertical structure of aerosol and cloud distributions on a global scale [*Winker et al.*, 2007, 2009]. Several studies validating CALIOP with ground-based measurements have shown reasonable agreements for the CALIOP Level 1 product with ground-based lidar [e.g., *Chazette et al.*, 2010; Kim et al., 2008, 2011].

The CALIOP Level 2 product, on the other hand, shows a much larger variation when compared with ground-based or airborne measurements. *Mielonen et al.* [2009] have found that 70% of the CALIOP Level 2 aerosol subtypes are in agreement with the AERONET-derived aerosol types. *Schuster et al.* [2012] found a CALIPSO 532 nm AOD bias of -13%, corresponding to an absolute bias of -0.029 relative to AERONET. However, the relative and absolute biases are reduced to -3% and -0.005, respectively, when they exclude dust aerosols. *Burton et al.* [2013] showed

that 62% of CALIOP ‘clean marine’, 54% of ‘polluted continental’, and 80% of ‘dust’ agree with airborne HSRL-1 classification results. However, agreement is poorer for CALIOP smoke (13%) and polluted dust (35%). *Kacenelenbogen et al.* [2011] have shown that CALIOP AOD is a factor of two lower than MODIS, POLDER, airborne HSRL and AERONET. *Bréon et al.* [2011] found that CALIOP-derived AODs show little resemblance to AERONET-derived AODs, with a root-mean-square (RMS) difference of 0.404 at 500 nm. *Omar et al.* [2013] showed that CALIOP AODs are lower than AERONET AOD, especially at low AODs. Furthermore, they reported that the median of relative AOD difference between CALIOP and AERONET (500 nm) is 25% of AERONET AOD for AOD > 0.1. *Misra et al.* [2012] reported the mean backscatter difference ranges from -0.004 to 0.023 km-1 sr-1 by comparing CALIOP Level 2 aerosol backscatter profile with ground-based Micro Pulse Lidar Network (MPL-NET) measurements.

Comparison of CALIOP AOD with ground-based instruments, such as sunphotometer and lidar, however, is more limited than space-borne passive sensors, such as MODIS, POLDER, MERIS, and SEVIRI. This is because CALIOP has a very narrow field of view (FOV) that corresponds to 70 m of the laser footprint at the Earth’s surface. Passive sensors have

much larger spatial resolution of up to several square kilometers. CALIOP can cover only 0.2% of the Earth's surface during one repeat cycle [*Kahn et al.*, 2008], thus making it difficult to find collocated data pairs between CALIOP and ground-based measurements [*Omar et al.*, 2013].

An alternative way for evaluating the accuracy CALIOP AOD is by comparing it with AOD from MODIS-Aqua. As part of the A-train satellite constellation, CALIPSO and Aqua satellites fly in close proximity. CALIPSO follows Aqua by 1-2 minutes providing nearly simultaneous and collocated observations. The expected error for CALIOP AOD is ±0.05 ± 40% over both land and ocean [*Winker et al.*, 2009; *Omar et al.*, 2013]. The MODIS AOD retrieval has less uncertainties, with expected errors of ±0.03 ± 5% over ocean and ±0.05 ± 15% over land [*Remer et al.*, 2005; *Levy et al.*, 2010]. *Kittaka et al.* [2011] reported that the CALIOP Version 2 product showed only a small global mean bias relative to MODIS Collection 5 for the period of June 2006 through August 2008, though the regional biases are large and vary with season. Global-mean AODs of CALIOP and MODIS over ocean for JJA (June to August) reported by *Kittaka et al.* [2011] are 0.076 and 0.083, respectively. *Oo and Holz* [2011] showed a mean AOD bias between MODIS and CALIOP of ~0.064 over the ocean using quality controlled and cloud screened data for

single aerosol layers. *Redemann et al.* [2012] found a RMS difference of 0.1 between CALIOP and MODIS AODs using quality-controlled and cloud screened data. However, none of these studies have compared AODs from the two sensors for different aerosol types.

In order to retrieve the aerosol extinction coefficient (or its column-integrated value, AOD) from CALIOP measurements, the aerosol type is determined *a priori* so that a type-specific lidar ratio (i.e., extinction-to-backscatter ratio) can be assigned to the aerosol layer. The lidar ratio is an essential parameter for aerosol extinction coefficient retrievals from elastic lidar measurements [*Fernald*, 1984]. Errors in the *a priori* prescription of this value can thus induce large errors in the retrieved AOD. Therefore, when validating CALIOP AOD using other instruments, errors associated with aerosol type or 'lidar ratio' should be considered. The validation of CALIOP AOD by segregating aerosol type can lead to an improvement of the accuracy of aerosol type classification and lidar ratio determination in CALIOP algorithm.

The goal of this study is to evaluate CALIOP AOD (Level 2 5-km Aerosol Product, Version 3.01) over ocean by comparing with collocated MODIS AOD (MYD04-L2 product, Collection 5.1). In order to figure out uncertainties in CALIOP AOD associated with aerosol type classification

and pre-determined lidar ratio, AODs from the two sensors are compared by considering aerosol subtypes classified by the CALIOP scene classification algorithms [*Omar et al.*, 2009; *Winker et al.*, 2009]. Potential sources for the discrepancies in AOD between the two sensors are discussed for each aerosol type.

2.2. Instruments and data

The A-Train constellation of satellites are Sun synchronous, near-polar orbiting satellites, which cover almost the whole globe (82°S - 82°N) from an altitude of ~700 km above the surface of the Earth and an orbital inclination of 98°. The A-train satellites cross the equator in ascending node at around 13:30 local solar time [*L'Ecuyer and Jiang*, 2010]. CALIPSO lags Aqua by one to two minutes. Thus, both satellites observe the same target within two minutes.

CALIOP uses a Nd:YAG laser that generates co-aligned pulses at 532 nm and 1064 nm, with a repetition frequency of 20.16 Hz producing 335 m of horizontal resolution along the ground track [*Winker et al.*, 2009]. Outgoing 532-nm pulses are linearly-polarized. Orthogonal polarizations of backscattered signals are measured to determine the linear

depolarization ratio, which provides information for determining the shape (spherical or nonspherical) of aerosol and cloud particles. The sampling vertical resolution of CALIOP for the 532 nm channel is 30 m from the surface to 8.2 km above mean sea level. The spatial resolutions of the CALIOP downlinked data throughout the atmosphere can be found in *Winker et al.* [*2009*].

CALIOP Level 2 algorithms consist of the following three major steps: (1) the selective iterative boundary locater (SIBYL) [*Vaughan et al.*, 2009], (2) the scene classification algorithm (SCA) [*Liu et al*., 2009; *Omar et al.*, 2009], and (3) the hybrid extinction retrieval algorithm (HERA) [*Winker et al.*, 2009, *Young and Vaughan*, 2009]. HERA is an iterative algorithm that retrieves aerosol extinction profiles for aerosol layers detected by SIBYL, using the lidar ratio determined a priori by SCA. The aerosol type classification is an essential step in CALIOP algorithm and has a direct impact on aerosol retrievals, since the lidar ratio is determined by aerosol type. The algorithm for the aerosol type classification is described in *Omar et al.* [2009].

MODIS measures radiance at 36 spectral bands in wavelengths ranging from 0.4 μm to 14.4 μm using calibrated reflectance data from

seven bands (0.47, 0.55, 0.66, 0.86, 1.24, 1.6 and 2.13 μm) to retrieve AOD. The spatial resolution is 250 m × 250 m for 0.66 and 0.86 μm, 500 m × 500 m for 0.47, 0.55, 1.24, 1.6, and 2.13 μm. During the MODIS retrieval, if all 20 × 20 pixels in a 10 × 10 km box are identified as "ocean", the ocean algorithm is implemented [*Remer et al.*, 2005]. After removing contaminated pixels, including cloud, sediment and glint masks, MODIS inversions attempt to minimize the difference between the observed spectral radiance in six MODIS channels and radiance pre-computed in a lookup table. The algorithm selects the best fit to the observed reflectance and reports AOD and other aerosol properties [*Levy et al.*, 2005; *Remer et al.*, 2005].

The data used in this study are CALIOP Level 2 aerosol layer and profile products (Version 3.01) and MODIS Level 2 aerosol product (Collection 5.1) over ocean, both from June 2006 to December 2010. 'Column_Optical_Depth_Aerosols_532' for CALIOP and 'Effective_Optical_Depth_Average_Ocean' at 550 nm for MODIS are used for the AOD comparison. CALIOP AODs in the Level 2 products are reported at a horizontal resolution of 5 km for Version 3. Horizontal resolution of MODIS AOD is 10 × 10 km at nadir. MODIS AODs over the land were not evaluated in this study because of higher uncertainty [*Remer*

et al., 2005; *Levy et al.*, 2010]. CALIOP provides data for both day and night, whereas MODIS AOD is available only for daytime. Therefore, comparisons of AOD between CALIOP and MODIS were made only for daytime data.

The uncertainty in CALIOP AOD can be caused by instrument calibration and normalization error, as well as errors in cloud-aerosol discrimination, layer boundary detection, multiple scattering assumption, and *a priori* lidar ratio [*Winker et al.*, 2009]. In many instances, the lidar ratio is one of the most significant sources of uncertainty in CALIOP AOD, with an uncertainty of 30-50%, depending on aerosol type [*Young et al.*, 2013]. Sensitivity tests to evaluate MODIS error sources were proposed by *Tanré et al.* [1997]. They report that the main sources of error in MODIS AOD are surface reflection, sensor calibration, contamination by glint, water-leaving radiance, and uncertainties involved in the lookup table such as aerosol size distribution, refractive index, and single scattering albedo.

AOD is reported at wavelengths of 532 nm and 550 nm for CALIOP and MODIS, respectively. Discrepancies in AOD due to different wavelengths can be approximated using an Ångström exponent (α) that

represents wavelength dependence of AOD. α is an indicator of effective aerosol particle size; $\alpha < 1$ indicates coarse-mode aerosols, such as dust and sea salt, and $\alpha \geq 2$ indicates fine-mode particles commonly associated with urban pollution and biomass burning [*Eck et al.*, 1999; *Schuster et al.*, 2006]. The difference between AOD at 532 nm and 550 nm increases as Ångström exponent increases and the typical difference is about 3% for the Ångström exponent of 1 and 6% for the Ångström exponent of 2. However, this difference is considered relatively small compared to uncertainties in AOD of both CALIOP [*Winker et al.*, 2009] and MODIS [*Remer et al.*, 2005], and, therefore, will be neglected in this study.

2.3. Data selection

The method used in this study to define spatial and temporal coincidence between CALIOP and MODIS for AOD comparison is nearly the same as that of *Kittaka et al.* [2011]. First, MODIS 10-km pixels whose centers are located less than 5 km from the CALIOP track are selected. Corresponding CALIOP data points located closer than 10 km from the center of the MODIS pixel were defined as collocated data points. Each selected MODIS pixel thus had three to five collocated CALIOP data

points. The collocated pairs used for the comparison are then MODIS pixel and the averaged value of these CALIOP data points. Figure 2.1 is a schematic diagram depicting a collocated MODIS pixel and CALIOP data points.

CALIOP AOD was obtained by vertical integration of aerosol extinction coefficient at 532 nm from the aerosol profile products. Since CALIOP identifies unique overlapping layers in the vertical, only AOD records with layers of single aerosol type throughout the column were used in the study. This was done to isolate specific aerosol types for unique one-to-one comparisons of single layer AOD with MODIS observations. ‘Feature_Classification_Flags’ of the CALIOP Level 2 layer products were used to determine the aerosol subtype. After filtering for single aerosol layers, approximately 20% of the CALIOP profiles were rejected.

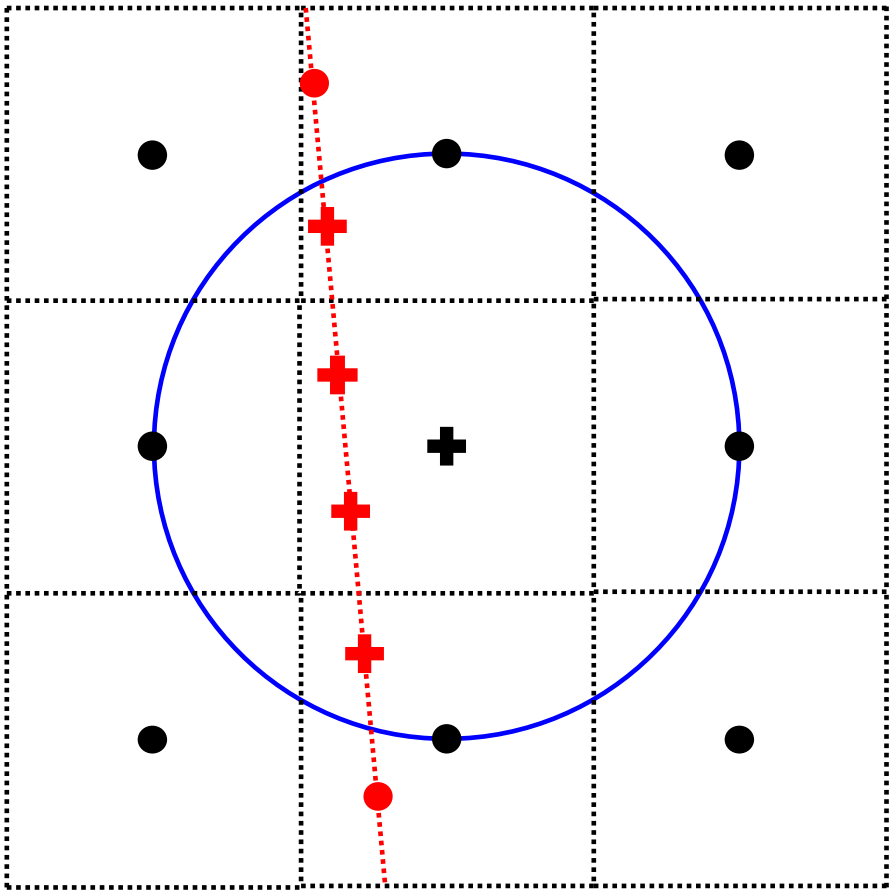

Figure 2.1. A schematic diagram representing collocated MODIS pixel (black crosshair) and CALIOP data points (red crosshair). Black dotted squares and red dotted line represent MODIS 10 × 10 km pixels and CALIPSO track, respectively. Black dots and crosses are the centers of MODIS pixels, and red dots and cross are CALIOP data points which have 5 km horizontal resolution. Blue circle shows the area covered within a radius of 10 km from the center of the MODIS pixel (black crosshair).

Cloud screening was independently applied for both CALIOP and MODIS data. CALIOP Level 2 data provides cloud optical depth (COD) and stratospheric optical depth (SOD). If any of these two values was not equal to zero, the collocated data pairs were not used. For the case of MODIS, “Cloud_Mask_QA” which represents cloud fraction is used to eliminate cloud contamination [*Ackerman et al.,* 1998]. The cloud fraction is determined using specific numerical thresholds of 1 km cloud mask pixels that meet certain criteria within the 10 × 10 km aerosol retrieval area. Only 10 × 10 km grid cells with less than 30% cloudy pixels were used in this study.

If optically-thick aerosol layers exist, the emitted laser sometimes cannot penetrate the layers, and becomes completely attenuated before reaching the earth’s surface. Such profiles are typically characterized by the failure of the lidar signal to detect the surface. Since in these cases, AODs from CALIOP are unreliable, fully-attenuated profiles are excluded. To remove these profiles, “Lidar_Surface_Elevation” of CALIOP Level 2 products, which represents an altitude of surface elevation detected by lidar return signal, was used. If CALIOP detects the Earth’s surface, then we assume that most of the layers in the atmosphere with an integrated attenuated backscatter above CALIOP’s detection threshold have also

been detected and included in the column AOD calculation. The profiles can be screened using a threshold integrated attenuated backscatter (e.g., 0.01 sr in *Kittaka et al.* [2011]) or the base altitude of the lowest layer (e.g., 250 m in *Campbell et al.* [2012, 2013]). These Kittaka and Campbell screening rubrics would reject only 2.6% and 7.8% of the collocated pairs used in this study, respectively. For biomass burning layers, however, 96.1% of our screened data are rejected by Campbell screening criteria because most of the smoke layers detected by CALIOP are elevated above 250 m. Contrary to this study, it should be noted that multiple aerosol types within a common layer column were included in *Campbell et al.* [2012, 2013].

The Extinction Quality Control (QC) flag and Cloud-Aerosol Discrimination (CAD) score of CALIOP Level 2 data files are also considered. Extinction QC is reported for each aerosol layer for which extinction was solved. If an aerosol layer is elevated, vertically isolated, and clear-air signals are detected above and below the layer, the extinction profile is solved using two-way transmittance [*Young and Vaughan*, 2009]. This is the so-called ‘constrained retrieval’. CALIOP algorithms employ an iterative solution to the lidar equation described in *Young and Vaughan* [2009] for unconstrained retrievals. However, sometimes the solutions for extinction do not converge with respect to the *a priori* lidar ratio selected.

In such cases, the CALIOP algorithm changes (by increasing or decreasing) the lidar ratio until the solution converges. In this study, the Extinction QC equals to 1 (constrained method using two-way transmittance) and 0 (unconstrained method without changing lidar ratio) were used. The sign of the CAD score, ranging between -100 (definitely aerosol) and 100 (definitely cloud), indicates confidence in the layer feature type. Positive values signify clouds, and negative values signify aerosols. CAD scores less than -80 (i.e., high confidence aerosol layers) are used for this study. 'Quality_Assurance_Ocean' is quality flag for MODIS ocean AOD discussed in *Hubanks* [2012]. No confidence MODIS ocean AODs denoted by QA flag 0 are rejected.

2.4. Results and discussion

Using the data selection method described above, nearly two million collocated data pairs were compared. Table 2.1 and Figure 2.2 show the results of the comparison for six different types of aerosol (clean marine, dust, polluted dust, polluted continental, biomass burning, and clean continental) classified by the CALIOP aerosol classification and lidar ratio selection algorithm [*Omar et al.*, 2009]. The mean AOD for all collocated

data pairs is 0.068 for CALIOP and 0.111 for MODIS, i.e., the mean MODIS AOD is 63% larger than CALIOP AOD. These mean values are not representative global mean AODs of the two sensors, because multiple layers with different aerosol types are not included. The difference reported in this study is larger than values reported in *Kittaka et al.* [2011], but closer to the biases reported by *Oo and Holz* [2011] and *Redemann et al.* [2012].

The discrepancies of AOD between the two sensors vary for the aerosol types reported by CALIOP. For most, mean MODIS AOD is higher than mean CALIOP AOD. For polluted continental and polluted dust, however, mean CALIOP AOD is higher. Large differences between MODIS and CALIOP were found for clean marine (mean MODIS AOD is 96% higher) and biomass burning (mean MODIS AOD 102% higher). A small bias and high correlation was found, though, for dust and polluted dust. *Schuster et al.* [2012] also reported a relatively large AOD bias for clean marine, biomass burning, and clean continental when comparing CALIOP and AERONET measurements. There are very few (less 0.031%) data pairs of the clean continental aerosol type. All of these are a result of uncertainties in determination of land and ocean borders for both CALIOP and MODIS, since the CALIOP aerosol type classification algorithm does

not allow clean continental aerosols over the ocean [*Omar et al.*, 2009]. We therefore did not consider the clean continental type for this study.

Table 2.1. Statistics of the comparison of CALIOP and MODIS AOD showing the mean ± standard deviation of the AOD, mean bias, relative(percent) bias, root-mean-square deviation (RMSD), correlation (R), and number of data pairs.

type	Mean±Standard Deviation		Mean bias	Relative bias (%)	RMSD	R	No. of data
	MODIS	CALIOP					
All	0.111±0.079	0.068±0.073	0.044	64	0.080	0.61	1808587
Clean Marine	0.110±0.064	0.056±0.038	0.053	95	0.072	0.65	1522590
Dust	0.236±0.179	0.209±0.217	0.027	12	0.139	0.78	49150
Polluted Continental	0.057±0.052	0.080±0.052	-0.023	-29	0.069	0.23	55295
Polluted Dust	0.105±0.098	0.123±0.132	-0.019	-15	0.107	0.62	173836
Biomass Burning	0.281±0.232	0.139±0.157	0.141	102	0.254	0.48	6614

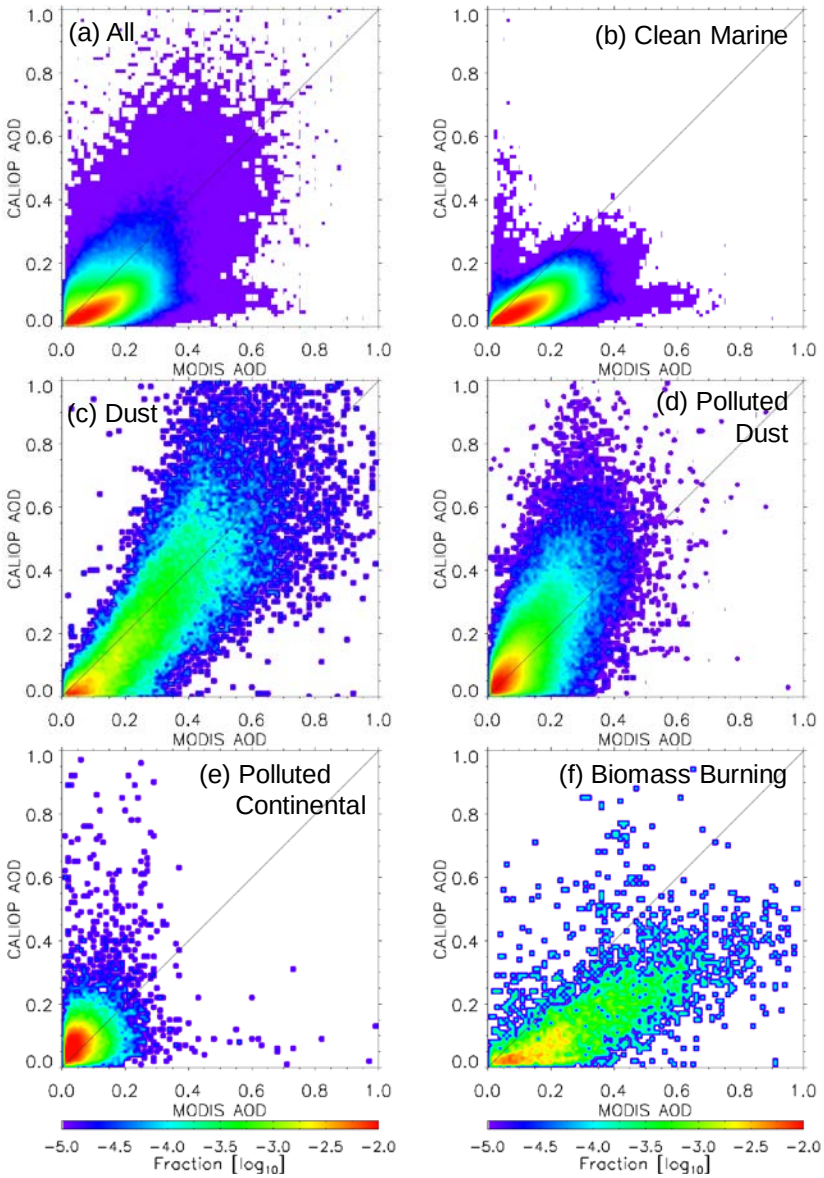

Figure 2.2. Frequency distributions of collocated CALIOP and MODIS AODs over ocean from June 2006 to December 2010 for single aerosol layers under a cloud-free condition: (a) all aerosol types, (b) clean marine, (c) dust, (d) polluted dust, (e) polluted continental, and (f) biomass burning aerosols.

2.4.1. Clean marine

While all other aerosol types are of continental origin, clean marine originates presumably in the ocean. It is the most dominant type of aerosol over the ocean, accounting for 84% of total aerosols observed (Table 2.1). A large number of these collocated data pairs occur over the remote oceans, whereas the occurrences of other aerosol types are mostly near shorelines.

The global distribution and meridional variation of AOD difference between the two instruments for clean marine is shown in Figures 2.3a and 2.3b, respectively. Differences are relatively large in the inter-tropical convergence zone (ITCZ) and sub-polar low region, and low in sub-tropical high region. Figure 2.4 shows the difference in the MODIS-CALIOP AOD and zonal mean wind speeds from NCEP/NCAR reanalysis data at sea surface level. The difference in AOD increases where surface wind is strong, especially for the Southern Hemisphere. Several studies have reported the enhancement of AOD under strong surface wind over remote oceans. *Anderson et al.* [2012] found a linear regression of τ_{bias} = 0.010 v – 0.024 after filtering the cloud fraction greater than 70%, where τ_{bias} is MODIS bias, and v is wind speed in m s^{-1}. *Smirnov et al.* [2012] showed that the slope of the linear regression between ship-based AOD

and wind speed (in m s^{-1}) is ~0.004-0.005. *O'Dowd et al.* [2010] reported a relation between the open ocean MODIS-derived AOD at 550nm and wind speed that follows a power-law, with the exponent ranging from 0.72 to 2.47 for a wind speed range of 2-18 m s^{-1}. In this study, the linear regressions between AOD and surface wind speed are τ_{CAL} = 0.003 v + 0.045 and τ_{MOD} = 0.008 v + 0.073, where v is wind speed (m s^{-1}), τ_{CAL} and τ_{MOD} are CALIOP and MODIS AOD, respectively, for the Southern Hemisphere. The zonal mean CALIOP and MODIS AODs have been averaged in 2.5 latitude degrees for comparison with the NCEP/NCAR reanalysis wind data.

CALIOP retrievals of extinction profile are not much affected by wind speed or surface reflectance/brightness, while the MODIS AOD retrieval is. Even though the MODIS algorithm takes into account sea surface reflectance under strong wind speed conditions by calculating the reflection of the sea surface from the rough ocean model [*Tanré et al.*, 1997], Figure 2.4 shows an overestimation of MODIS AOD caused by sea surface reflection over the rough ocean still exists. In the northern hemisphere, on the other hand, the difference of AOD and surface wind speed are not as strongly correlated. Although wind speeds in the Northern Hemisphere are relatively weak near the surface, the difference in AOD is

still large. We attribute this to the potential misclassification of continental aerosols as clean marine, thus resulting in lower values of CALIOP AOD due to offsets in their corresponding *a priori* lidar ratios.

The difference in clean marine AOD between the two sensors varies with geographical region (Figure 2.3b). Large differences occur along the coasts of South and East Asia and the Mid-Atlantic Ocean near Africa, where the transport of aerosol particles from the adjacent continents frequently occurs. In these regions, biomass burning and polluted continental are difficult to distinguish from clean marine using the two direct measurements CALIOP makes: attenuated backscatter and volume depolarization ratio. The CALIOP algorithm defines clean marine as optically thick layers consisting of spherical particles and polluted continental as optically thin layers with some non-spherical particles in the marine boundary layer [*Omar et al.*, 2009]. This classification might not be suitable for cases in the ocean close to aerosol source regions. Among the six aerosol types, clean marine has the smallest lidar ratio (20 sr), whereas biomass burning and polluted continental have the largest (70 sr). Therefore, misclassification of biomass burning or polluted continental as clean marine significantly depresses CALIOP AOD and increases the AOD difference between the two sensors.

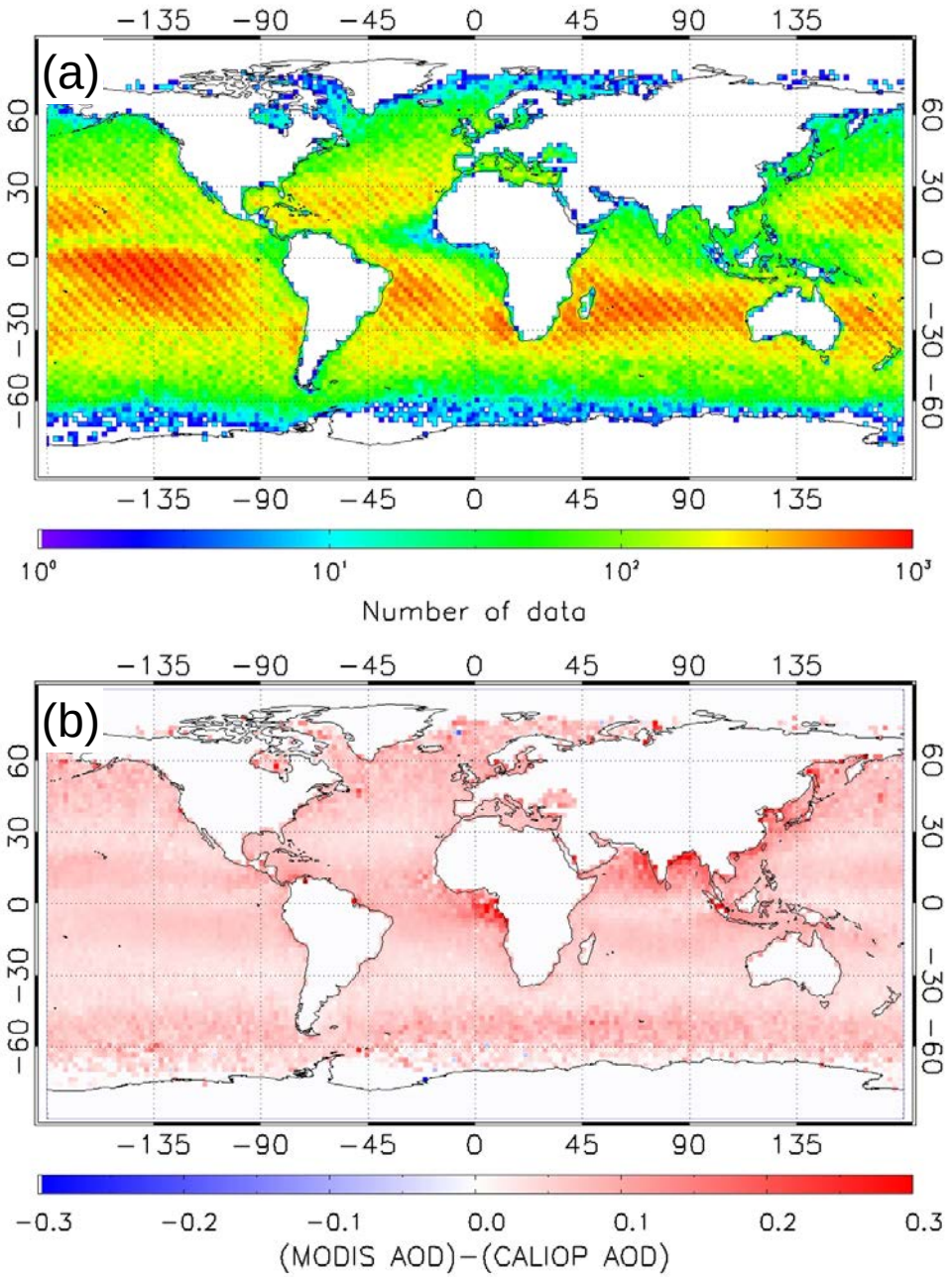

Figure 2.3. Global distribution of (a) the number of collocated data pairs and (b) difference between CALIOP and MODIS AODs for clean marine.

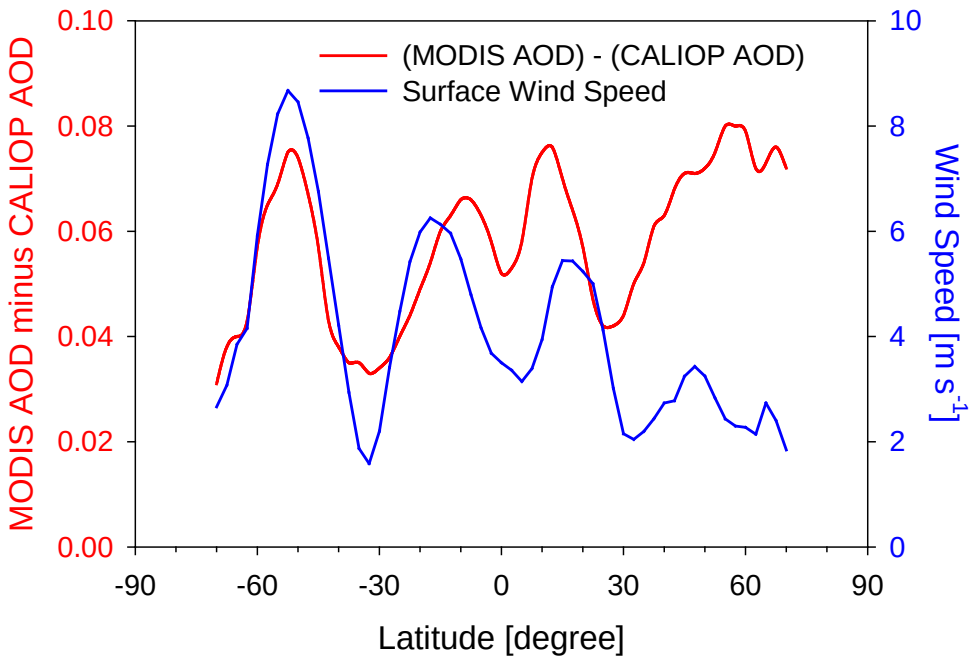

Figure 2.4. Zonal mean of AOD difference between CALIOP and MODIS and sea-level wind speed over oceans from June 2006 to December 2010.

2.4.2. Dust

Dust is predominantly non-spherical in shape with a relatively large depolarization ratio making its classification relatively unambiguous with respect to other common aerosol particles [e.g., *Freudenthaler et al.*, 2009; *Kai et al.*, 2008; *Sugimoto et al.*, 2002]. In general, the difference in dust AOD between the two instruments is smaller than the differences for other aerosol types (Table 2.1). Figure 2.2c also shows that dust AODs from the two sensors are better correlated than other aerosol types despite the large variance.

The global distribution of collocated dust data pairs is shown in Figure 2.5a. Dust appears more frequently near source regions, such as North Africa, Arabia, and East Asia, and AOD differences between the two sensors vary accordingly (Figure 2.5b). Mean MODIS AOD is larger than CALIOP AOD in East Asia, while the two mean AODs are comparable near the Saharan and Arabian Deserts. This variation in AOD difference implies that the optical properties of dust from Saharan and Arabian deserts are different from the optical properties of East Asian dust. Since CALIOP assumes that the lidar ratio for all dust is 40 sr, the difference in optical properties between East Asian and Saharan/Arabian dust has an impact on the accuracy CALIOP's AOD retrievals. Given the finding in

Figure 2.5, it is thus plausible, that the lidar ratio for East Asian dust is larger than the lidar ratio of Saharan and Arabian desert dust. The CALIOP algorithm lidar ratio for dust is comparable to *Voss et al.* [2001] for African dust (41 ± 8 sr) and *Cattrall et al.* [2005] for non-Asian desert dust (42 ± 4 sr). Several studies for the lidar ratio of Asian dust, however, report relatively larger values than Saharan dust: 42 - 55 sr by *Liu et al.* [2002], 50.4 ± 9.5 sr by *Murayama et al.* [2003], and 45.5 ± 8.6 sr by *Noh et al.* [2007]. Contrarily, *Schuster et al.* [2012] suggested a dust lidar ratio of 50-55 for Saharan dust after comparing CALIOP AODs with AERONET, and *Müller et al.* [2007] reported 55 ± 5 sr and 59 ± 11 sr for Saharan dust from Raman lidar measurements.

CALIOP algorithms classify dust aerosol when the estimated depolarization ratio (δ_v) is greater than 0.2, everywhere except for the polar regions [*Omar et al.*, 2009]. δ_v is an approximation of the particulate depolarization ratio (δ) defined by Eq. (9) in *Omar et al.* [2009]. δ, the depolarization due to only particles, is obtained after the retrieval of aerosol extinction profile. But for the retrieval, aerosol type, or the lidar ratio is required *a priori*. In order to determine the lidar ratio, therefore, δ_v is first estimated from the volume depolarization ratio, which is a sum of the depolarization due to particles and air molecules.

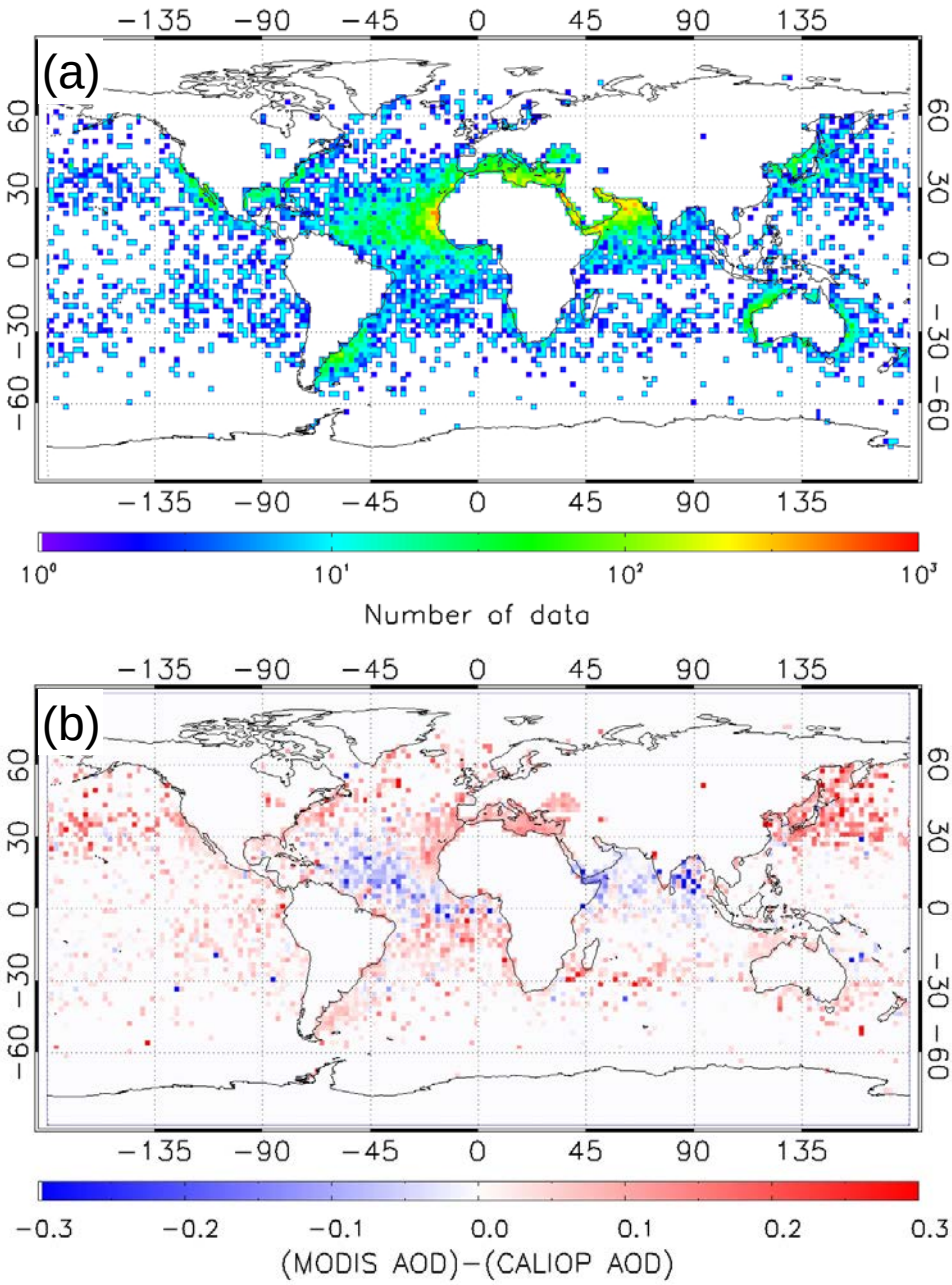

Figure 2.5. Same as Figure 2.3, except for dust.

To examine the relationship of the MODIS-CALIOP AOD differences and the depolarization ratio we define an extinction-normalized depolarization ratio, as a proxy for the particulate depolarization ratio obtained by following equation:

$$\bar{\delta} = \frac{\sum_{z_{base}}^{z_{top}} \sigma(z)\delta(z)}{\sum_{z_{base}}^{z_{top}} \sigma(z)} \quad \text{(EQ1)}$$

where z is the altitude with the resolution of 60 m; the subscripts “top” and “base” represent the top and the base height of the aerosol layer; and σ is the particulate extinction coefficient. Figure 2.6a shows frequency distributions of δ for dust, polluted dust, and clean marine.

δ is greater than 0.2 for most of the dust layers in Figure 2.6. However, for about 9% of the dust data used in this study, δ is less than 0.2. *Burton et al.* [2013] point out that in cases of strong attenuation and weak depolarization spurious classification of dust and polluted dust is likely.

Figure 2.6b shows the relation between the difference in AOD and $\bar{\delta}$ for dust, polluted dust and clean marine. While the differences of AOD for polluted dust and clean marine exhibit weak relations with $\bar{\delta}$, the difference of AOD for dust shows a very distinguishable dependence on $\bar{\delta}$.

When considering only collocated data pairs having $\bar{\delta}$ greater than 0.2 and assuming that the MODIS AOD and CALIOP classification of dust is correct, the increasing trend of the AOD difference with $\bar{\delta}$ implies that the lidar ratio of dust should increase as $\bar{\delta}$ increases.

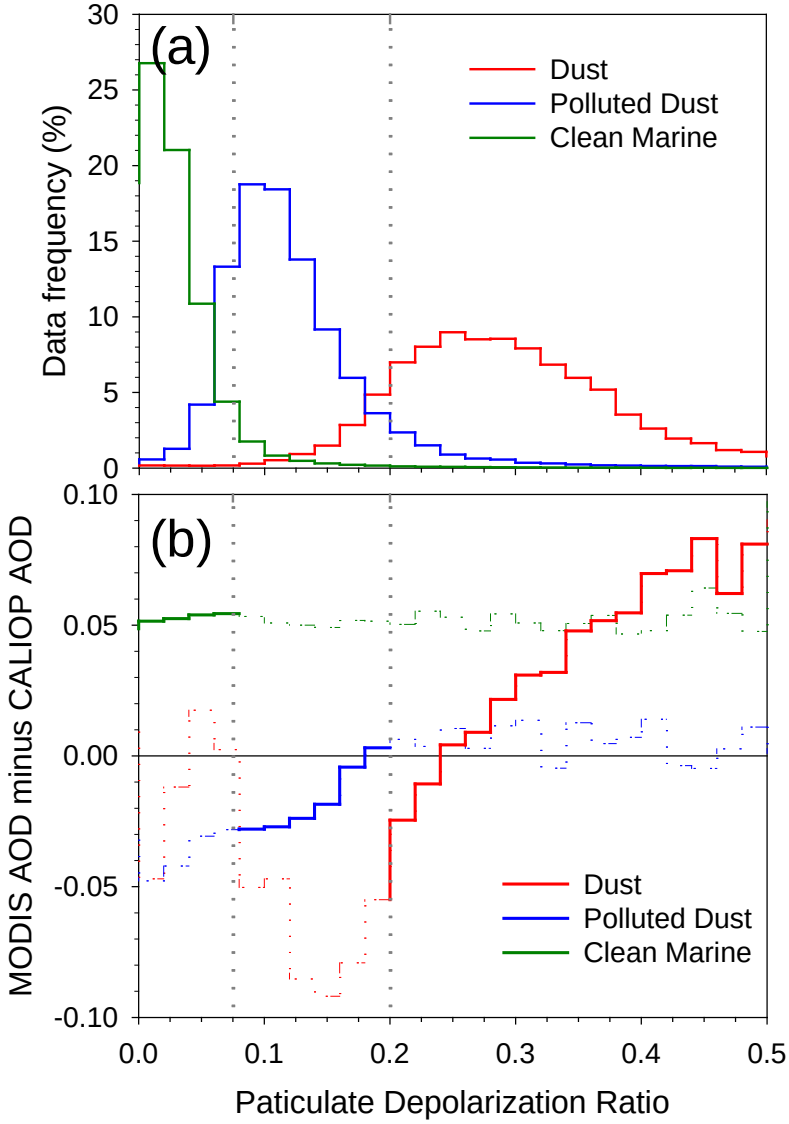

Figure 2.6. Variations in (a) data frequency and (b) AOD difference versus particulate depolarization ratio ($\overline{\boldsymbol{\delta}}$) for dust (red), polluted dust (blue), and clean marine (green). The criteria of depolarization ratio for the polluted dust (0.75) and dust (0.2) are shown in gray vertical dashed lines. For each type, the solid line denotes the region for which the algorithm threshold matches the $\overline{\boldsymbol{\delta}}$.

2.4.3. Polluted dust

Polluted dust is defined as dust mixed with biomass burning, and is identified when δ_v has the range between 0.075 and 0.2 regardless of elevation or region except for the poles [*Omar et al.*, 2009]. A lidar ratio of 55 sr is used in the CALIOP algorithms for polluted dust. A possible reason for higher CALIOP AOD compared to MODIS AOD for polluted dust is misclassification of aerosol type in CALIOP algorithm. If any aerosols which have lower lidar ratios than polluted dust, such as clean marine or dust are misclassified as polluted dust, CALIOP AOD will be larger than the true value. Since CALIOP aerosol classification does not include mixtures of dust and marine aerosols, it is possible for these mixtures to be classified as polluted dust as shown by *Burton et al.* [2013]. Such mixtures would have an effective lidar ratio between 20 and 40 sr, and therefore lower than the polluted dust ratio of 55 sr. Such a misclassification would therefore lead to a higher CALIOP AOD than the true value. Figure 2.7 shows global distributions of the number of collocated data points and difference between CALIOP and MODIS AODs for polluted dust. The number of data points increases near the continents where source regions of dust and biomass burning are close. The number is still relatively significant over remote oceans. As

mentioned above, polluted dust is identified using only δ_v over the ocean, which is only an approximation of the particulate depolarization. However, $\bar{\delta}$ is not exactly same as δ_v, and using δ_v instead of $\bar{\delta}$ can affect the classification of polluted dust, dust and clean marine aerosols. Figure 2.6a shows that 19.6% of polluted dust has $\bar{\delta}$ less than 0.075 or greater than 0.2, 11.2% of clean marine has $\bar{\delta}$ greater than 0.075 and 6.9% of dust has $\bar{\delta}$ less than 0.2.

Low SNR in the perpendicular 532 nm channel enhanced by high background solar radiation during daytime is one possible source for error in δ_v estimation affecting polluted dust classification. Figure 2.8 shows global distributions of the number of CALIOP data points of polluted dust for daytime and nighttime. The number of data points is high over the remote ocean for the daytime, whereas the number decreases as the distance from the source regions increases at night. This result implies that other aerosols (probably clean marine) could be misclassified as polluted dust over the ocean particularly during the daytime when the SNR is lower, which in turn would make CALIOP AOD higher than MODIS AOD on average.

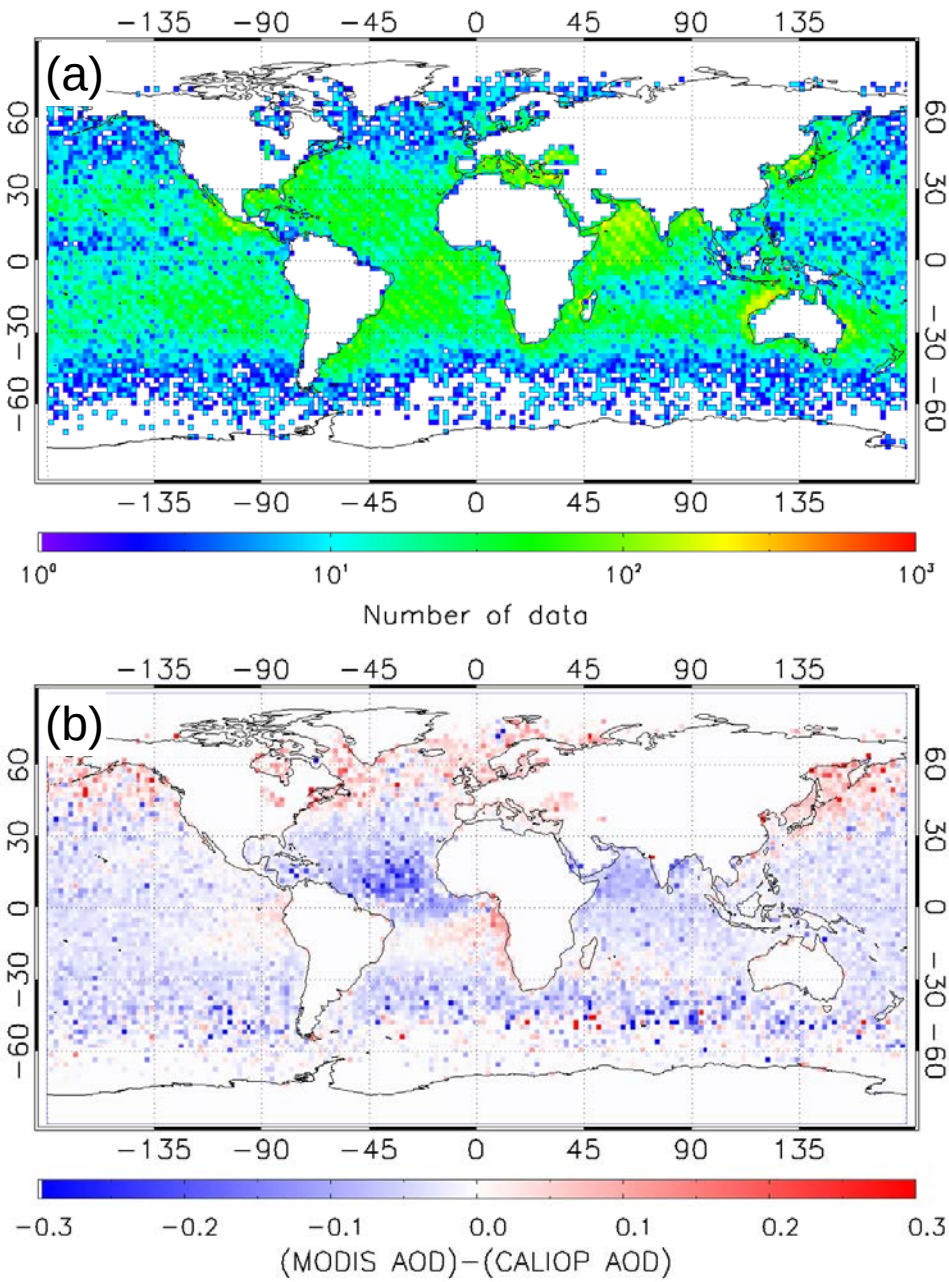

Figure 2.7. Same as Figure 2.3, except for polluted dust.

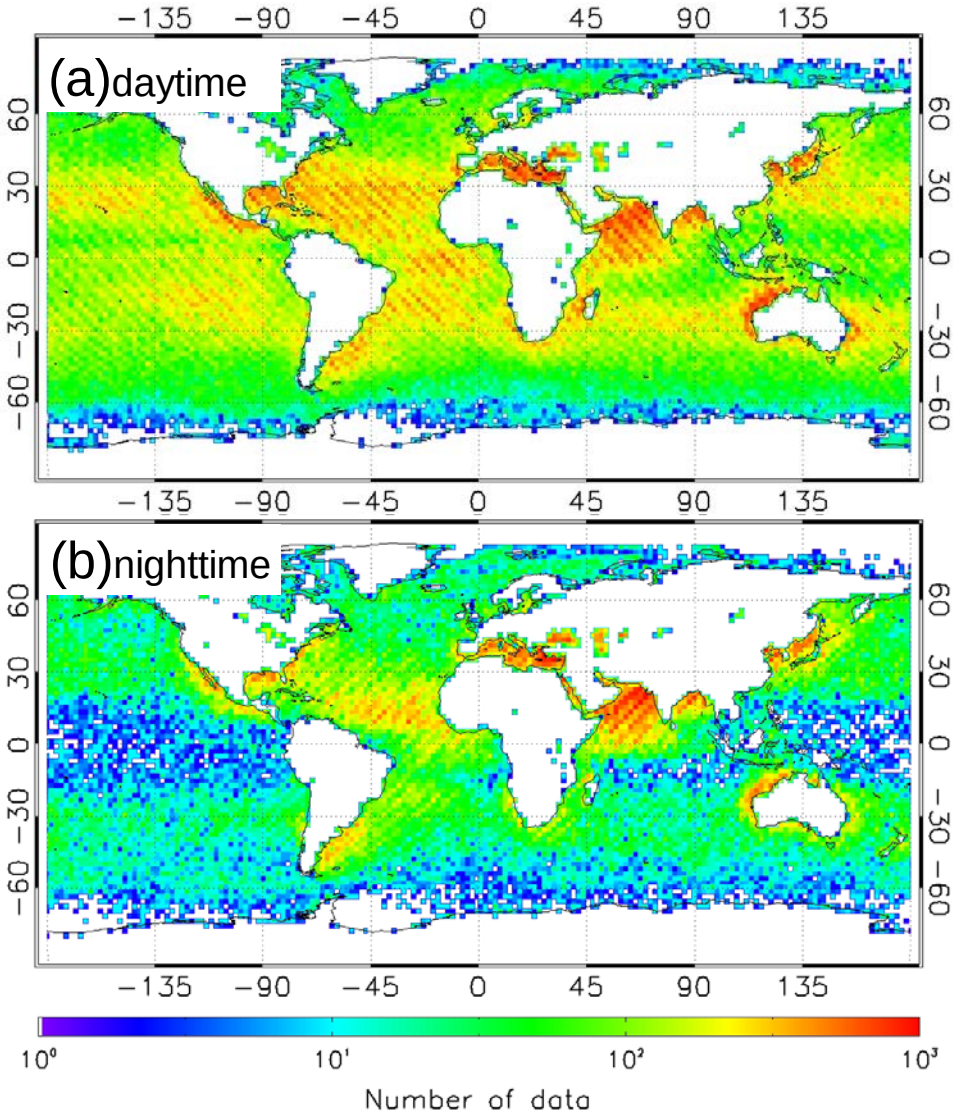

Figure 2.8. Global distribution of the number of CALIOP data points during (a) daytime and (b) nighttime for polluted dust.

2.4.4. Polluted continental

Omar et al. [2009] defined polluted continental as optically thin layers composed of mostly spherical particles with a layer-integrated attenuated backscatter at 532 nm (γ') less than 0.01 and δ_v greater than 0.05. Because optically-thin layers are classified as polluted continental, AODs for polluted continental over the ocean are even lower than those of clean marine (Table 1). As shown in Figure 6 of *Winker et al.* [2009], the retrieval error of MODIS AOD increases dramatically at AODs less than 0.1. Figure 2.2e shows that most of polluted continental AODs are less than 0.1 making the AOD comparison challenging.

Figure 2.9 shows the global distribution of numbers of collocated data pairs and differences of AOD between the two sensors for polluted continental over the ocean. Similar to polluted dust, the number of collocated data pairs for polluted continental is high not only along coastlines but also over remote ocean locations. Figure 2.10 also shows that the number of CALIOP data points for polluted continental over the remote ocean for daytime is high compared to that at nighttime, and implies a low SNR for γ' and δ_v during daytime is responsible for the misclassification of clean marine which is most common over remote oceans as polluted continental.

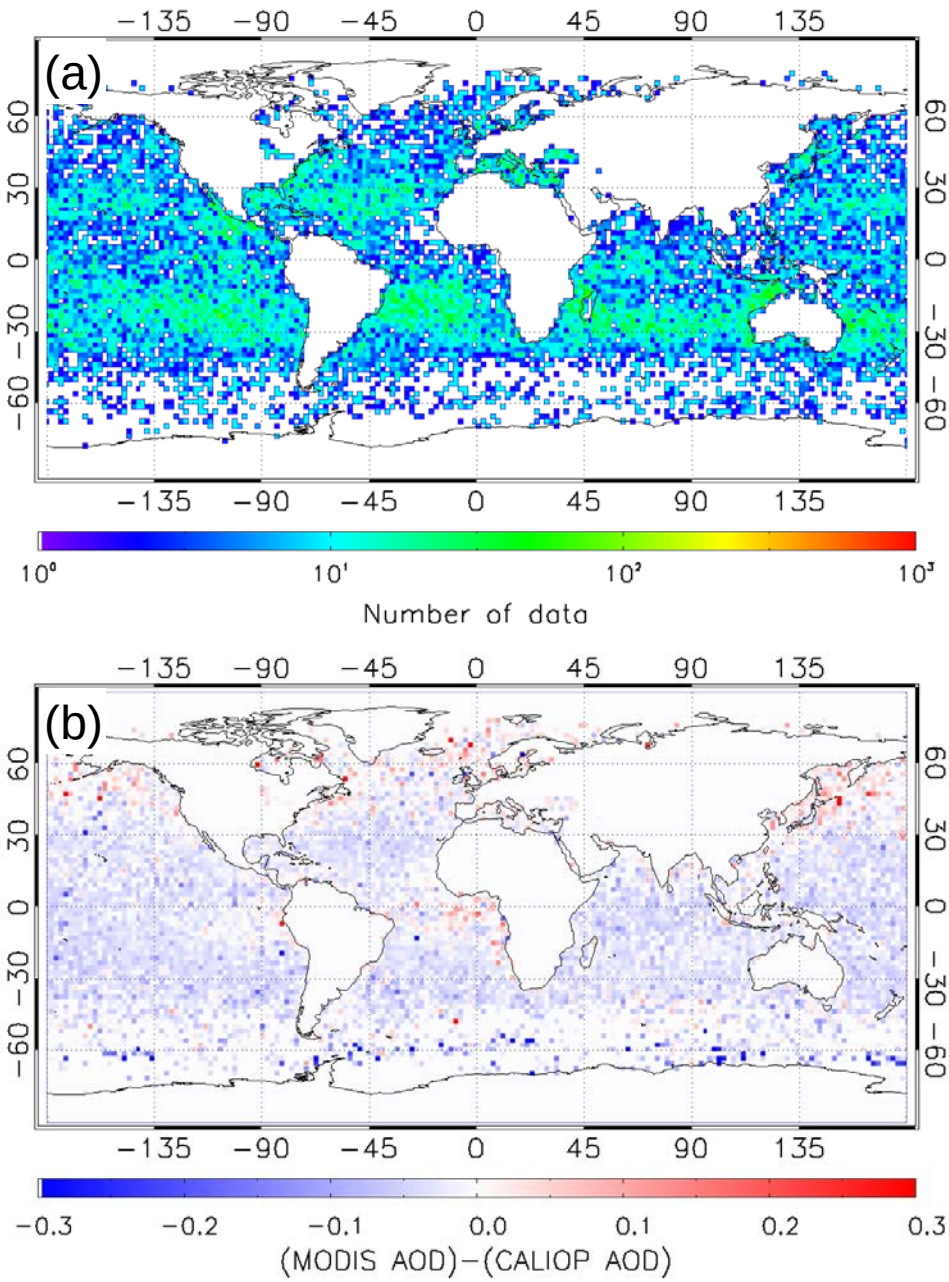

Figure 2.9. Same as Figure 2.3, except for polluted continental.

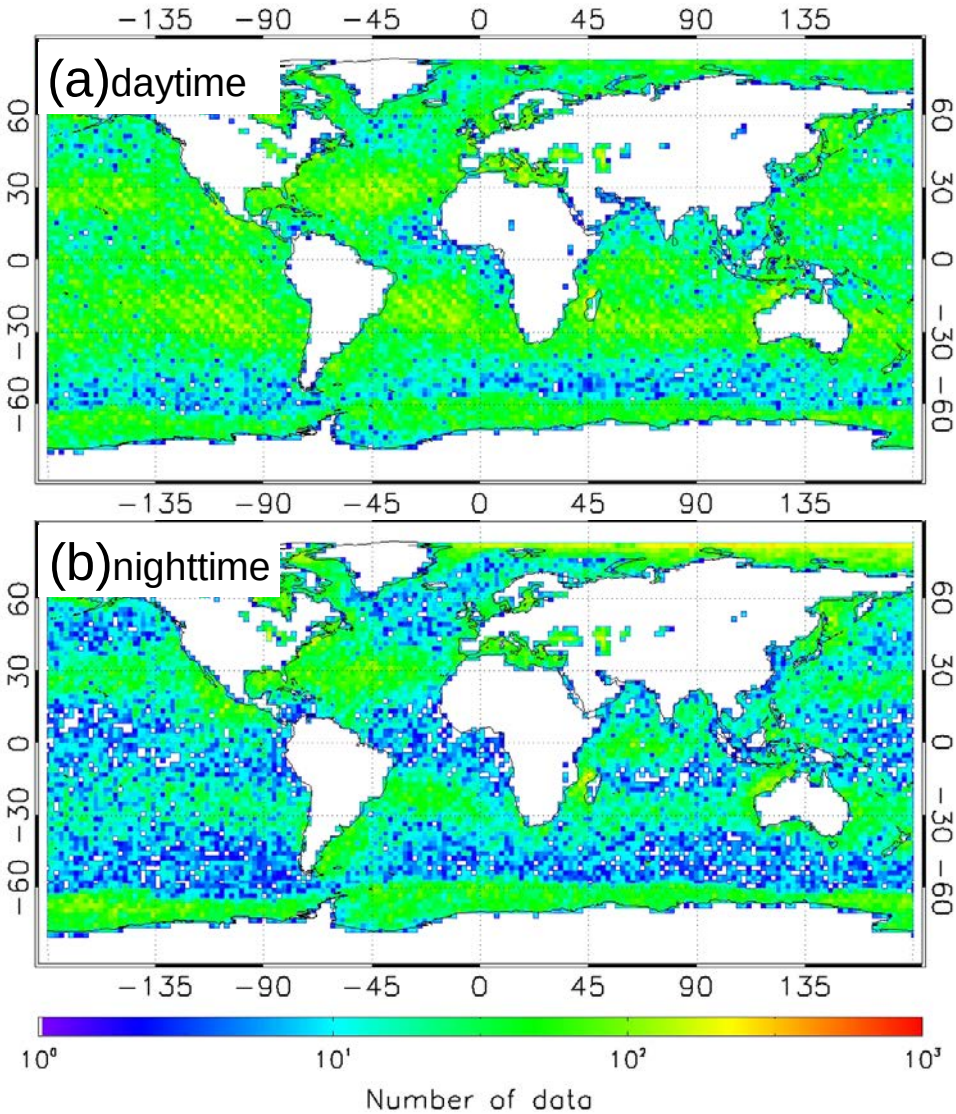

Figure 2.10. Same as Figure 2.8, except for polluted continental.

2.4.5. Biomass burning

Biomass burning, also referred to as smoke in the CALIOP algorithms, shows the largest difference of AOD between the two sensors. The mean AOD of MODIS (0.281 ± 0.232) is about twice that of the CALIOP AOD (0.139 ± 0.157). Collocated data pairs appear most frequently in the South Atlantic Ocean, west of Africa (Figure 2.11a), which is considered a primary global source region of biomass burning [*Duncan et al*., 2003]. CALIOP AOD is generally lower than MODIS AOD regardless of region (Figure 2.11b). The CALIOP lidar ratio for smoke is quite high at 70 sr and consistent with the values obtained by *Ansmann et al.* [2001], *Voss et al.* [2001], and *Cattrall et al.* [2005]. It is therefore unlikely that the low CALIOP AOD is a result of an underestimated smoke lidar ratio.

Biomass burning aerosols are buoyant at the source and thus more likely to be elevated above the marine boundary layer when transported over the ocean. In the CALIOP aerosol classification algorithms, all elevated non-dust aerosol layers over the ocean are identified as biomass burning [*Omar et al.*, 2009]. CALIOP, being a down-looking lidar system, readily detects the top height compared to the base height of a cloud or an aerosol layer. This is because the signal undergoes significant attenuation as it travels through optically ‘thick’ layers [*Vaughan et al.*, 2005; *Kim et*

al., 2011]. For most of the aerosol layers located near the surface, it is not necessary to find the base altitude as most often the layer reaches the surface. For the elevated layers, however, the base altitude is important in determining CALIOP AOD. Because biomass burning aerosols are more likely to be elevated and separated from the boundary layer, the correct location of the base height is crucial for AOD determination.

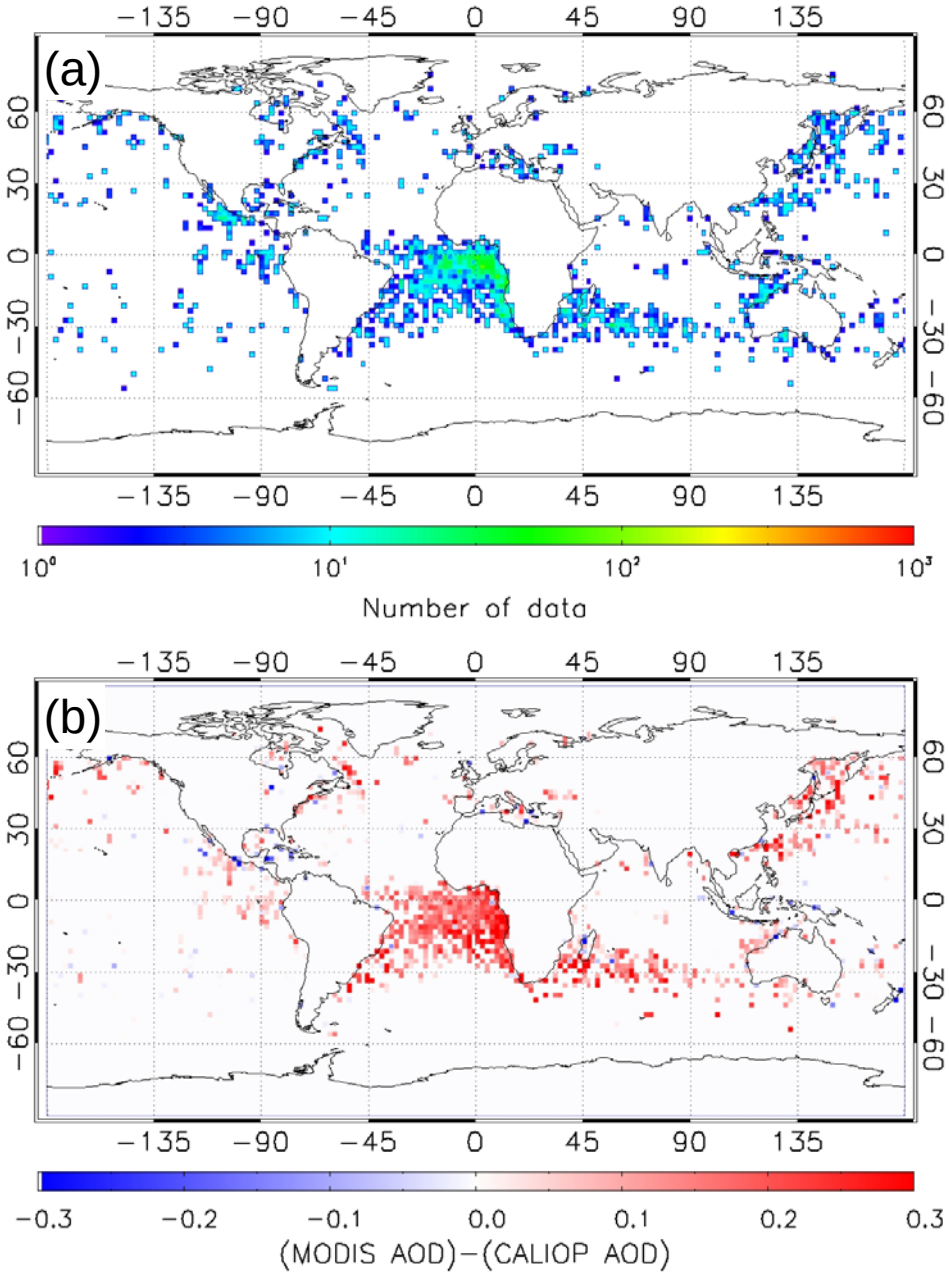

Figure 2.11. Same as Figure 2.3, except for biomass burning.

Figures 2.12 and 2.13 are examples of (a) the total attenuated backscatter at 532 nm for CALIOP Level 1B data, (b) aerosol extinction profile at 532 nm from Level 2 5-km profile data, and (c) column integrated AOD from CALIOP and MODIS for the collocated data pairs of biomass burning measured over the Southern Atlantic. In both figures, the layer top altitudes are easily distinguishable but the base altitudes determined by the CALIOP algorithms are quite variable and possibly uncertain. The base altitudes for the aerosol layer in Figure 2.12 are near 3-4 km and no other aerosol layers are detected below, whereas the base altitudes for Figure 2.13 extend to the surface. When comparing AOD for these two cases, a distinct contrast is found. The CALIOP AODs are similar or slightly larger than MODIS AOD for Figure 2.13c while MODIS AOD is nearly twice that of CALIOP AOD for Figure 2.12c. In this study, the mean layer base altitude for the collocated data pairs of biomass burning is 3.1 km. Also, 71.5% of the collocated data pairs have the base altitude higher than 2 km, which implies that the most of CALIOP AOD for biomass burning does not extend into the marine boundary layer.

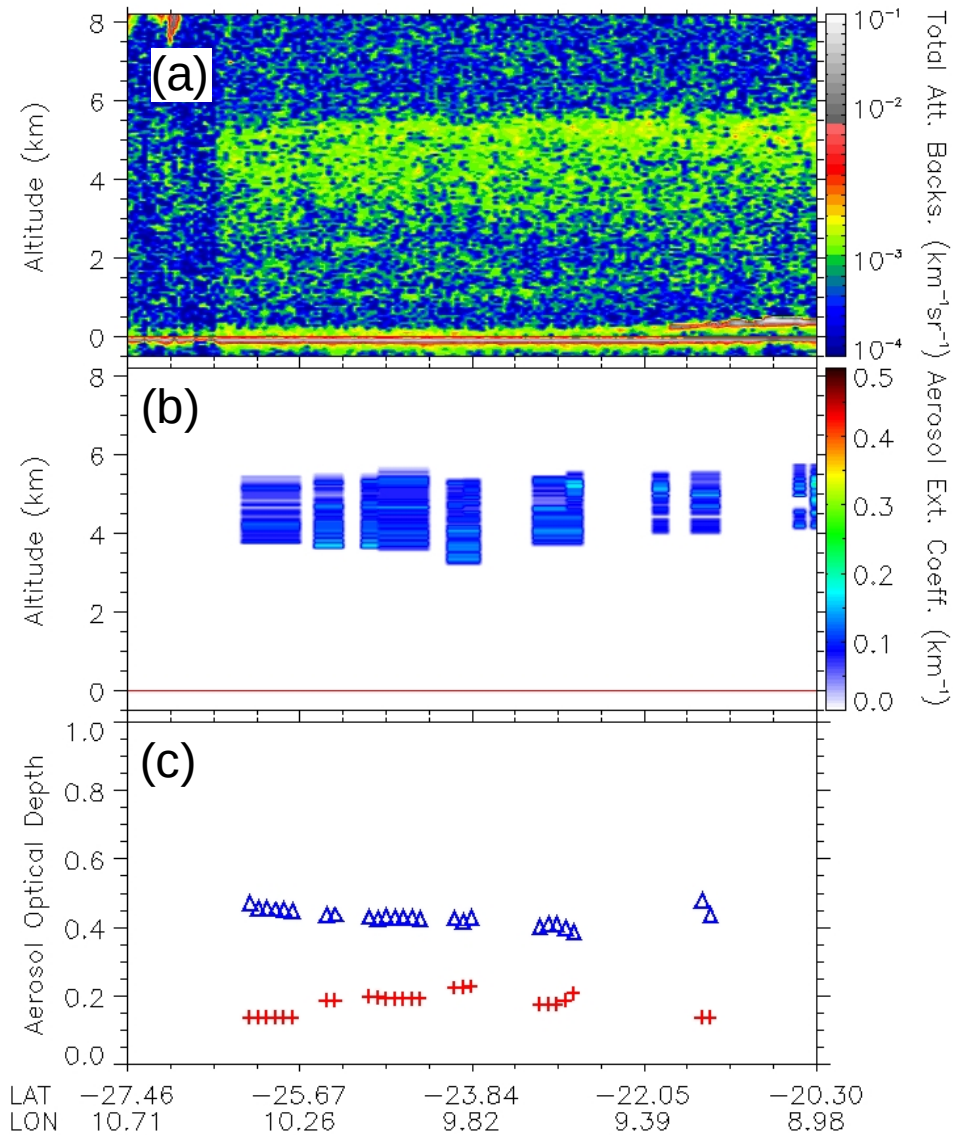

Figure 2.12. (a) CALIOP Level 1 total attenuated backscatter at 532 nm, (b) CALIOP Level 2 5-km aerosol extinction profile, and (c) column integrated AODs from CALIOP (red cross) and collocated MODIS AOD (blue triangle) for the biomass burning aerosols from 13:19 UTC to 13:21 UTC, October 6, 2010.

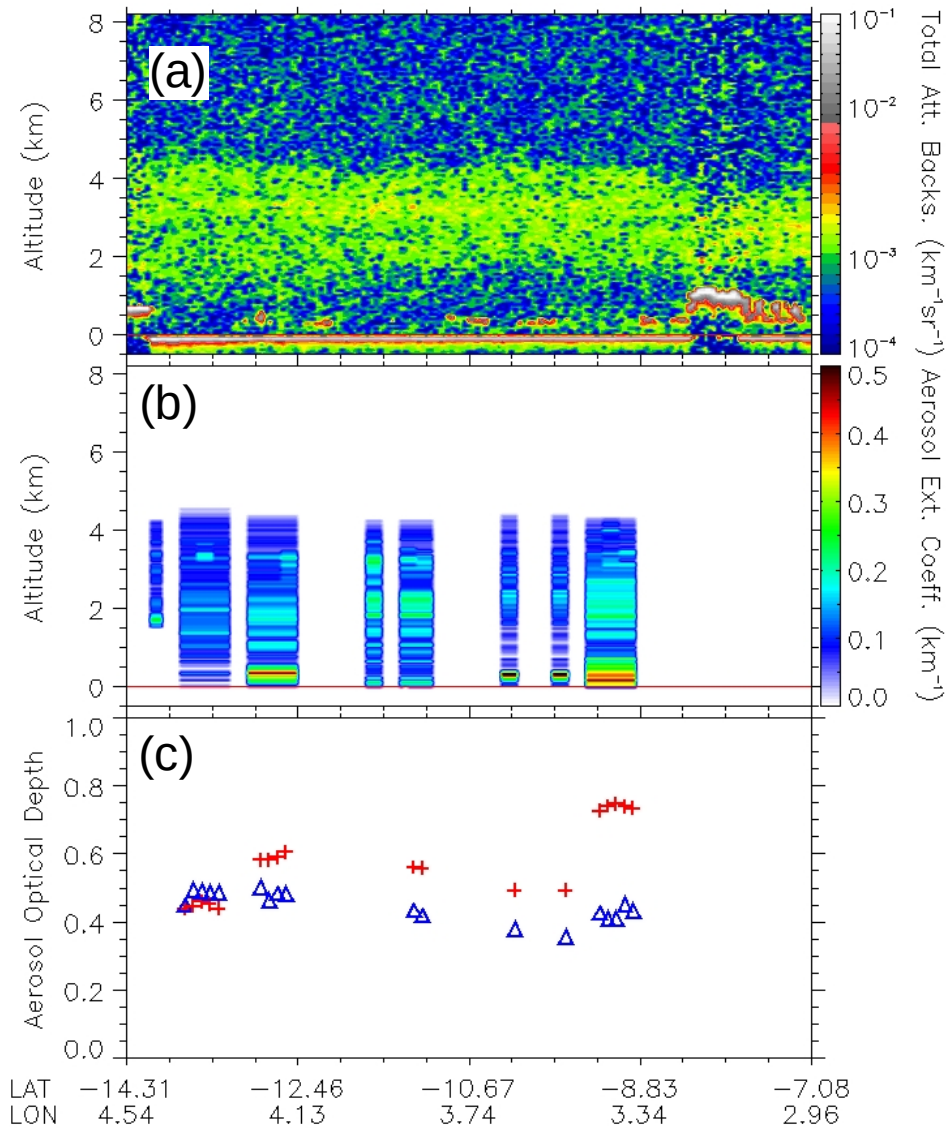

Figure 2.13. Same as Figure 2.12, except from 13:34 UTC to 13:36 UTC, October 4, 2010.

Figure 2.14 shows aerosol extinction profiles from CALIOP Level 2 Aerosol Profile product (blue) and retrieved in this study using same retrieval algorithm with *Young and Vaughan* [2009] from CALIOP Level 1 product (red). This profile comes from the center of Figure 2.12, from -24.15° to -24.69° in latitude. For that region, CALIOP Level 2 product does not report aerosol layers blow 3.5 km from the surface. Our retrieval matches relatively well with CALIOP L2 products for detected aerosol layers from 3.5 km to 5.8 km. However, our retrieval shows that aerosol extinction is still high enough below the detected aerosol layer. Thus, AOD increases from 0.19 to 0.40. As shown in this figure, surface reflection is not fully removed in our retrieval. If we remove aerosol extinction near the surface (below 300 m), AOD is found to be 0.34 which is still higher than AOD from CALIOP Level 2 product.

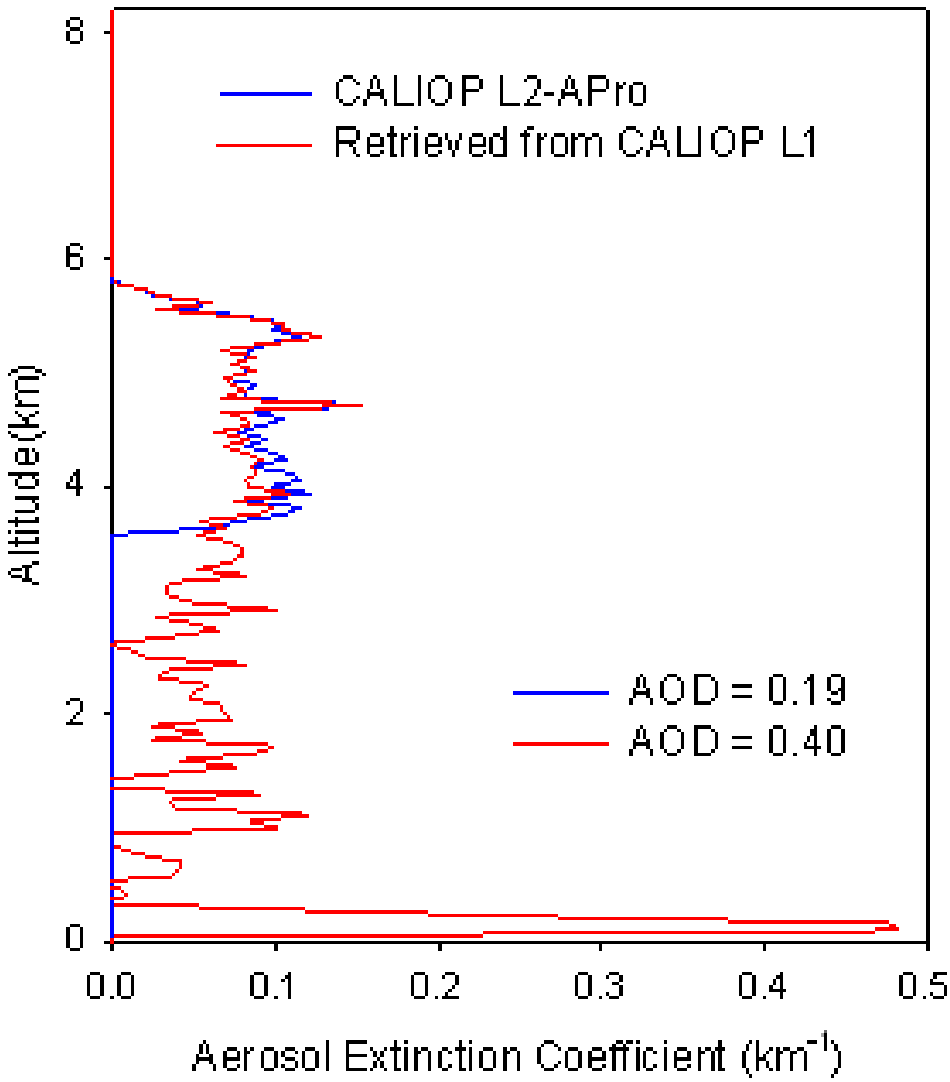

Figure 2.14. Aerosol extinction profiles from CALIOP 5-km Level 2 Aerosol Profile Product (blue) and retrieved in this study from CALIOP 333-m Level 1 product using same retrieval algorithm with Young and Vaughan [2009] from the top of the layer to the surface level (red). The aerosol extinction profiles correspond to the center of Figure 2.12, from -24.15° to -24.69° in latitude.

2.5. Summary

Nearly two million collocated AOD data pairs have been compared over oceans for cloud-free conditions using CALIOP Level 2 aerosol layer and profile products (Version 3.01) and MODIS Level 2 aerosol product (Collection 5.1) from June 2006 to December 2010. MODIS 10-km pixel and CALIOP profiles closer than 10 km from MODIS pixel are chosen as a collocated data pair. In order to consider errors associated with aerosol type classification and pre-determined lidar ratio, CALIOP AODs with layers of a single aerosol type throughout the column were selected for the comparison. The mean MODIS AOD is 63% larger than that of CALIOP AOD for all aerosol types. When considering aerosol types defined in CALIOP algorithm, the differences in AOD between the two sensors show some dependence on the type of aerosol. MODIS AOD is higher than CALIOP AOD for most aerosol types except for polluted dust and polluted continental.

AOD differences between MODIS and CALIOP for clean marine (relative bias of 96%) show latitude dependency, which is related to the surface wind speed, especially for the southern hemisphere. Because CALIOP AOD is not affected by surface conditions, the latitudinal variation in the AOD difference is likely due to surface related retrieval

errors of MODIS AOD. A strong surface wind brightens the ocean and thus can contribute to the higher MODIS AOD.

Dust AOD from CALIOP and MODIS are in good agreement with a relative bias of 13%. However, they show distinct regional variations. MODIS AOD is much higher than CALIOP AOD for the Asian dust, while MODIS AOD is almost similar or sometimes lower for the dust from Saharan and Arabian deserts. The AOD difference for dust also shows strong dependence on extinction-normalized particulate depolarization ratio ($\bar{\delta}$). The increasing trend of the AOD difference with $\bar{\delta}$ implies that the lidar ratio for dust should increase as $\bar{\delta}$ increases, if the MODIS AOD is correct.

Mean AOD of CALIOP is larger than that of MODIS for polluted dust (relative bias of -15%) and polluted continental (relative bias of -29%). It is possible that the lidar ratios for these aerosols are overestimated or that some other aerosols with smaller lidar ratio are misclassified if MODIS AOD is assumed to be correct. The large number of collocated data pairs for polluted dust and polluted continental over the remote ocean, far from their source region, may be an indication that other aerosols such as clean marine are being misclassified as polluted dust and polluted continental.

A large difference in AOD (102%) between CALIOP and MODIS was found for biomass burning. A reason for the low CALIOP AOD is due to the errors in determining the layer base altitude. By definition in the CALIOP algorithms, biomass burning aerosol layers are all elevated. It is therefore critical to determine the base altitude correctly in order to account for all aerosols in the column. This can be a challenge for satellite based down-looking lidar systems especially in the presence of highly attenuating smoke layers frequently encountered near biomass burning source regions. In this study, most of the biomass burning layers do not extend into the boundary layer which may have led to the underestimation of the CALIOP AOD.

This study has shown several areas where both the CALIOP and MODIS algorithms can be improved. It is possible that MODIS retrievals are affected by sea surface wind speeds in the Southern Hemisphere and the algorithms might benefit from updated surface models and dynamic wind fields to account for ocean surface reflectance. The CALIOP algorithms can increase the accuracy of the Asian dust AODs by adopting regionally variable dust lidar ratios. Additionally, an examination of the layer base altitude for smoke layers and comparison with independent measurements to determine what corrections if any to the calculation of

the AOD for smoke are warranted. As the study has shown, the effect of the daytime SNR on the depolarization ratio has important consequences for the aerosol classification scheme. While there are no easy solutions to some of the findings of this study CALIPSO team is working on several fronts to mitigate some of these shortcomings in the upcoming algorithm release.

CHAPTER 3.
EVALUATION OF CALIOP LIDAR RATIO USING AOD CONSTRAINED METHOD

3.1. Introduction

CALIOP data products are available in three “levels” that reflect the degree of processing involved [*King et al.*, 2004]. Level 1 data products include the calibrated attenuated backscatter profiles at the two wavelengths (532 nm and 1064 nm) along with various ancillary atmospheric and navigational data. The fundamental sampling resolution of CALIOP is 30 m vertical and 335 m horizontal. The laser pulse repetition frequency of 20.16 Hz produces footprints every 333 m along the ground [*Winker et al.*, 2009], which corresponds to the horizontal resolution of CALIOP Level 1 Products. The vertical resolution of CALIOP Level 1 Products is 30 m from -0.5 to 8.2 km and averaged vertically above an altitude of 8.2 km [*Winker et al.*, 2009]. CALIOP Level 2 Products are created from the Level 1 Products. Primary Level 2 data products from the lidar are the location of atmospheric regions that

contains particulate matter (clouds and aerosols), the identification of these particles according to type. CALIOP Level 2 Products consist of “Layer Product” and “Profile Product”. The Layer Products provide the spatial and optical characteristics of each feature found, and include quantities such as layer base and top altitudes, integrated attenuated backscatter, layer-integrated volume depolarization ratio, and optical depth. The Profile Products report profiles of particle extinction, backscatter, and additional profile information (e.g., particulate depolarization ratios) derived from these fundamental products. The horizontal resolution of CALIOP Aerosol Level 2 Products is 5 km and the vertical resolution of CALIOP Aerosol Level 2 Profile Products is 60 m from -0.5 km to 20.2 km. CALIPSO Level 3 Aerosol Product reports monthly mean profiles of aerosol optical properties on a uniform spatial grid. It is intended to be a tropospheric product, so data are only reported below altitudes of 12 km.

The CALIOP level 2 algorithms retrieve the aerosol extinction profiles from the CALIOP Level 1 Products. To retrieve aerosol extinction profile from lidar measurements, the lidar equation should be solved. *Klett* [1985] or *Fernald* [1984] methods are typically used especially for the ground-based lidar. These methods adopt an analytic solution for the lidar equation assuming aerosol free atmosphere. Then, aerosol extinction

profiles are retrieved for each level to the ground. One of the biggest advantages of these methods is that the solution is very stable for ground-based lidar system. Also, the calibration constant of the lidar equation is eliminated during the retrieval. However, these methods are commonly unstable for down-looking lidar systems such as space-borne and air-borne lidar systems. The CALIOP level 2 algorithm uses a numerical solution to retrieve aerosol extinction profiles [*Young and Vaughan*, 2009].

To solve the lidar equation using analytic or numerical solutions from elastic lidar measurements, $\boldsymbol{S_{aer}}$ should be determined and it is frequently either assumed or inferred from additional measurements. In the CALIOP algorithm, $\boldsymbol{S_{aer}}$ is determined by aerosol type classification based on the cluster analysis of a multiyear (1993-2002) AEROENT dataset [*Omar et al.*, 2005]. $\boldsymbol{S_{aer}}$ is considered to be constant over certain intervals within each backscatter profile, as determined by the layer detection and scene classification algorithms. However, a pre-determined $\boldsymbol{S_{aer}}$ has large uncertainty, higher than 30% [*Omar et al.*, 2009].

As denoted in *Winker et al*. [2013], uncertainty in $\boldsymbol{S_{aer}}$ is the largest source of uncertainty in the CALIOP AOD. Current CALIOP level 2 algorithm uses pre-determined $\boldsymbol{S_{aer}}$ for classified aerosol types. However,

not only using single values of $\boldsymbol{S_{aer}}$ for each aerosol type but also aerosol classification algorithm could be sources of uncertainties in aerosol extinction retrieval. In this study, aerosol extinction profiles are retrieved from CALIOP Level 1 Products using independently measured AOD from AERONET or MODIS-Aqua as a constraint without assuming aerosol type or $\boldsymbol{S_{aer}}$. By comparing the retrieved $\boldsymbol{S_{aer}}$ with that value of CALIOP Level 2 algorithm, the uncertainties of currently used $\boldsymbol{S_{aer}}$ in CALIOP algorithm was evaluated, especially for dust aerosol which is considered as the most accurately classified among CALIOP Level 2 aerosol subtypes.

3.2. Methodology

3.2.1. Aerosol extinction retrieval

In order to retrieve aerosol extinction coefficients from the measurements of elastic backscatter lidar, the lidar equation [EQ2] should be solved.

$$P(z) = \frac{C}{z^2}[\beta_{aer}(z) + \beta_{mol}(z)]e^{-2\int_0^z[\sigma_{aer}(r)+\sigma_{mol}(r)]dr} \qquad \text{[EQ 2]}$$

Here, $P(z)$ is the returned lidar signal from the altitude z, C is the constant including all range-independent parameters, β_{aer} and β_{mol} are the volume aerosol backscatter coefficient of aerosols and molecules, σ_{aer} and σ_{mol} represent the volume aerosol extinction coefficients of aerosol and molecules, respectively.

Normally, β_{aer} and β_{mol} are calculated using air temperature and pressure profiles for the ‘Standard Atmosphere’ or using data from radio sonde profiling. The CALIOP Level 2 product provides ‘Molecular Number Density’ which is obtained from the ancillary meteorological data

provided by the GMAO (http://gmao.gsfc.nasa.gov/ operations/). The calibration constant (C) in [EQ 2] can be calculated or eliminated by assuming aerosol free atmosphere. However, even if the vertical information of molecules (β_{mol}, σ_{mol}) and the calibration constant (C) are known, [EQ 2] cannot be solved because it still has two unknowns: aerosol extinction and backscatter coefficients. To solve this ill-posed equation, we should know $\boldsymbol{S_{aer}}$ which represents the ratio between aerosol backscatter and extinction coefficients as follows.

$$S_{aer}(z) = \frac{\beta_{aer}(z)}{\sigma_{aer}(z)} \qquad \text{[EQ 3]}$$

To derive analytic solution of [EQ 2], *Sasano et al.* (1985) used normalized total extinction coefficient y(z) defined as

$$\mathrm{y}(z) = \sigma_{aer}(z) + \frac{S_{aer}(z)}{S_{mol}}\sigma_{mol}(z). \qquad \text{[EQ 4]}$$

Here, $\boldsymbol{S_{mol}}$ is molecular lidar ratio which is not dependent on height. Then we can obtain following equation by substituting above equation for [EQ 2] and taking the logarithm and differentiating them with z.

$$\frac{d\ln\left(S_{aer}(z)P(z)z^2 e^{-2\left[\frac{S_{aer}}{S_{mol}}-1\right]\int_0^z \sigma_{mol}(r)dr}\right)}{dz} = \frac{1}{\mathrm{y}(z)}\frac{d\mathrm{y}(z)}{dz} - 2\mathrm{y}(z) \qquad \text{[EQ 5]}$$

[EQ 5] is known as Bernoulli's differential equation and has following solution [*Klett*, 1981; *Fernald*, 1984, *Sasano et al.*, 1985].

$$\sigma_{aer}(z) + \frac{S_{aer}}{S_{mol}}\sigma_{mol}(z) = \qquad \text{[EQ 6]}$$

$$\frac{S_{aer}P(z)z^2 e^{-2\left[\frac{S_{aer}}{S_{mol}}-1\right]\int_{z_0}^z \sigma_{mol}(r)dr}}{\frac{S_{mol}P(z_0){z_0}^2}{\sigma_{mol}(z_0)} - 2\int_{z_0}^z S_{aer}P(r)r^2 e^{-2\left[\frac{S_{aer}}{S_{mol}}-1\right]\int_{z_0}^r \sigma_{mol}(r`)dr`}dr}$$

where, z_0 is reference altitude where the aerosol extinction is assumed to be zero. In this equation $\boldsymbol{S_{aer}}$ is assumed constant with altitude.

The analytic solution described above is widely used for ground-based lidar measurements due to its stableness. For the down-looking lidar system such as CALIOP, however, the integration of [EQ 6] is performed in forward direction. Thus, the denominator sometimes can be infinitesimal and [EQ 6] becomes unstable. For this reason, CALIOP level 2 algorithm uses an iterative solution [*Young and Vaughan*, 2009]. [EQ 2] can be rewired for down-looking lidar systems as follows.

$$P'(z) = \frac{P(z)z^2}{C} = [\beta_{aer}(z) + \beta_{mol}(z)]T_{aer}^2(0,z)T_{mol}^2(0,z) \qquad \text{[EQ 7]}$$

Here, $P'(z)$ is range corrected lidar signal, T_{aer}^2 and T_{mol}^2 are two-way transmittance for aerosol and air molecules, respectively. To solve [EQ 7], the "renormalized" attenuated backscatter is calculated using the renormalization factor defined as follows.

$$R_N(z_N) = T^2_{aer}(0, z_N)T^2_{mol}(0, z_N). \qquad \text{[EQ 7]}$$

Thus, [EQ 7] can be rewritten as

$$P'_N(z) = [\beta_{aer}(z) + \beta_{mol}(z)]T^2_{aer}(z_N, z)T^2_{mol}(z_N, z) \qquad \text{[EQ 8]}$$

Solving for the particulate backscattering coefficient at range z, we have

$$\beta_{aer}(z) = \frac{P'_N(z)}{T^2_{aer}(z_N,z)T^2_{mol}(z_N,z)} - \beta_{mol}(z). \qquad \text{[EQ 9]}$$

In [EQ 9], however, $T^2_{aer}(z_N, z)$ is also a function of $\beta_{aer}(z)$. Therefore, we have to find a solution to an equation of the form $x = F(x)$. Equations of this form are commonly solved using fixed-point iteration algorithms and CALIOP level 2 algorithm uses a Newtonian (Newton-Raphson) method iteration. In this method, successive estimates, *k*, of the particulate

backscatter at any range, z, from the lidar are obtained from the following formula:

$$\beta_{aer,k+1}(z) = \beta_{aer,k}(z) - \frac{f[\beta_{aer,k}(z)]}{f'[\beta_{aer,k}(z)]}. \qquad \text{[EQ 10]}$$

Here, $f\left[\beta_{aer,k}(z)\right]$ is

$$f\left[\beta_{aer,k}(z)\right] = \frac{P'_N(z)}{T^2_{mol}(z_N, z)} \exp\left[2\int_{z_N}^{z} \sigma_{aer}(r)dr\right] - \beta_{mol}(z) - \beta_{aer,k}(z)$$

[EQ 11]

and $f'\left[\beta_{aer,k}(z)\right]$ is the derivative of $f\left[\beta_{aer,k}(z)\right]$ with respect to $\beta_{aer}(z)$ at $\beta_{aer,k}(z)$,

$$f'\left[\beta_{aer,k}(z)\right] = \frac{S_{aer}\,\delta z\,P'_N(z)}{T^2_{mol}(z_N,z)} \exp\left[2\int_{z_N}^{z} \sigma_{aer}(r)dr\right] - 1 \qquad \text{[EQ 12]}$$

where δz is the range increment at range z. The retrieved profile of $\beta_{aer}(z)$ may diverge from the correct values if incorrect estimates of the lidar ratio, multiple scattering function (assumed 1 for aerosols), or correction for the attenuation of overlying features are used. When the solution diverges, the CALIOP level 2 algorithm adjust the lidar ratio to prevent divergence in features.

3.2.2. Lidar ratio determination

Aerosol extinction profiles can be retrieved from lidar measurements by solving lidar equation as described in previous section. To solve this equation, however, $\boldsymbol{S_{aer}}$ should be known. It is normally assumed or inferred from order independent observations. In this study, AOD from independently measured from AERONET or MODIS-Aqua are used as a constraint to determine $\boldsymbol{S_{aer}}$. Figure 3.1 shows a schematic flow chart of the algorithm used in this study.

Aerosol extinction profiles are firstly retrieved using $\boldsymbol{S_{aer}}$ of 10 sr or any arbitrary value. By integrating aerosol extinction profile vertically, we can obtain AOD from CALIOP measurement. Then, the CALIOP-derived AOD is compared with MODIS AOD. If the difference of AOD between

two sensors is larger than 0.5%, $\boldsymbol{S_{aer}}$ is adjusted and aerosol extinction profile is calculated again. Final $\boldsymbol{S_{aer}}$ and aerosol extinction profile is determined when the difference of AOD between two sensors is less than 0.5%.

As mentioned in section 2.3, $\boldsymbol{S_{aer}}$ is assumed as constant with altitude which means this algorithm produce vertically averaged values of $\boldsymbol{S_{aer}}$. This assumption can cause error in aerosol vertical structure, but vertically integrated aerosol loading (AOD) is not changed. For the single aerosol layers, this assumption is acceptable. For the multi-layers with different aerosol types, however, this assumption causes the errors in aerosol extinction profiles [*Sasano et al.*, 1985]. In this study, in order to minimize this uncertainty, only single aerosol layers are considered to determine $\boldsymbol{S_{aer}}$.

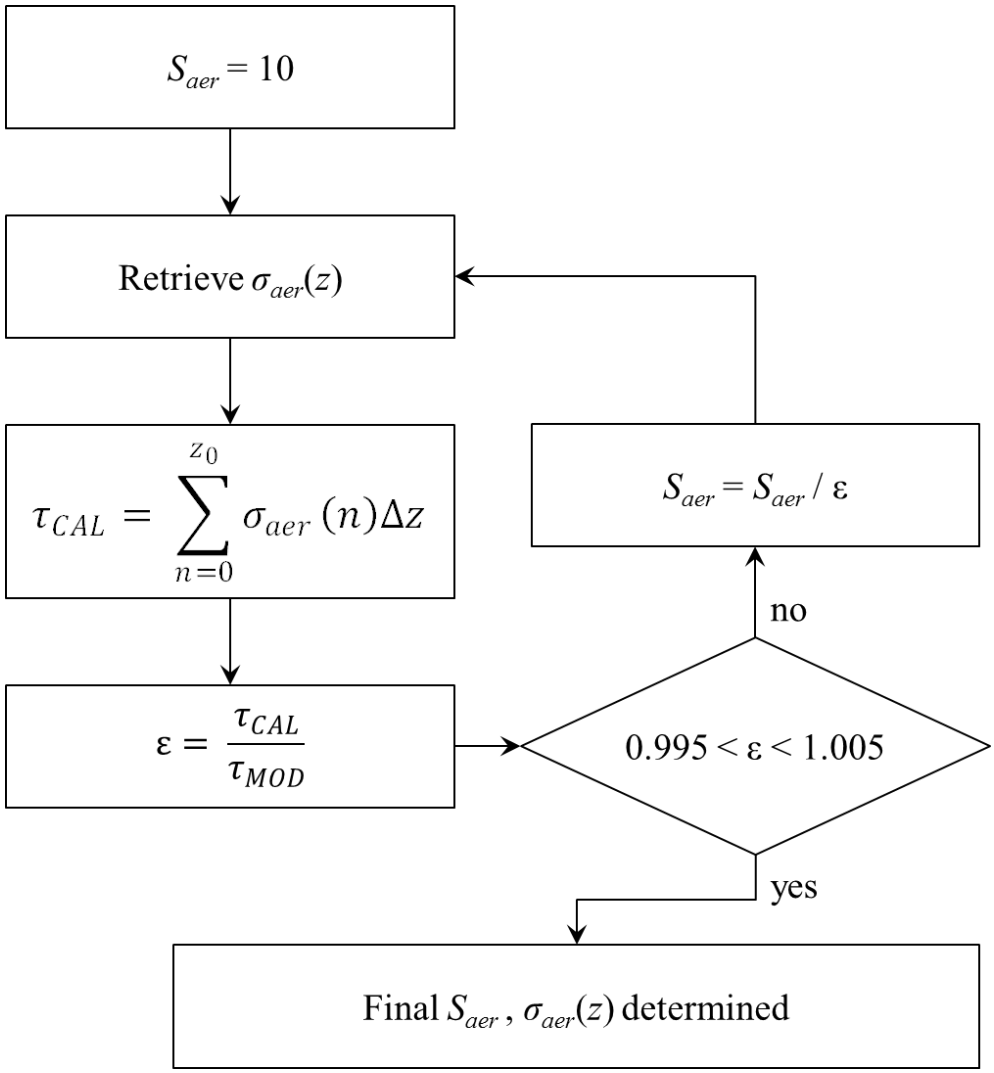

Figure 3.1. Flow chart of the algorithm for determination of the lidar ratio and extinction profile. τ_{CAL} and τ_{MOD} are the AOD from CALIOP and MODIS.

3.3. Determination of lidar ratio from Ground-based Lidar and sky radiometer Measurements

The method described above was successfully applied to determine $\boldsymbol{S_{aer}}$ using 4-year measurements of elastic-backscatter lidar and sky radiometer at Seoul National University of Seoul, Korea. AOD from sky radiometer was adjusted from 500 nm to 532 nm using Ångstöm exponent.

Figure 3.2 shows the seasonal variation of $\boldsymbol{S_{aer}}$, Ångstöm exponent, total depolarization ratio and AOD. Here, Ångstöm exponent and AOD are obtained from sky radiometer and depolarization ratio(*DR*) is vertically integrated values defined as follows.

$$DR = \frac{\sum_{n=0}^{z_0} \delta(n)\sigma_{aer}(n)}{\sum_{n=0}^{z_0} \sigma_{aer}(n)} \qquad \text{[EQ 13]}$$

where, $\delta(n)$ and $\sigma_{aer}(n)$ are total depolarization ratio and aerosol extinction coefficient for nth layer. Aerosol depolarization ratio for dust often exceeds 0.3 and total depolarization ratio is a little bit lower. But the integrated total depolarization ratio used in this study is much less than that of dust layer because it is weighted mean values for the whole layers.

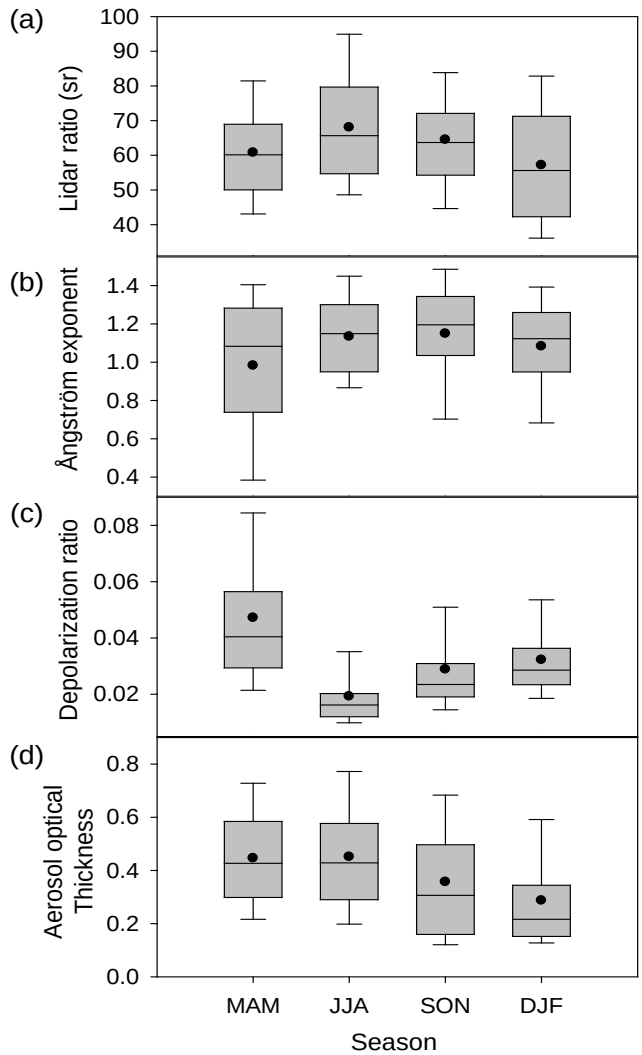

Figure 3.2. Seasonal variation of (a) lidar ratio, (b) Ångström exponent, (c) integrated total depolarization ratio and (d) aerosol optical thickness at Seoul, Korea. Top and bottom of boxes and whiskers represent 75th, 25th, 95th and 5th percentile, respectively. Lines in the boxes are median values and dots represent mean values. Lidar ratio and depolarization ratio are at 532 nm, and Ångström exponent is determined from AOD at five wave length (400, 500, 675, 870, and 1020 nm).

The mean lidar ratio (with standard deviation) based on 4 years of measurements is found to be 61.7±16.5 sr, and has the range of 20 – 110 sr. Relatively weak seasonal variations are noted with a maximum in JJA (68.1±16.8 sr) and a minimum in DJF (57.2±17.9 sr). The impact of Asian dust was clearly noticeable in MAM (spring) through the low values of Ångstöm exponent and high values of depolarization ratio.

From these four-year data, $\boldsymbol{S_{aer}}$ values for some dominant aerosol types are analyzed. Pollution aerosols and dust aerosols can be distinguishable using Ångstöm exponent which provides information about aerosol size [*Jeong and Li*, 2005; *Jung et al.*, 2010]. In this study, dust and pollution aerosols are defined when the Ångstöm exponent belongs to minimum 10% (<0.6) and maximum 10% (>1.4), respectively. Clean or background aerosol is also considered when the AOD belongs to minimum 10% (<0.2). The lidar ratios for clean, dust, and polluted conditions are estimated to be 45.0±9.5 sr, 51.7±13.7 sr, and 62.2±13.2 sr, respectively (Figure 3.3). While the lidar ratio for the polluted condition appears to be consistent with previous studies [e.g., *Ansmann et al.*, 2001; *Cattrall et al.*, 2005; *Barnaba and Gobbi*, 2004], clean conditions tend to have larger ratios, compared to previous estimates and currently used values in CALIOP algorithm [e.g., *Ansmann et al.*, 2001; *Voss et al.*, 2001;

Liu et al., 2002; *Catrall et al.*, 2005; *Muller et al.*, 2007; *Omar et al.*, 2009].

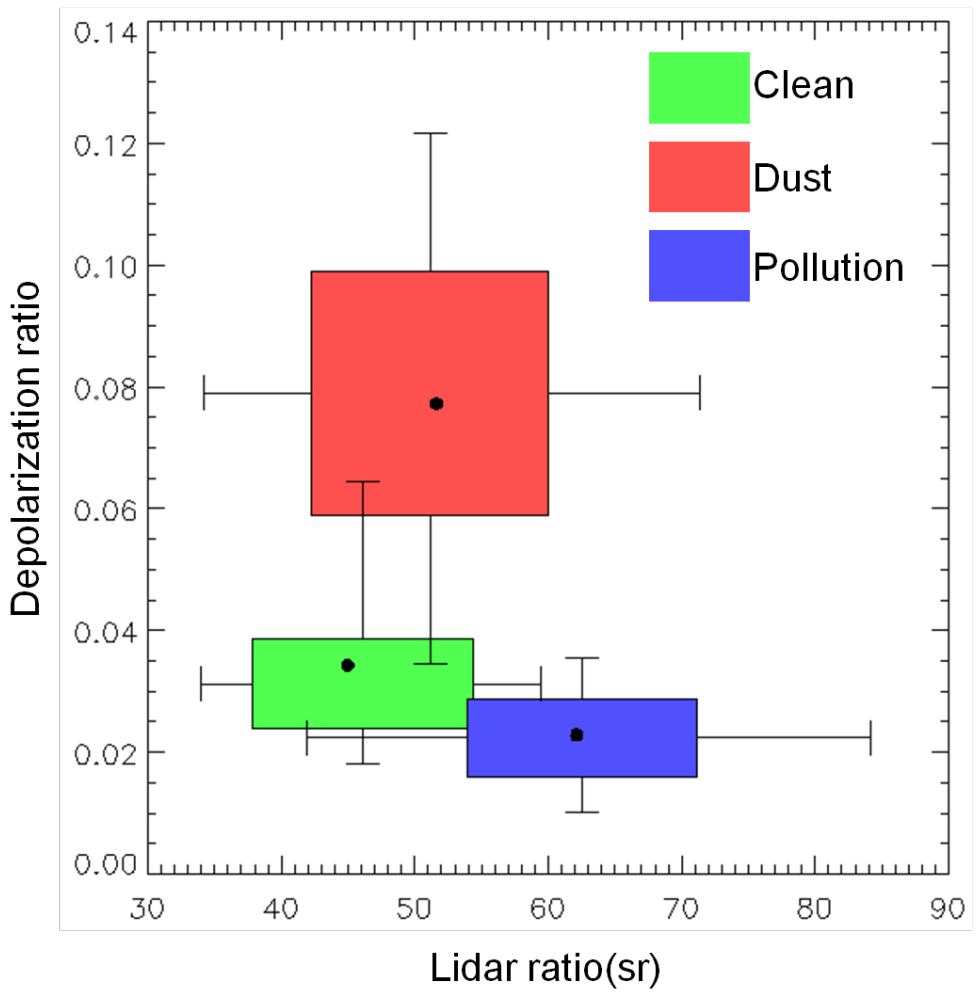

Figure 3.3. Box plots of lidar ratio versus integrated total depolarization ratio at 532 nm for different aerosol types. The boxes represent 25 and 75 percentile and whiskers are 5 and 95 percentile.

Lidar ratios are also retrieved using ground-based lidar and AERONET sun/sky radiometer during Distributed Regional Aerosol Gridded Observation Networks (DRAGON) Northeast Asia Campaign 2012. DRAGON NE Asia Campaign was held in Korea and Japan from March to May 2012, composed by NASA AERONET. During the campaign, lidars from the National Institute for Environmental Studies (NIES) of Japan and AERONET sun/sky radiometers were collocated and operated together at six observatories (Seoul, Gosan, Fukue, Osaka, Chiba, and Tsukuba). In this study, lidar ratio is retrieved for Seoul and Osaka where stable measurements were performed for both lidar and sun/sky radiometer during whole campaign period.

Figure 3.4 shows frequency distributions of lidar ratios at Seoul and Osaka during the campaign. Mean (and standard deviation) lidar ratios at Seoul and Osaka were retrieved as 65.41±21.42 sr and 65.04±20.62 sr, respectively. Mean lidar ratios from two observatories are almost same and comparable to the lidar ratio for pollution [e.g., *Ansmann et al.,* 2001; *Cattrall et al.,* 2005; *Barnaba and Gobbi*, 2004], which implies that the dominant aerosol type in those cities during the campaign is polluted aerosol. One difference between the two cities is that the lidar ratios in Seoul have broader range than Osaka.

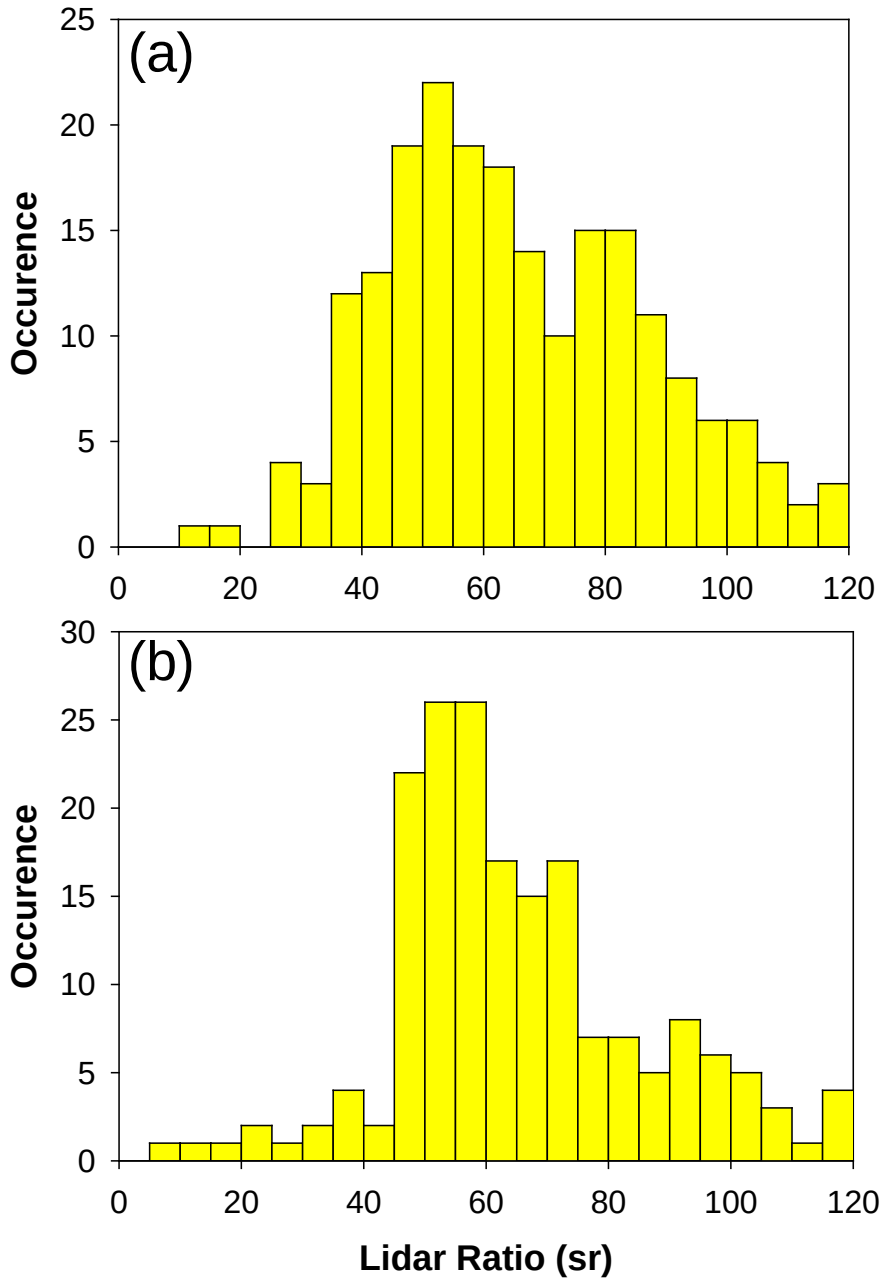

Figure 3.4. Occurrence distribution of lidar ratios retrieved from NIES lidar measurements using collocated AOD as a constraint in (a) Seoul and (b) Osaka during DRAGON NE-Asia Campaign from March to May 2013.

Figure 3.5 and 3.6 are results from lidar and AERONET for dust event during the campaign from April 27 to April 29. Depolarization ratio was small and Ångström exponent was large in Seoul on April 26 (Figure 3.5). This implies that the small and spherical-shaped polluted aerosols were dominant on this day. Then, depolarization ratio increased and Ångström exponent decreased on April 27, which indicates dust plume arrived. Lidar ratios during dust event were retrieved to 40-60 sr (48.02±9.38 sr) which is higher than CALIOP (40 sr). Dust plume passed over Korea and reached Osaka on April 28 (Figure 3.6). Depolarization ratio was increased to ~0.15, but not much large as observed in Seoul. Lidar ratios for dust plume in Osaka are 50~80 sr which are much larger than Seoul. Higher lidar ratios in Osaka than Seoul for dust are due to mixing with polluted aerosols during transport from Korea to Japan. Relatively lower depolarization ratio in Osaka compared to Seoul also shows that dust plume is mixed with spherical-shaped aerosols.

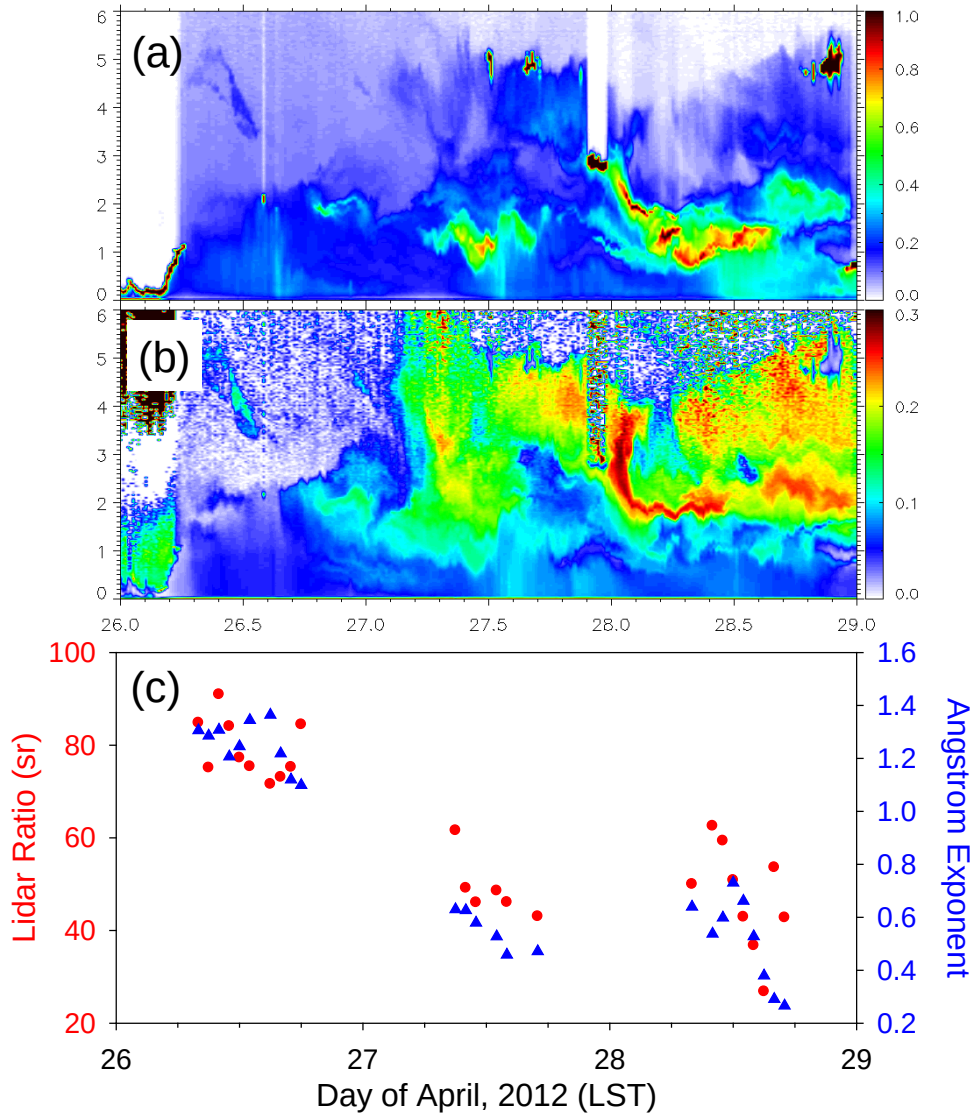

Figure 3.5. (a) Total attenuated backscatter, (b) depolarization ratio, (c) lidar ratios and Ångström exponent from lidar and AERONET measurements in Seoul from 26 to 28 April 2013.

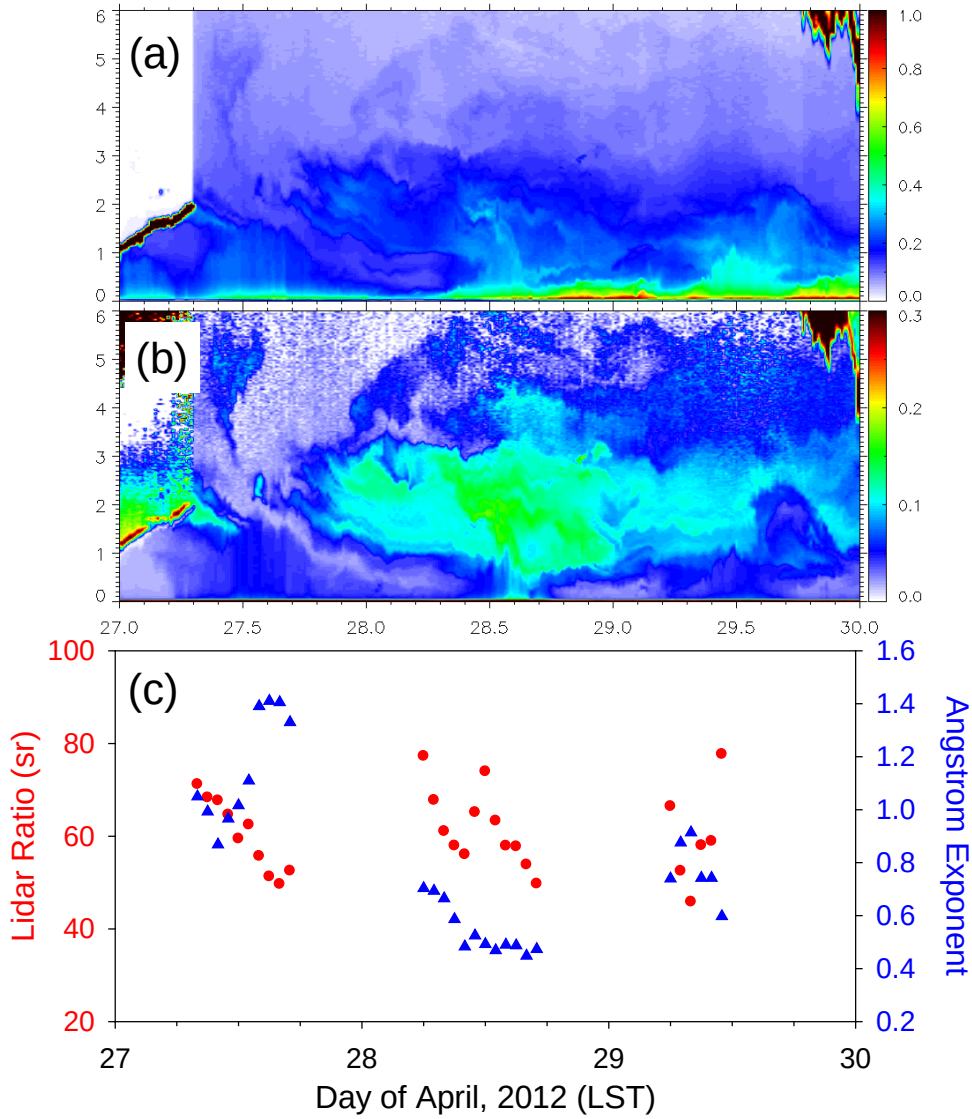

Figure 3.6. Same as Figure 3.5, but in Osaka from 27 to 29 April 2013.

3.4. Determination of lidar ratio from CALIOP and AERONET measurements

Retrieving aerosol extinction from CALIOP is quite different from ground-based lidars as explained in Section 3.2. An iteration method, same as CALIOP level 2 algorithm [*Young and Vaughan*, 2009], was used in this study. To assess the performance of retrieval algorithm, AODs retrieved in this study (AOD_Ret) from CALIOP Level 1 Product were compared AODs from CALIOP Level 2 Product (AOD_CAL). Figure 3.7 is a scatter plot of AOD_Ret and AOD_CAL. 4464 CALIOP profiles for dust aerosol were retrieved in 2010. As mentioned above, CALIOP Level 1 Product has horizontal resolution of 333 m, whereas the horizontal resolution of CALIOP Level 2 Product is 5 km. Thus, fifteen CALIOP Level 1 profiles are averaged to retrieve the aerosol extinction coefficient. To remove surface returns in of CALIOP Level 1 profiles, lidar signals below the surface level were assumed to be zero. Since CALIOP level 2 algorithm retrieves aerosol extinction coefficient only for the detected aerosol layers, the retrieval was performed for same layers.

The linear regression shows that retrieval algorithm used in this study performs properly with the correlation coefficient of 0.975. Only few profiles have large difference between AOD_Ret and AOD_CAL. Most of

these cases are related with failure in separating surface returns.

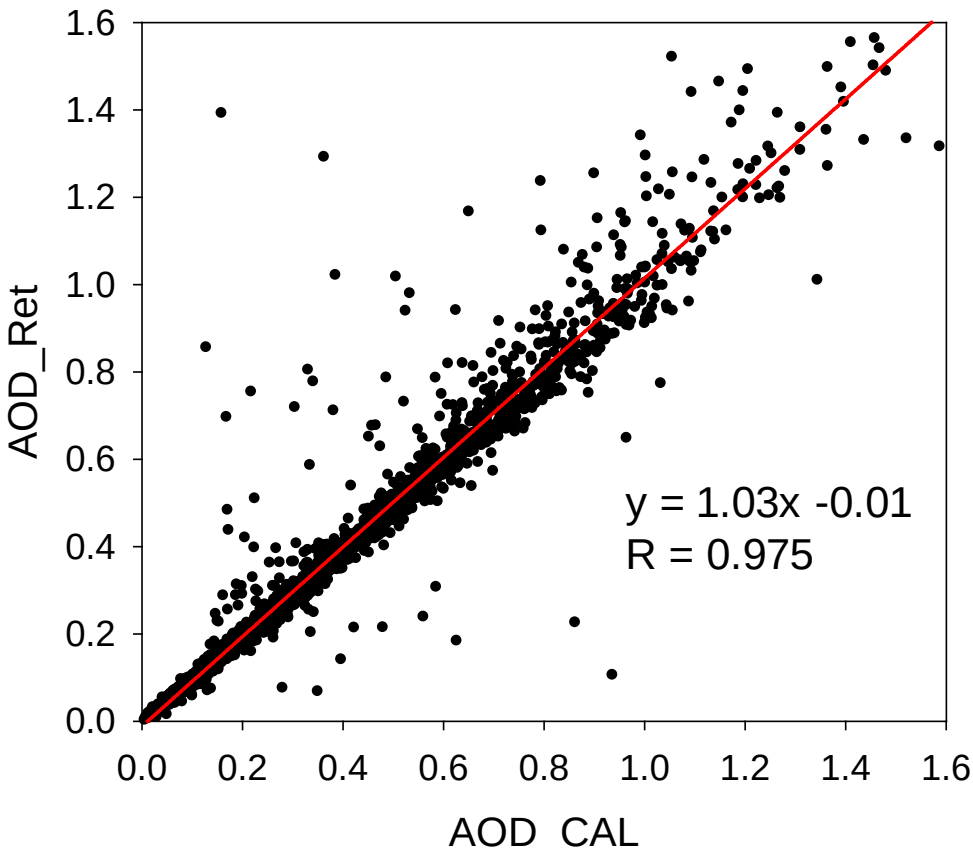

Figure 3.7. Scatter plot of AOD retrieved in this study (AOD_Ret) and CALIOP Level 2 Product (AOD_CAL) for dust aerosols in 2010. Red line represents a linear regression of the data. 4644 profiles have used.

Using the method described in Section 3.2, lidar ratios were retrieved from CALIOP Level 1 Product using AERONET AOD as a constraint for Saharan dust. 15 AERONET sites were chosen where CALIPSO satellite passes nearby. CALIOP profiles within 10 km from AERONET site were selected and AERONET AODs measured within 15 minutes from CALIPSO closest overpass time were averaged. Figure 3.8(a) shows a distribution of retrieved lidar ratio for Saharan dust. The mean (and standard deviation) retrieved lidar ratio was 50.5±19.5 sr. For dust aerosols classified in CALIOP algorithm, the mean lidar ratio decreased to 47.5±16.5 sr (Figure 3.8b). But this value is still larger than currently used lidar ratio for dust in CALIOP algorithm [*Omar et al.*, 2009].

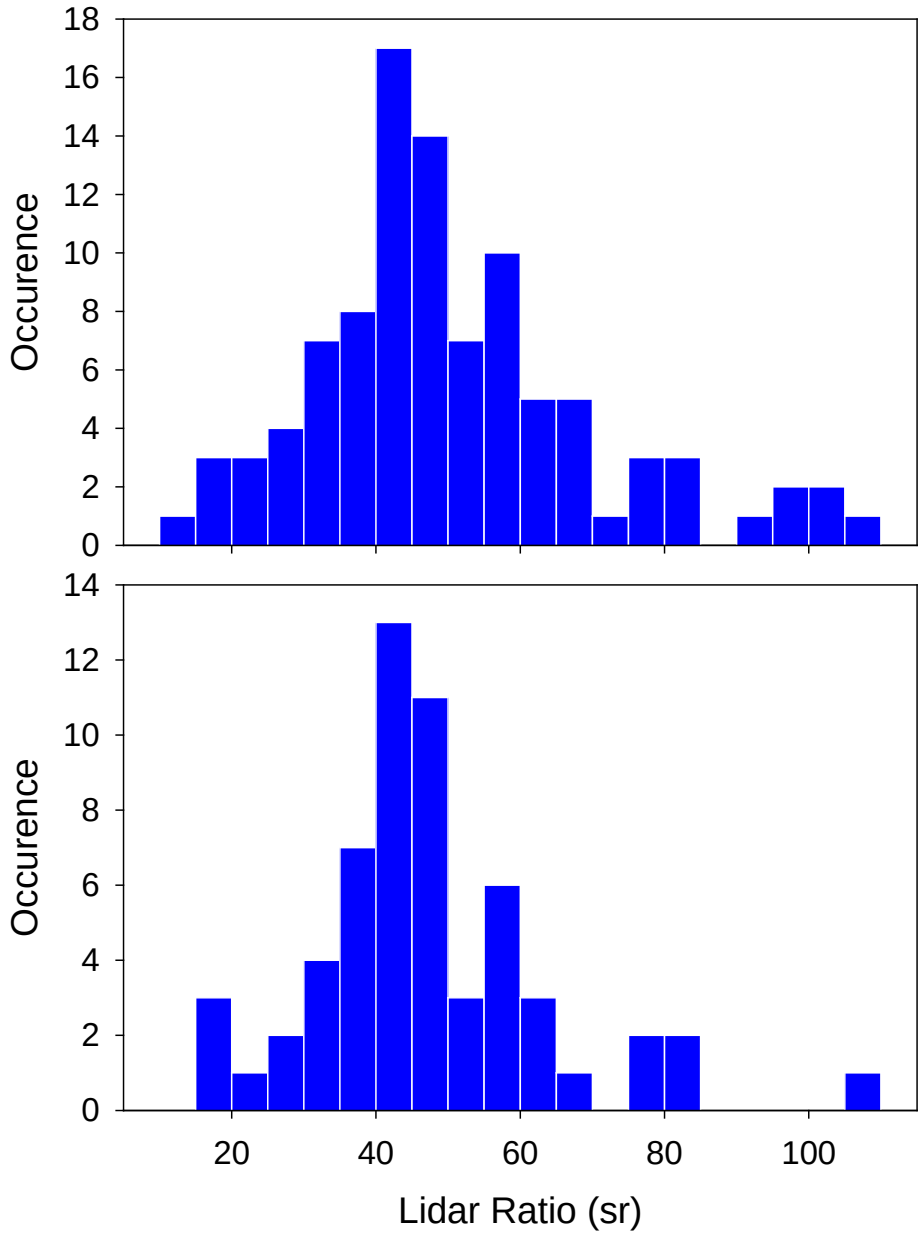

Figure 3.8. Number distribution of retrieved lidar ratios from CALIOP Level 1 Products over near-Saharan AERONET sites for (a) whole retrieved results and for (b) dust aerosols classified in CALIOP algorithm.

3.5. Determination of lidar ratio from CALIOP and MODIS measurements

Aerosol lidar ratio and extinction coefficient are retrieved from CALIOP measurements using MODIS-Aqua AOD as a constraint. CALIOP Level 1 ValStage1 data (Version 3.01) and MODIS-Aqua Level 2 aerosol data (MYD04-L2) are used from January to December 2010. For both instruments, cloud screened and quality assured data over the ocean are used.

Figure 3.9 and 3.10 are examples of CALIOP vertical profiles and retrieved aerosol optical properties. Figure 3.9 shows a typical case of marine boundary aerosol layer. Aerosols are detected from surface to 1~2 km above the surface and most of them classified as clean marine (Figure 3.9d). MODIS AOD is larger than CALIOP AOD for most profiles (Figure 3.9e). Two main differences in aerosol extinction retrieval between AOD constrained method (Figure 3.9c) and CALIOP Level 2 Profile Product (Figure 3.9b) are lidar ratio and retrieving range. In this study, aerosol extinction retrieved for whole profile from the surface to 8.2 km using adjusted lidar ratio, whereas CALIOP Level 2 algorithm retrieves only for detected aerosol layer with pre-determined lidar ratio. Figure 3.9(f) shows

CALIOP lidar ratios have single value of 20 sr for clean marine aerosol, but retrieved lidar ratios have range from 10 sr to 40 sr.

Dust and polluted dust plumes are observed in Figure 3.10. MODIS AOD is generally larger than CALIOP AOD for clean marine aerosols as shown in Figure 3.9. On the other hand, AODs from the two sensors are relatively well matched for dust and polluted dust aerosols (0°-5°N in Figure 3.9). Retrieved liar ratios for dust and polluted dust are relatively larger than clean marine with the range from 20 sr to 60 sr (Figure 3.9f).

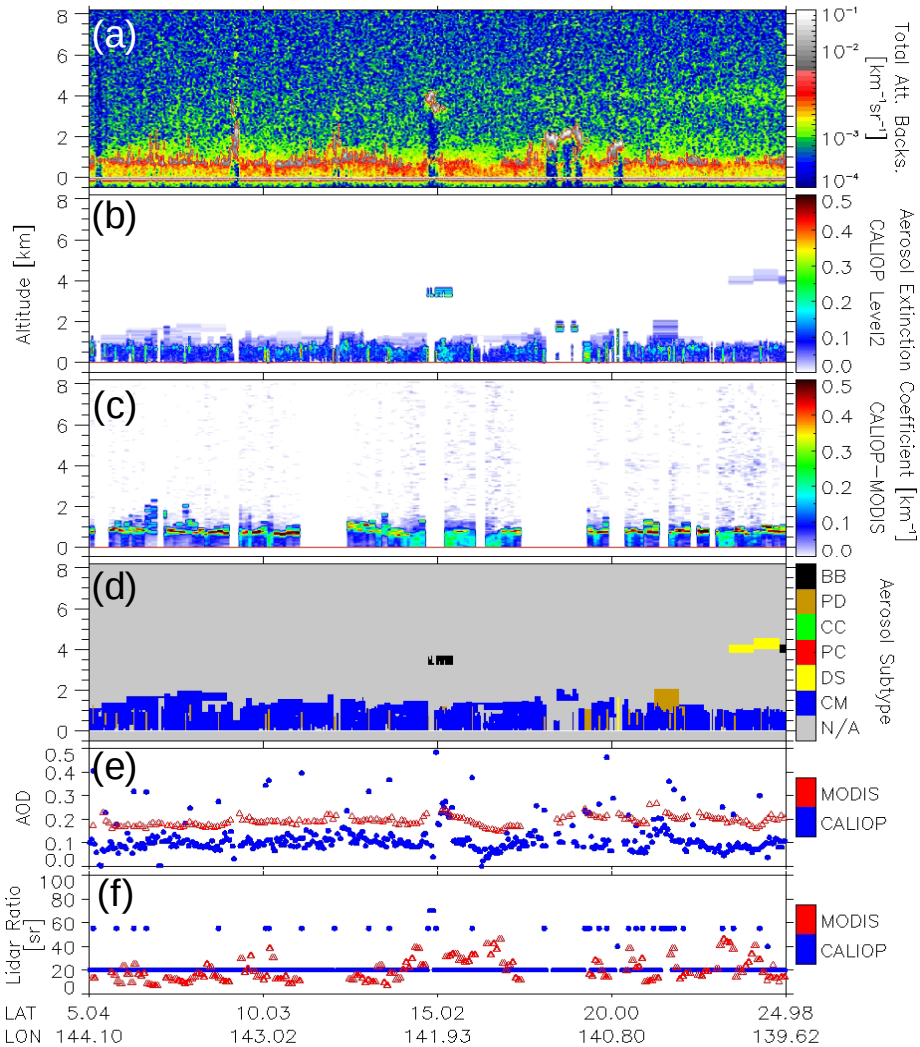

Figure 3.9. (a) Total attenuated backscatter, (b) aerosol extinction from CALIOP Level 2 Product, (c) aerosol extinction retrieved in this study, (d) aerosol subtype (e) aerosol optical depth from MODIS (red triangle) and CALIOP Level 2 Product (blue circle), and (f) lidar ratios for dominant aerosol subtype in CALIOP Level 2 Product (blue circle) and retrieved in this study using MODIS AOD as a constraint (red triangle) observed on 15 March 2010 ~04UTC over Western Pacific.

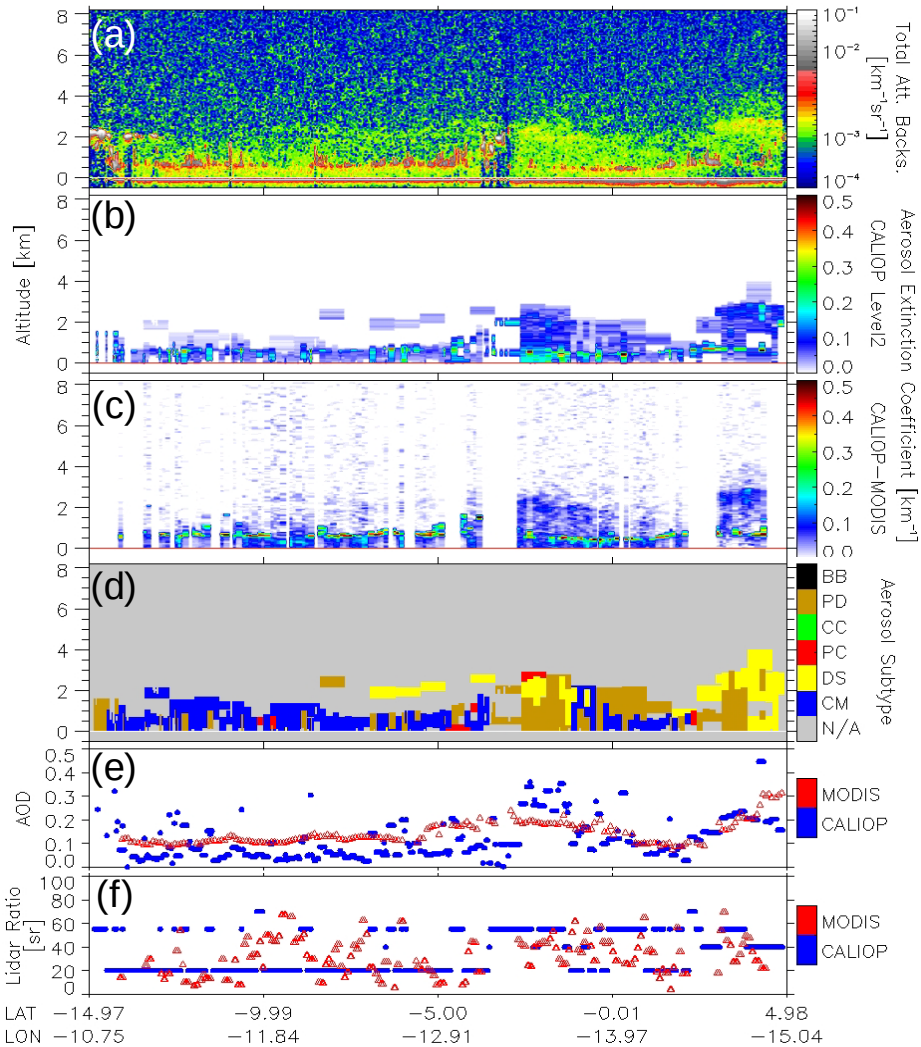

Figure 3.10. Same as Figure 3.9, but observed on 16 March 2010 ~14UTC over Mid Atlantic.

Figure 3.11 and 3.12 show frequency distributions of retrieved lidar ratios using AOD constrained method. Mean value of the retrieved lidar ratios for clean marine (25.66±23.68 sr) is slightly larger than 20 sr which is currently used in CALIOP algorithm (Figure 3.11a). However, its distribution with the median of 20.40 sr, in Figure 3.11(a), shows that currently used lidar ratio (20 ar) and aerosol type classification for clean marine aerosol in CALIOP algorithm is acceptable in spite of large standard deviation.

The mean lidar ratio retrieved from CALIOP and MODIS measurements using AOD constrained method for dust aerosol (46.32±14.44 sr) shows very similar values, shown in Section 3.3 and 3.4, which implies currently used lidar ratio for dust in CALIOP algorithm need to be increased (Figure 3.11b). Especially for Asian dust (110°E - 180°E, 20°N – 50°N), the lidar ratios are retrieved much larger. This result also suggests that the lidar ratios for dust have regional variation as mentioned in Section 2.4.2.

The mean retrieved lidar ratios for polluted dust, biomass burning, and polluted continental aerosols are 47.41±19.57 sr, 59.15±20.69 sr, and 56.91±24.12 sr, respectively, 14-19% less than those values in CALIOP

algorithm (Figure 3.12). The mean lidar ratio for biomass burning was expected to be larger than 70 sr, which is used in CALIOP algorithm, because MODIS AOD is much larger than CALIOP AOD for biomass burning as shown in Section 2.4.5. In this study, however, unlike CALIOP Level 2 algorithm, aerosol extinction retrieval is performed from 8.2 km to the surface not from the layer top altitude to the layer base altitude. As a result, CALIOP AOD can increase compared to CALIOP Level 2 product and the mean lidar ratio can be retrieved less than 70 sr for biomass burning aerosol. This result shows that CALIOP AOD for biomass burning would be larger when the retrieval is performed for whole profile. Thus error in layer detection is a significant source of uncertainty in CALIOP AOD for biomass burning.

Currently used lidar ratios in CALIOP algorithm for polluted dust, polluted continental, and biomass burning aerosols are consistent with other previous studies [e.g., *Ansmann et al.*, 2001; *Voss et al.*, 2001; *Catrall et al.*, 2005]. Therefore, discrepancies in lidar ratios between CALIOP algorithm and this study for those aerosols are thought be due to errors in aerosol type classification rather than errors in lidar ratio itself.

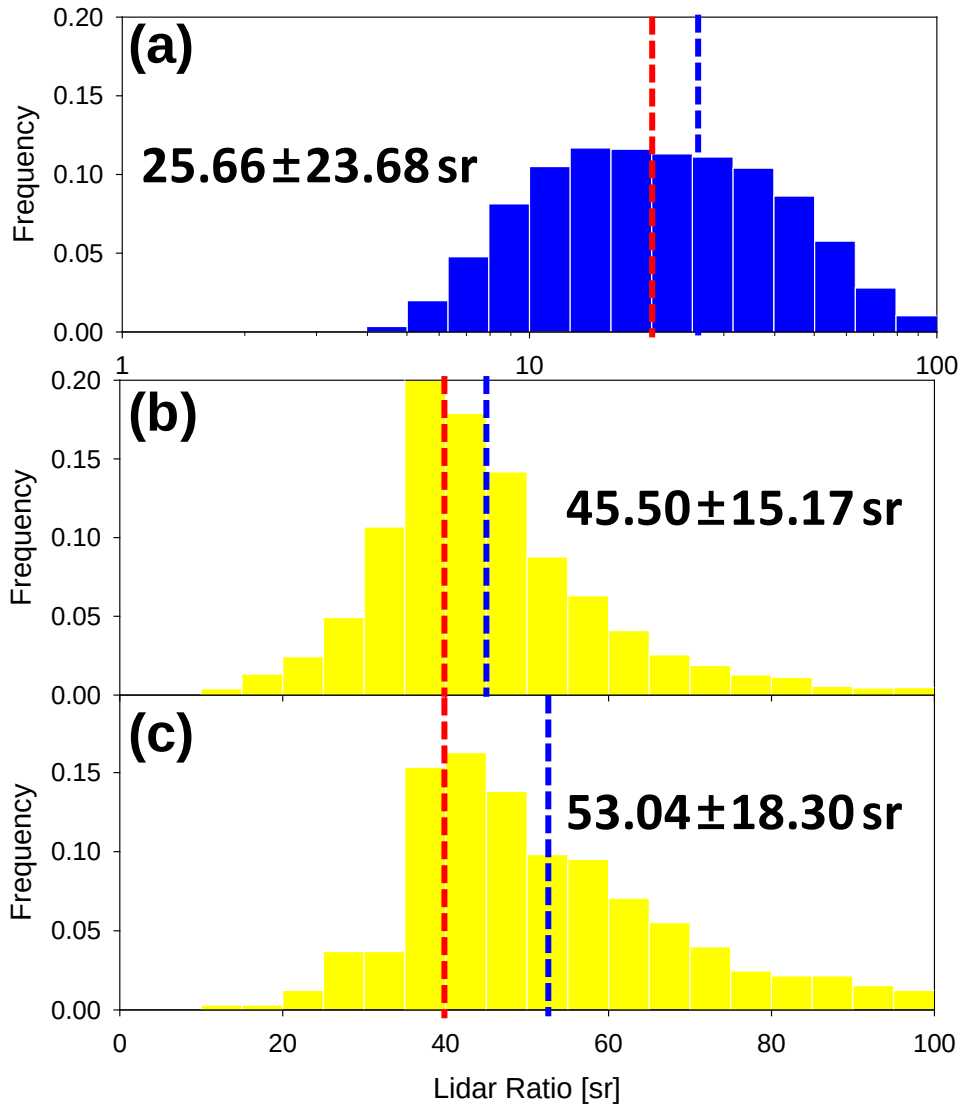

Figure 3.11. Frequency distributions of retrieved lidar ratios from CALIOP and MODIS measurements using AOD constrained method for (a) clean marine (log scale), (b) dust, and (c) Asian dust aerosols. Red and blue dashed lines represent currently used lidar ratios in CALIOP algorithm and mean values retrieved in this study, respectively. Mean (and standard deviation) lidar ratios are also shown.

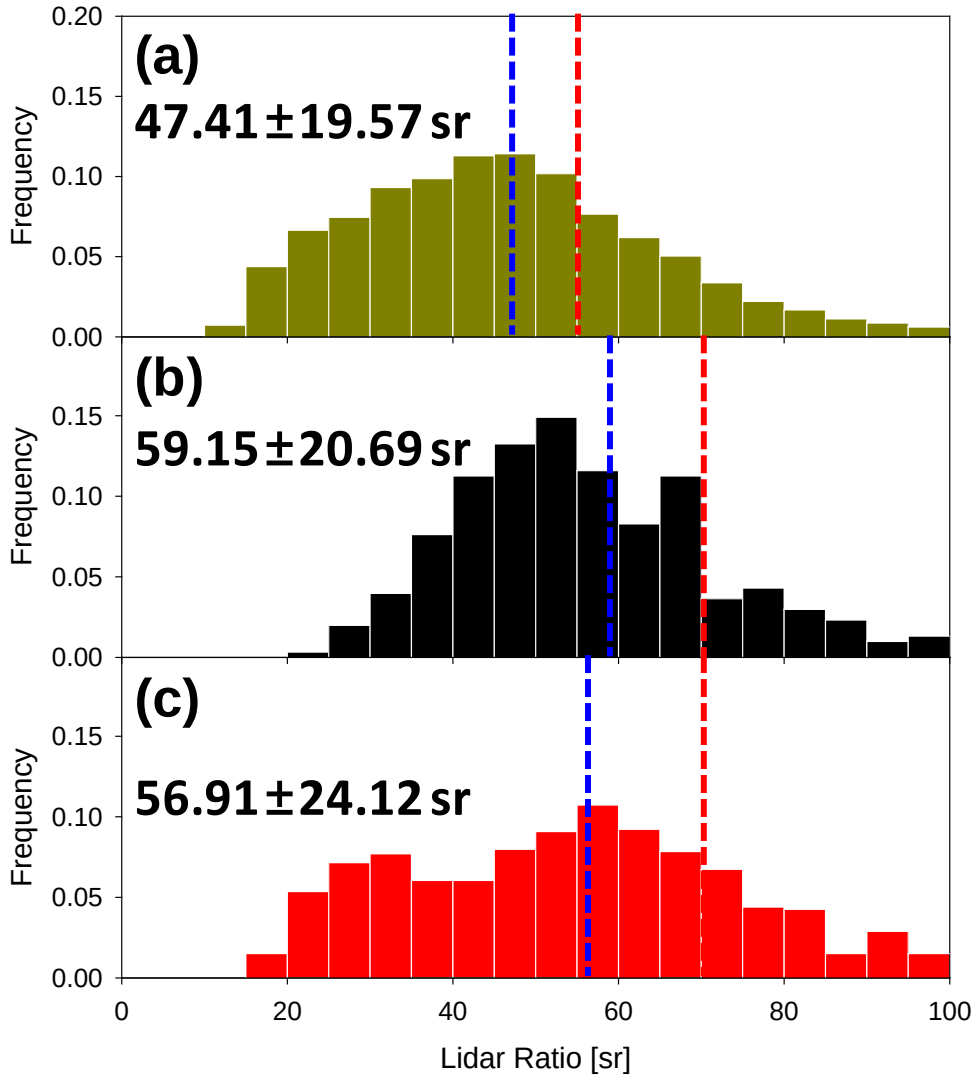

Figure 3.12. Same as Figure 3.11 but for (a) polluted dust, (b) biomass burning, and (c) polluted continental aerosols.

3.6. Summary

Aerosol extinction profile can be retrieved from lidar measurement by solving lidar equation. The Raman lidar technique [*Ansmann et al.*, 1990] and the high spectral resolution lidar (HSRL) technique [*Shipley et al.*, 1983] can derive aerosol extinction profiles needless to assume the S_{aer} by separating aerosol returns from molecular returns. However, the elastic backscatter lidar, which is most commonly used lidar system, cannot derive aerosol extinction directly from the measurement. In order to retrieve aerosol extinction from elastic backscatter lidar, $\boldsymbol{S_{aer}}$ should be determined and it is frequently either assumed or inferred from additional measurements.

Because uncertainty in S_{aer} is the largest source of uncertainty in the CALIOP AOD, it is desirable to improve S_{aer} values used in CALIOP algorithm to retrieve accurate AOD (or aerosol extinction). Current CALIOP level 2 algorithm uses pre-determined $\boldsymbol{S_{aer}}$ for classified aerosol types. However, not only using single values of $\boldsymbol{S_{aer}}$ for each aerosol type but also aerosol classification algorithm could be sources of uncertainties in aerosol extinction retrieval. In this study, to improve currently used $\boldsymbol{S_{aer}}$ in CALIOP level 2 algorithm, $\boldsymbol{S_{aer}}$ is determined

from CALIOP by using AOD from AERONET and MODIS-Aqua as a constraint without any assumption.

Using 4-year measurements (2006-2010) of elastic-backscatter lidar and SKYNET sun/sky radiometer at Seoul National University of Seoul, Korea, mean lidar ratio is estimated to be 61.7±16.5 sr. Lidar ratios are also retrieved using ground-based lidar and AERONET sun/sky radiometer during Distributed Regional Aerosol Gridded Observation Networks (DRAGON) Northeast Asia Campaign 2012. Mean lidar ratios at Seoul and Osaka were retrieved as 65.41±21.42 sr and 65.04±20.62 sr, respectively. Mean lidar ratios from Seoul and Osaka, which are metropolitan cities in East Asia, are almost same and comparable to the lidar ratio for pollution used in CALIOP algorithm (70 sr).

Dust aerosol is easily recognized from depolarization ratio measurements due to its non-spherical shape. *Burton et al.* [2013] reported that aerosol type classification for dust is the most accurate in CALIOP algorithm. For this reason, lidar ratios are retrieved mainly focused on dust aerosol and compared other studies and CALIOP Level 2 Product. The lidar ratio for dust conditions are estimated to be 51.7±13.7 sr using 4-year measurements of elastic-backscatter lidar and SKYNET sun/sky

radiometer at Seoul National University of Seoul, Korea. During DRAGON 2012 NE Asia campaign, lidar ratio for dust event on 27-28 April 2012 in Seoul is retrieved as 48.02±9.38 sr from elastic-backscatter lidar and AERONET sun/sky radiometer. From a synergy of CALIOP and AERONET, lidar ratio for Saharan/Arabian dust is derived to be 47.45±16.52 sr. Lastly, using CALIOP and MODIS measurements together, dust lidar ratio is retrieved as 45.50±15.17 sr. All the lidar ratios for dust aerosol retrieved in this study using AOD constrained method show larger values than currently used lidar ratio for dust in CALIOP algorithm (40 sr), which suggests that dust lidar ratio in CALIOP algorithm is underestimated and needs to be increased. Moreover, the retrieved lidar ratio for Asian dust (110°E - 180°E, 20°N – 50°N) appears as 53.04±18.30 sr, which is much larger than global mean of dust lidar ratio (45.50±15.17 sr). This result implies that the lidar ratios for dust have regional variation.

CHAPTER 4.
SUMMARY AND FURTHERWORKS

Aerosol extinction profile is one of the most important parameter to estimate aerosol radiative forcing, especially when calculating atmospheric heating by aerosol. CALIOP is a very useful instrument that provides aerosol vertical profiles over the glove. However, current CALIOP-derived AOD (or aerosol extinction) has large uncertainty compared to other passive sensors. The expected error for CALIOP AOD is ±0.05 ± 40% over both land and ocean [*Winker et al.*, 2009; *Omar et al.*, 2013], whereas the MODIS AOD retrieval has less uncertainties, with expected errors of ±0.03 ± 5% over ocean and ±0.05 ± 15% over land [*Remer et al.*, 2005; *Levy et al.*, 2010].

In order to retrieve the aerosol extinction coefficient (or AOD) from CALIOP measurements, the aerosol type is determined *a priori* so that a type-specific lidar ratio can be assigned to the aerosol layer. The lidar ratio is an essential parameter for aerosol extinction coefficient retrievals from elastic lidar measurements [*Fernald*, 1984]. Errors in the *a priori* prescription of this value can thus induce large errors in the retrieved AOD.

Therefore, when validating CALIOP AOD using other instruments, errors associated with aerosol type or ‘lidar ratio’ should be considered. The validation of CALIOP AOD by segregating aerosol type can lead to an improvement of the accuracy of aerosol type classification and lidar ratio determination in CALIOP algorithm.

Nearly two million collocated AOD data pairs over oceans from CALIOP and MODIS from June 2006 to December 2010 have been compared to evaluate the CALIOP AODs in this study. The mean MODIS AOD is 61% larger than that of CALIOP AOD. When considering aerosol types defined in CALIOP algorithm, the differences in AOD between the two sensors show some dependence on the type of aerosol. MODIS AOD is higher than CALIOP AOD for most aerosol types except for polluted dust and polluted continental.

The AOD comparison between CALIOP and MODIS shows that the CALIOP algorithms can increase the accuracy of the Asian dust AODs by adopting regionally variable dust lidar ratios. Additionally, an examination of the layer base altitude for smoke layers and comparing with independent measurements to determine what corrections if any to the calculation of the AOD for smoke are warranted. As the study has shown,

the effect of the daytime SNR on the depolarization ratio has important consequences for the aerosol classification scheme.

It is desirable to improve lidar ratios used in CALIOP algorithm to retrieve accurate AOD (or aerosol extinction) because the lidar ratio is a crucial source of uncertainties in CALIOP aerosol retrieval. In this study, lidar ratios were retrieved from CALIOP measurements using independently measured AOD from AERONET and MODIS as a constraint. By comparing retrieved lidar ratios with pre-determined lidar ratios in CALIOP algorithm for each aerosol type, the accuracy of currently used lidar ratio in CALIOP algorithm will be assessed and the algorithm for determining lidar ratio and classifying aerosol types will be improved.

Lidar ratios for dust are retrieved as 51.7±13.7 sr and 48.02±9.38 sr from ground-based elastic lidar and sun/sky radiometer measurements. The CALIOP-derived lidar ratio for dusts using AODs from AERONET and MODIS are found to be 47.45±16.52 sr and 46.32±14.44 sr, respectively. These results are larger than currently used lidar ratio for dust in CALIOP algorithm (40 sr), which suggests that currently used lidar ratio for dust in CALIOP algorithm needs to be increased. Moreover,

retrieved lidar ratio for Asian dust is estimated to be 53.04±18.30 sr from a synergy of CALIOP and MODIS, which is much larger than other regions. This result implies that the lidar ratios for dust have regional variation.

Although aerosol lidar ratios used in CALIOP algorithm have relatively large uncertainty (lager then 30% as shown in *Young et al.*. [2013]), their mean values are consistent with other previous studies (e.g., *Ansmann et al.*, [2001], *Voss et al.*, [2001], *Catrall et al.*, [2005]). Thus, in order to produce more accurate AOD and aerosol extinction from CALIOP measurements, it is reliable to improve the aerosol type classification in CALIOP algorithm, except for dust aerosol which is classified accurately compared to other types. Several results reported in this study can provide suggestions to improve aerosol type classification in CALIOP algorithm.

REFERENCES

Ackerman, S. A., K. I. Strabala, W. P. Menzel, R. A. Frey, C. C. Moeller, and L. E. Gumley, 1998: Discriminating clear sky from clouds with MODIS, *J. Geophys. Res.*, 103(D24), 32141–32157, doi:10.1029/1998JD200032.

Anderson, J. C., J. Wang, J. Zeng, M. Petrenko, G. G. Leptoukh, and C. Ichoku, 2012: Accuracy assessment of Aqua-MODIS aerosol optical depth over coastal regions: importance of quality flag and sea surface wind speed, *Atmos. Meas. Tech. Discuss.*, 5, 5205-5243, doi:10.5194/amtd-5-5205-2012.

Ansmann, A., F. Wagner, D. Althausen, D. Müller, A. Herber, and U. Wandinger, 2001: European pollution outbreaks during ACE 2: Lofted aerosol plumes observed with Raman lidar at the Portuguese coast, *Journal of Geophysical Research*, **106**, 20725–20733, doi:10.1029/2000JD000091.

Barnaba, F., and G. P. Gobbi, 2004: Modeling the aerosol extinction versus backscatter relationship for lidar applications: Maritime and continental conditions, *J. Atmos. Oceanic Technol.*, **21**, 428–442.

Boucher, O., D. Randall, P. Artaxo, C. Bretherton, G. Feingold, P. Forster, V.-M. Kerminen, Y. Kondo, H. Liao, U. Lohmann, P. Rasch, S. K. Satheesh, S. Sherwood, B. Stevens and X. Y. Zhang, 2013: Clouds and Aerosols. In: Climate Change 2013: The Physical Science Basis. Contribution of Working Group I to the Fifth Assessment Report of the Intergovernmental Panel on Climate Change [Stocker, T. F.,D. Qin, G.-K. Plattner, M. Tignor, S. K. Allen, J. Boschung, A. Nauels, Y. Xia, V. Bex and P. M. Midgley (eds.)]. *Cambridge University Press, Cambridge*, United Kingdom and New York, NY, USA, in press.

Bréon, F-M., A. Vermeulen, and J. Descloitres, 2011: An evaluation of satellite aerosol products against sunphotometer measurements, *Remote Sens. Environ.*, 115, 3102-3111, doi:10.1016/j.rse.2011.06.017.

Burton, S. P., R. A. Ferrare, M. A. Vaughan, A. H. Omar, R. R. Rogers, C. A. Hostetler, and J. W. Hair, 2013: Aerosol classification from airborne HSRL and comparisons with the CALIPSO vertical feature mask, *Atmos. Meas. Tech. Discuss.*, 6, 1815-1858, doi:10.5194/amtd-6-1815-2013.

Burton, S. P., R. A. Ferrare, C. A. Hostetler, J. W. Hair, C. Kittaka, M. A. Vaughan, M. D. Obland, R. R. Rogers, A. L. Cook, D. B. Harper, and L. A. Remer, 2010: Using airborne high spectral resolution lidar data to evaluate combined active plus passive retrievals of aerosol extinction profiles, *Journal of Geophysical Research*, **115**, D00H15, doi:10.1029/2009JD012130.

Campbell, J. R., J. L. Tackett, J. S. Reid, J. Zhang, C. A. Curtis, E. J. Hyer, W. R. Sessions, D. L. Westphal, J. M. Prospero, E. J. Welton, A. H. Omar, M. A. Vaughan, and D. M. Winker, 2012: Evaluating nighttime CALIOP 0.532 μm aerosol optical depth and extinction coefficient retrievals, *Atmos. Meas. Tech.*, 5, 2143-2160, doi:10.5194/amt-5-2143-2012.

Campbell, J. R., J. S. Reid, D. L. Westphal, J. L. Zhang, J. L. Tackett, B. N. Chew, E. J. Welton, A. Shimizu, N. Sugimoto, K. Aoki, and D. M. Winker, 2013: Characterizing the vertical profile of aerosol particle extinction and linear depolarization over Southeast Asia and the Maritime Continent: The 2007-2009 view from CALIOP, *Atmos. Res.*, 122, 520-543.

Cattrall, C., J. Reagan, K. Thome, and O. Dubovik, 2005: Variability of aerosol and spectral lidar and backscatter and extinction ratios of key aerosol types derived from selected Aerosol Robotic Network locations, *J. Geophys. Res.*, 110, D10S11, doi:10.1029/2004JD005124.

Chazette, P., J.-C. Raut, F. Dulac, S. Berthier, S.-W. Kim, P. Royer, J. Sanak, S. Loaec, and H. Grigaut-Desbrosses, 2010: Simultaneous observations of lower tropospheric continental aerosols with a ground-based, an airborne, and the spaceborne CALIOP lidar systems, *J. Geophys. Res.*, 115, D00H31, doi:10.1029/2009JD012341.

Doherty, Sarah J., Theodore L. Anderson, and Robert J. Charlson, 1999: Measurement of the Lidar Ratio for Atmospheric Aerosols with a 180° Backscatter Nephelometer, *Applied Optics*, **38**, 1823-1832.

Dubovik, O., A. Sinyuk, T. Lapyonok, B. N. Holben, M. Mishchenko, P. Yang, T. F. Eck, H. Volten, O. Munoz, B. Veihelmann, van der Zander, M Sorokin, and I. Slutsker, 2006: Application of spheroid models to account for aerosol particle nonsphericity in remote sensing of desert dust, *Journal of Geophysical Research*, **111**, D11208, doi:10.1029/2005JD006619.

Duncan, B. N., R. V. Martin, A. C. Staudt, R. Yevich, and J. A. Logan, 2003: Interannual and seasonal variability of biomass burning emissions constrained by satellite observations, *J. Geophys. Res.*, 108(D2), 4100, doi:10.1029/2002JD002378.

Eck, T., B. N. Holben, J. Reid, O. Dubovik, A. Smirnov, N. O'Neill, I. Slutsker, and S. Kinne, 1999: Wavelength dependence of the optical depth of biomass burning, urban, and desert dust aerosols, *J. Geophys. Res.*, 104(D24), 31333– 31349.

Fernald, F. G., 1984: Analysis of atmospheric lidar observations: some comments, *Applied Optics*, **23**, 652-653.

Freudenthaler, V., M. Esselborn, M. Wiegner, B. Heese, M. Tesche, A. Ansmann, D. Muller, D. Althausen, M. Wirth, A. Fix, G. Ehret, P. Knippertz, C. Toledano, J. Gasteiger, M. Garhammer, and M. Seefeldner, 2009: Depolarization ratio profiling at several wavelengths in pure Saharan dust during SAMUM 2006, *Tellus B*, 61, 165–179. doi: 10.1111/j.1600-0889.2008.00396.

Hansen, J.E., M. Sato and R. Ruedy, 1997: Radiative forcing and climate response. *Journal of Geophysical Research*, **102**, 6831-6864, 1997.

Huang, J., Q. Fu, J. Su, Q. Tang, P. Minnis, Y. Hu, Y. Yi, and Q. Zhao, 2009: Taklimakan dust aerosol radiative heating derived from CALIPSO observations using the Fu-Liou radiation model with CERES constraints, *Atmospheric Chemistry and Physics*, **9**, 4011–4021.

Hubanks, P. A., 2012: MODIS Atmosphere QA Plan for Collection 005 and 051, 63 pp., available at: http://modis-atmos.gsfc.nasa.gov/_docs/QA_Plan_2012_01_12.pdf.

Jeong, Myeong-jae and Zhanqing Li, 2005: Quality, compatibility, and synergy analyses of global aerosol products derived from the advanced very high resolution radiometer and Total Ozone Mapping Spectrometer, Journal of Geophysical Research, 110, D10S08, doi:10.1029/2004JD004647.

Jung, J.,, Y. J. Kim, K. Y. Lee, M. G.-Cayetano, T. Batmunkh, J.-H. Koo, and J. Kim, 2010: Spectral optical properties of long-range transport Asian dust and pollution aerosols over Northeast Asia in 2007 and 2008, Atmospheric Chemistry and Physics, 10, 5391–5408, doi:10.5194/acp-10-5391-2010.

Kacenelenbogen, M., M. A. Vaughan, J. Redemann, R. M. Hoff, R. R. Rogers, R. A. Ferrare, P. B. Russell, C. A. Hostetler, J. W. Hair, and B. N. Holben, 2011: An accuracy assessment of the CALIOP/CALIPSO version 2/version 3 daytime aerosol extinction product based on a detailed multi-sensor, multi-platform case study, *Atmos. Chem. Phys.*, 11, 3981-4000, doi:10.5194/acpd-10-27967-2010.

Kahn, R. A., Y. Chen, D. L. Nelson, F.-Y. Leung, Q. Li, D. J. Diner, and J. A. Logan, 2008: Wildfire smoke injection heights: Two perspectives from space, *Geophysical Research Letters*, **35**, L04809, doi:10.1029/2007GL032165.

Kai, K., Y. Nagata, N. Tsunematsu, T. Matsumura, H.-S. KIM, T. Matsumoto, S. Hu, H. Zhou, M. Abo, and T. Nagai, 2008: The Structure of the dust layer over the Taklimakan Desert during the dust storm in April 2002 as observed using a depolarization lidar, *J. Meteor. Soc. Japan*, 86, 1-16.

Kaufman, Y. J., J. M. Haywood, P. V. Hobbs, W. Hart, R. Kleidman, and B. Schmid, 2003: Remote sensing of vertical distributions of smoke

aerosol off the coast of Africa, *Geophysical Research Letters*, **30(16)**, 1831, doi:10.1029/2003GL017068.

Kim, S.-W., S. Berthier, P. Chazette, J.-C. Raut, F. Dulac, and S.-C. Yoon, 2008: Validation of aerosol and cloud layer structures from the space-borne lidar CALIOP using Seoul National University ground-based lidar, *Atmos. Chem. Phys.*, 8, 3705-3720.

Kim, S.-W., E.-S. Chung, S.-C. Yoon, B.-J. Sohn, and N. Sugimoto, 2011: Intercomparisons of cloud-top and cloud-base heights from ground-based Lidar, CloudSat and CALIPSO measurements, *Int. J. Remote Sens.*, 32, 1179-1197, doi:10.1080/01431160903527439.

King, M., J. Closs, S. Spangler, R. Greenstone, S. Wharton, and M. Myers, 2004: *EOS Data Products Handbook.* Vol. 1. EOS Project Science Office, NASA Goddard Space Flight Center, Greenbelt, MD, 260 pp. [Available from EOS Project Science Office, Code 900, NASA Goddard Space Flight Center, Greenbelt, MD 20771; or online at http://eospso.gsfc.nasa.gov/ftp_docs/data_products_1.pdf.]

Kittaka, C., D. M. Winker, M. A. Vaughan, A. Omar, and L. A. Remer, 2010: Intercomparison of CALIOP and MODIS aerosol optical

depth retrievals, *Atmospheric Measurement Techniques*, **4**, 131–141, doi:10.5194/amt-4-131-2011

Klett, J. D., 1981: Stable analytical inversion solution for processing lidar returns, *Applied Optics*, **20(2)**, 211-220.

L'Ecuyer, T. S., and J. H. Jiang, 2010: Touring the atmosphere aboard the A-Train, *Phys. Today*, 63(7), 36–41, doi:10.1063/1.3463626.

Léon, J.-F., D. Tanré, J. Pelon, Y. J. Kaufman, J. M. Haywood, and B. Chatenet, 2003: Profiling of a Saharan dust outbreak based on a synergy between active and passive remote sensing, *Journal of Geophysical Research*, **108(D18)**, 8575, doi:10.1029/2002JD002774.

Levy, R. C., L. A. Remer, J. V. Martins, Y. J. Kaufman, A. Plana-Fattori, J. Redemann, and B. Wenny, 2005: Evaluation of the MODIS aerosol retrievals over ocean and land during CLAMS, *J. Atmos. Sci.*, 62(4), 974-992.

Levy, R. C., L. A. Remer, R. G. Kleidman, S. Mattoo, C. Ichoku, R. Kahn, and T. F. Eck, 2010: Global evaluation of the Collection 5 MODIS dark-target aerosol products over land, *Atmos. Chem. Phys.*, 10, 10399–10420, doi:10.5194/acp-10-10399-2010.

Liu, Z., N. Sugimoto, and T. Murayama, 2002: Extinction-To-Backscatter Ratio of Asian Dust Observed With High-Spectral-Resolution Lidar and Raman Lidar, *App. Opt.*, 41, 2760-2767.

Liu, Z. Y., M. Vaughan, D. Winker, C. Kittaka, B. Getzewich, R. Kuehn, A. Omar, K. Powell, C. Trepte, and C. Hostetler, 2009: The CALIPSO lidar cloud and aerosol discrimination: Version 2 algorithm and initial assessment of performance, *J. Atmos. Ocean. Tech.*, 26, 1198–1213.

McPherson, C. J., J. A. Reagan, J. Schafer, D. Giles, R. Ferrare, J. Hair, and C. Hostetler, 2010: AERONET, airborne HSRL, and CALIPSO aerosol retrievals compared and combined: A case study, *Journal of Geophysical Research*, **115**, D00H21, doi:10.1029/2009JD012389.

Mielonen, T., A. Arola, M. Komppula, J. Kukkonen, J. Koskinen, G. de Leeuw, and K. E. J. Lehtinen, 2009: Comparison of CALIOP Level 2 aerosol subtypes to aerosol types derived from AERONET inversion data, *Geophys. Res. Lett.*, 36, L18804, doi:10.1029/2009GL039609.

Misra, Amit, S. N. Tripathi, D. S. Kaul, Ellsworth J. Welton, 2012: Study of MPLNET-Derived Aerosol Climatology over Kanpur, India, and Validation of CALIPSO Level 2 Version 3 Backscatter and Extinction Products, *J. Atmos. Oceanic Technol.*, 29, 1285-1294.

Müller, D., F. Wagner, D. Althausen, U. Wandinger, and A. Ansmann, 2000: Physical properties of the Indian aerosol plume derived from six-wavelength lidar observations on 25 March 1999 of the Indian Ocean Experiment, *Geophys. Res. Lett.*, **27**, 1403–1406.

Murayama, T., S. Masonis, J. Redemann, T. L. Anderson, B. Schmid, J. M. Livingston, P. B. Russell, B. Huebert, S. G. Howell, C. S. McNaughton, A. Clarke, M. Abo, A. Shimizu, N. Sugimoto, M. Yabuki, H. Kuze, S. Fukagawa, K. Maxwell-Meier, R. J. Weber, D. A. Orsini, B. Blomquist, A. Bandy, and D. Thornton, 2003: An intercomparison of lidar-derived aerosol optical properties with airborne measurements near Tokyo during ACE-Asia, *J. Geophys. Res.*, 108(D23), 8651, doi:10.1029/2002JD003259.

Noh, Y. M., Y. J. Kim, B. C. Choi, and T. Murayama, 2007: Aerosol lidar ratio characteristics measured by a multi-wavelength Raman lidar system at Anmyeon Island, Korea, *Atmos. Res.*, 86, 76-87, doi:10.1016/j.atmosres.2007.03.006.

O'Dowd, C., C. Scannell, J. Mulcahy, and S. G. Jennings, 2010: Wind speed influences on marine aerosol optical depth, *Adv. Meteorol.*, 2010, 830846, doi:10.1155/2010/830846.

Omar A. H., D. M. Winker, C. Kittaka, M. A. Vaughan, Z. Lou, Y. Hu, C. R. Trepte, R. R. Rogers, R. A. Ferrare, K-P Lee, R. E. Kuehn, and Chris A. Hostetler, 2009: The CALIPSO Automated Aerosol Classification and Lidar Ratio Selection Algorithm, *Journal of Atmospheric and Oceanic Technology*, **26**, 1994–2014, doi: 10.1175/2009JTECHA1231.1.

Omar, A. H., J.-G. Won, D. M. Winker, S.-C. Yoon, O. Dubovik, and M. P. McCormick, 2005: Development of global aerosol models using cluster analysis of Aerosol Robotic Network (AERONET) measurements. *Journal of Geophysical Research*, **110**, D10S14, doi:10.1029/2004JD004874.

Omar, A. H., D. M. Winker, J. L. Tackett, D. M. Giles, J. Kar, Z. Liu, M. A. Vaughan, K. A. Powell, and C. R. Trepte, 2013: CALIOP and AERONET aerosol optical depth comparisons: One size fits none, *J. Geophys. Res.*, 118, 1-19, doi:10.1002/jgrd.50330.

Oo, M., R. Holz, 2011: Improving the CALIOP aerosol optical depth using combined MODIS-CALIOP observations and CALIOP integrated attenuated total color ratio, *Journal of Geophysical Research*, **116**, D14201, doi:10.1029/ 2010JD014894

Ramana, M. V., V. Ramanathan, Y. Feng, S-C. Yoon, S-W. Kim, G. R.

Carmichael and J. J. Schauer, 2010: Warming influenced by the ratio of black carbon to sulphate and the black-carbon source, *Nature Geoscience*, **3**, 542–545, doi:10.1038/ngeo918.

Ramanathan, V., M. V. Ramana, G. Roberts, D. Kim, C. Corrigan, C. Chung, and D. Winker, 2007: Warming trends in Asia amplified by brown cloud solar absorption, *Nature*, **448**, 575–578, doi:10.1038/nature06019.

Remer, L. A., Y. J. Kaufman, D. DTanr´e, S. Mattoo, D.A. Chu, J. V. Martins, R.-R. Li, C. Cichoku, R. C. Levy, R. G. Kleidman, T. F. Eck, E. Vermote, and B. N. Holben, 2005: The MODIS Aerosol Algorithm, Products, and Validation, *Journal of Atmospheric Science*, **62**, 947–973.

Sasano, Y., E. V. Browell, and S. Ismail, 1985: Error caused by using a constant extinction/backscattering ratio in the lidar solution, *Applied Optics*, **24**, 3929-3932.

Schuster, G. L., O. Dubovik, and B. N. Holben, 2006: Angstrom exponent and bimodal aerosol size distributions, *J. Geophys. Res.*, 111, D07207, doi:10.1029/2005JD006328.

Schuster, G. L., M. Vaughan, D. MacDonnell, W. Su, D. Winker, O. Dubovik, T. Lapyonok, and C. Trepte, 2012: Comparison of CALIPSO aerosol optical depth retrievals to AERONET measurements, and a climatology for the lidar ratio of dust, *Atmos. Chem. Phys.*, 12, 7431-7452, doi:10.5194/acp-12-7431-2012, 2012.

Shipley, S. T., D. H. Tracy, E. W. Eloranta, J. T. Tauger, J. T. Sroga, F. L. Roesler, and J. A. Weinman, 1983: High spectral resolution lidar to measure optical scattering properties of atmospheric aerosols. 1: Theory and instrumentation, *Applied Optics*, **22**, 3716-3724.

Smirnov, A., A. M. Sayer, B. N. Holben, N. C. Hsu, S. M. Sakerin, A. Macke, N. B. Nelson, Y. Courcoux, T. J. Smyth, P. Croot, P. K. Quinn, J. Sciare, S. K. Gulev, S. Piketh, R. Losno, S. Kinne, and V. F. Radionov, 2012: Effect of wind speed on aerosol optical depth over remote oceans, based on data from the Maritime Aerosol Network, *Atmos. Meas. Tech.*, 5, 377-388, doi:10.5194/amt-5-377-2012.

Sugimoto, N., I. Matsui, A. Shimizu, I. Uno, K. Asai, T. Endoh, and T. Nakajima, 2002: Observation of dust and anthropogenic aerosol plumes in the Northwest Pacific with a two-wavelength polarization

lidar on board the research vessel Mirai, *Geophys. Res. Lett.*, 29(19), 1901, doi:10.1029/2002GL015112.

Tanré, D., Y. J. Kaufman, M. Herman, and S. Mattoo, 1997: Remote sensing of aerosol properties over oceans using the MODIS/EOS spectral radiances, *J. Geophys. Res.*, 102, 16971–16988.

Vaughan, M. A., D. M. Winker, and K. A. Powell, 2005: CALIOP algorithm theoretical basis document— Part 2: Feature Detection and Layer Properties Algorithms, Release 1.01, PC-SCI-202, *NASA Langley Research Center*, Hampton, VA, 87pp.

Vaughan, M. A, K. A. Powell, R. E. Kuehn, S. A. Young, D. M. Winker, C. A. Hostetler, W. H. Hunt, Z. Liu, M. J. McGill, and B. J. Getzewich, 2009: Fully Automated Detection of Cloud and Aerosol Layers in the CALIPSO Lidar Measurements, *Journal of Atmospheric and Oceanic Technology*, **26**, 2034–2050, doi: 10.1175/2009JTECHA1228.1.

Voss, K. J., E. J. Welton, P. K. Quinn, J. Johnson, A. M. Thompson, and H. R. Gordon, 2001: Lidar measurements during Aerosols99, *J. of Geophys. Res.*, 106, 20821–20831, doi:10.1029/2001JD900217.

Welton, E. J., Voss, K. J., Gordon, H. R., Maring, H., Smirnov, A., Holben, B., Schmid, B., Livingston, J. M., Russell, P. B., Durkee, P. A., Formenti, P. and Andreae, M. O., 2000: Ground-based lidar measurements of aerosols during ACE-2: instrument description, results, and comparisons with other ground-based and airborne measurements. *Tellus B*, **52**, 636–651, doi:10.1034/j.1600-0889.2000.00025.

Winker, D. M., J. Pelon, and M. P. McCormick, 2003: The CALIPSO mission: Spaceborne lidar for observations of aerosols and clouds. Lidar Remote Sensing for Industry and Environment Monitoring III, U. N. Singh, T. Itabe, and Z. Liu, Eds., *International Society for Optical Engineering (SPIE Proceedings, Vol. 4893)*, doi:10.1117/12.466539.

Winker, D. M., M. A. Vaughan, A. Omar, Y. Hu, K. A. Powell, Z. Liu, W. H. Hunt, and S. A. Young, 2009: Overview of the CALIPSO Mission and CALIOP Data Processing Algorithms, *Journal of Atmospheric and Oceanic Technology*, **26**, 2310–2323, doi: 10.1175/2009JTECHA1281.1.

Winker, D. M., W. H. Hunt, and M. J. McGill, 2007, Initial performance assessment of CALIOP, *Geophysical Research Letters*, **34**, L19803, doi:10.1029/ 2007GL030135

Won, J.-G., S.-C. Yoon, S.-W. Kim, A. Jefferson, E. G. Dutton, and B. Holben, 2004: Estimation of direct radiative forcing of Asian dust aerosols with Sun/sky radiometer and lidar measurements at Gosan, Korea, *Journal of the Meteorological Society Japan*, **82**, 115–130.

Young, S. A., M. A. Vaughan, 2009: The Retrieval of Profiles of Particulate Extinction from Cloud-Aerosol Lidar Infrared Pathfinder Satellite Observations (CALIPSO) Data: Algorithm Description. *Journal of Atmospheric and Oceanic Technology*, **26**, 1105–1119, doi: 10.1175/2008JTECHA1221.1.

Young, S. A., M. A. Vaughan, R. E. Kuehn, D. M. Winker, 2013: The Retrieval of Profiles of Particulate Extinction from Cloud–Aerosol Lidar and Infrared Pathfinder Satellite Observations (CALIPSO) Data: Uncertainty and Error Sensitivity Analyses. *J. Atmos. Oceanic Technol.*, **30**, 395–428, doi: http://dx.doi.org/10.1175/JTECH-D-12-00046.1

국문초록

CALIOP (the Cloud-Aerosol Lidar with Orthogonal Polarization)은 CALIPSO (the Cloud-Aerosol Lidar and Infrared Pathfinder Satellite Observation) 위성에 탑재된 라이다로 전구에 걸쳐 대기의 연직 분포를 관측하는 유용한 기기이다. 그러나 CALIOP 에서 제공하는 에어로졸 광학두께 (AOD; aerosol optical depth)는 기존의 다른 위성 관측 결과에 비해 정확도가 낮은 것이 현실이다. CALIOP AOD 의 정확도를 평가하고 오차 발생 원인을 분석하기 위해 MODIS AOD 자료와 비교•검증을 수행하였다. 비교•검증에는 MODIS AOD 의 정확도가 높은 해양 자료만을 사용하였으며 2006 년 6 월부터 2010 년 12 월까지의 자료를 이용하여 CALIOP 에서 구분된 여섯 종류의 에어로졸 (clean marine, dust, polluted dust, polluted continental, biomass burning)로 나누어 분석하였다. 550 nm 에서의 MODIS AOD 는 평균 0.111 ± 0.079 로 CALIOP AOD (0.068 ± 0.073) 보다 약 63% 높게 나타났다. Clean marine 의 경우, MODIS AOD 가 0.110 ± 0.064 로 CALIOP AOD (0.056 ± 0.038)보다 거의 두 배 가까이 높게 나타났으며 위도에 따라 두 기기의 AOD 차이가 변하는 모습을

보였다. 이는 해수면 풍속이 강할 때, 지표면 알베도 (albedo)가 증가하여 MODIS AOD 가 과대모의 되기 때문으로 판단된다. Dust 에어로졸의 AOD 차이는 다른 에어로졸에 비해 적게 나타났지만 지역에 따른 변화가 뚜렷하게 나타났다. 또한, 에어로졸에 편광소멸도가 증가함에 따라 두 기기의 AOD 차이가 증가하는 모습도 확인할 수 있었다. Polluted dust 와 polluted continental 에어로졸은 CALIOP AOD 가 각각 15%와 29% 크게 나타났다. 특히, 두 종류의 에어로졸은 육지에서 유입되는 에어로졸이 거의 없을 것으로 예상되는 먼 바다에서도 관측 빈도가 높아 clean marine 에어로졸이 잘못 구분될 수 있음을 추측해 볼 수 있었다. Biomass burning 에어로졸은 CALIOP 알고리즘에서 상층에 떠 있는 에어로졸로 정의되어 하층의 에어로졸을 감지하지 못하는 사례가 많았으며 이로 인해 CALIOP AOD 가 매우 낮게 산출되는 것을 확인하였다.

현재 CALIOP Level 2 알고리즘은 에어로졸 종류에 따라 미리 정해진 라이다 상수 (lidar ratio)를 사용하여 에어로졸 소산계수를 산출하고 있다. 그러나 에어로졸 종류를 구분하고 구분된 에어로졸에 따라 단일한 라이다 상수 값을 사용하기 때문에 CALIOP AOD 에 오차가 발생할 수 있다. 본 연구에서는 라이다로부터 에어로졸 소산계수 및 AOD 를 산출하는데 가장

큰 오차의 원인인 라이다 상수를 가정하지 않고 MODIS 나 AERONET 등의 관측으로 얻은 AOD 값을 이용하여 직접 구하였다. 서울대학교에서 지상 라이다와 SKYNET 선/스카이 레디오미터로 2006 년부터 2010 년까지 관측 결과를 이용하여 라이다 상수를 산출한 결과 평균 61.7±16.5 sr 로 나타났다. 또한, 2012 년 3-5 월 한반도와 일본에서 수행된 DRAGON 캠페인 기간 동안 AERONET 과 라이다의 공동관측 결과를 이용하여 서울과 오사카에서 캠페인 기간 라이다 상수를 계산한 결과, 각각 65.41±21.42 sr, 65.04±20.62 sr 로 나타났다. 이러한 결과는 기존의 선행연구에서 보고한 오염물질의 라이다 상수 및 현재 CALIOP 에서 사용하고 있는 polluted continental 의 라이다 상수인 70 sr 과 비슷한 결과이다.

Dust 에어로졸은 현재 CALIOP 알고리즘 상에서 에어로졸 종류 구분의 정확도가 상대적으로 가장 정확한 것으로 보고되고 있다 [*Burton et al.,* 2013]. 따라서 본 연구에서는 dust 에 초점을 맞추어 라이다 상수를 직접 산출하고 현재 CALIOP 알고리즘에서 사용 중인 40 sr 과 비교하여 보았다. 서울에서 2006 년부터 2010 년까지 황사 사례에서의 라이다 상수를 산출한 결과는 51.7±13.7 sr 로 나타났다. 2012 년 DRAGON 캠페인 기간 황사가 발생했던 2012 년 4 월 27-28 일

서울에서의 라이다 상수는 48.02±9.38 sr 로 비슷한 값을 보였다. CALIOP 과 AERONET 자료를 이용하여 사하라 사막 지역의 dust 에 대해 라이다 상수를 산출한 결과는 47.45±16.52 sr 로 나타났으며 CALIOP 과 MODIS 자료로부터 산출된 dust 의 라이다 상수는 45.50±15.17 sr 이었다. 특히, CALIOP 과 MODIS 자료를 이용하여 동아시아 지역에서의 dust 라이다 상수 산출 결과는 53.04±18.30 sr 로 전구 평균 보다 높은 값을 보였다. 이와 같이 dust 의 라이다 상수는 40 sr 보다 모두 높은 값을 보여 현재 CALIOP 알고리즘에서 사용하고 있는 값보다 큰 값을 사용할 필요가 있음을 보여준다. 또한, 동아시아에서는 더욱 큰 값을 보여 지역에 따라 다른 값을 사용할 필요성이 있음을 알 수 있었다.

주요어: CALIOP, 에어로졸 광학두께, 에어로졸 종류, 라이다 상수, MODIS

학 번: 2005-20504